KOONS, RACHEL CLAUDIA, M.S. DECEMBER 2018 GEOLOGY

DISCREPANCY OF ORGANIC RICHNESS WITHIN THE OATKA CREEK AND UNION SPRINGS OF THE MARCELLUS FORMATION

Thesis Advisor: Jeremy C. Williams

The Appalachian Basin has attracted attention because of its considerable shale plays that yield high volumes of natural gas. Within this basin, the Marcellus formation has become a prime target for study not only because of the potential profit it may generate in terms of economic resources, but also because it offers insight into the type of paleoenvironment favorable for black shale deposition. While establishing analogues between past and present black shale environments is complex, the Marcellus most readily lends itself to comparison with the Black Sea, a modern environment referred to as the type euxinic basin. However, while both basins may fit into the same general restricted basin model, the similar stratification system that developed and ultimately led to favorable organic matter preservation in each was likely the result of different processes. Due to plate tectonic activity in the larger scale context of the Appalachian Basin, the Marcellus formation was influenced by the Acadian Orogen that manifested from the closing of the Rhea Ocean and convergence of Laurentia with Gondwana. These mountains were responsible for establishing the arid, evaporitic environment that produced a halocline in the basin in which the Marcellus formed. The halocline had the benefit of creating anoxic bottom waters in which the preservation of organic matter was favorably enhanced.

We collected six stratigraphic columns totaling in 104 samples from the basal black shale member, the Union Springs, at an active aggregate quarry in Seneca Falls, New York. An additional 18 samples from a single stratigraphic column of the upper black shale member, the Oatka Creek, was collected from the same site. Using a multi-proxy geochemical approach to test for the oxygen conditions at the time of deposition, the Marcellus black shales were evaluated for the environmental factors that contributed to their organic richness and to determine if any changes occurred between the deposition of each black shale based on fine-scale geochemical resolution. We examined the relationships between total organic carbon (TOC), pyritic sulfur (S_{pyr}), pyritic iron (Fe_{pyr}), and acid soluble iron in the Union Springs and Oatka Creek samples, which allowed for classification of each of the black shale environments as oxic, dysoxic, or anoxic/euxinic based on a degree of pyritization (DOP) value. Ultimately, we determined that in the localized area of study, the oxygen conditions were similar for the deposition of both black shale members which exhibited almost exclusively anoxic/euxinic DOP values and TOC values that were highly comparable and suggestive of favorable preservation conditions.

DISCREPANCY OF ORGANIC RICHNESS WITHIN THE OATKA CREEK AND UNION SPRINGS OF THE MARCELLUS FORMATION

A thesis submitted

To Kent State University in partial

Fulfillment of the requirements for the

Degree of Master of Sciences

By

Rachel Claudia Koons

December, 2018

© Copyright

All rights reserved

Except for previously published materials

Thesis written by

Rachel Claudia Koons

B.S., The Ohio State University, 2014

M.S., Kent State University, 2018

Approved by

Jeremy C. Williams, Advisor

Daniel K. Holm, Chair, Department of Geology

James L. Blank, Dean, College of Arts and Sciences

LIST OF FIGURES

LIST OF TABLES

Acknowledgements

First and foremost, a big thanks is owed to my thesis advisor, Dr. Jeremy Williams, for all of his guidance and support in the formulation and completion of this project. If not for a snap decision to return to school, I would still be serving tea in California. It is due to Dr. Williams's diligence and backing that I secured a place in the graduate program at Kent State University as quickly as I decided to apply. Aside from the lingering fear of breaking every piece of remotely expensive-looking instrumentation, I am grateful for these last two years that have provided valuable hands-on experience and the freedom to present my findings with my own words.

I would like to thank my labmates, Daniel Wood, Diana Simone, and Bryan Ice, for their assistance with instrumentation training, sample collection and preparation, analytical runs, and data collection. More significantly, I thank you for being there and sharing in the bemoaning of the perpetual state of zombiehood known to practically every graduate student. It was much needed and appreciated.

To undergraduate lab assistants Shannon Joseph and Nicolle Di Domenico, thank you for your willingness to be roped into my project and the time you spent in front of the DOP set-up. The work you put in was critical for completing an essential part of this research and I really appreciate it. Thank you to Shannon for your help with writing the EA SOP.

To Ph.D. student Alan Stebbins at University of Massachusetts Boston, thank you for your time and patience with training me in the DOP procedure. You were a great teacher and always responded to the various questions I sent your way throughout the past year.

To Nick Johnson from the Department of Biological Sciences at Kent State University, thank you for your assistance with running the ICP-OES.

I would like to acknowledge Dr. Joseph Ortiz of Kent State University and Dr. Thomas Darrah of The Ohio State University for sitting on my thesis committee and offering helpful edits and suggestions for improving the quality of the questions I asked and the methods I used to tackle them.

If this thesis has any coherency and panache embedded within its words, it's largely thanks to my fellow KSU graduate students and Dr. Anne Jefferson who have greatly assisted in their peer review of the first rough (like, *really* rough) drafts of this work.

Last but not least, many thanks to Lisa Koons (mother), Keith Koons (father), and Billy Eymold (fiancé). Mom and Dad, you may not keep on top of the kind of research I do, but you have always let me know how proud you are of me and that means a whole lot more. To Billy, thank you for tagging along during the sample collection trip even though it left us absolutely drenched by the sudden rain shower while you were intent on procuring the perfect hand specimens. Also, I love you and such. Double also, I can finally start getting around to all of that wedding planning I should be doing.

Chapter 1: Proposal of Research

Project Description: We will perform a geochemical analysis on the Devonian-aged Marcellus formation for the purpose of reconstructing the paleoenvironment and determining which factors were present and favorable for black shale deposition, and more precisely, to specify which controls on organic matter preservation differed between the upper Oatka Creek member and lower Union Springs member to explain their disparity in organic matter richness.

Statement of Work

1.1 Introduction

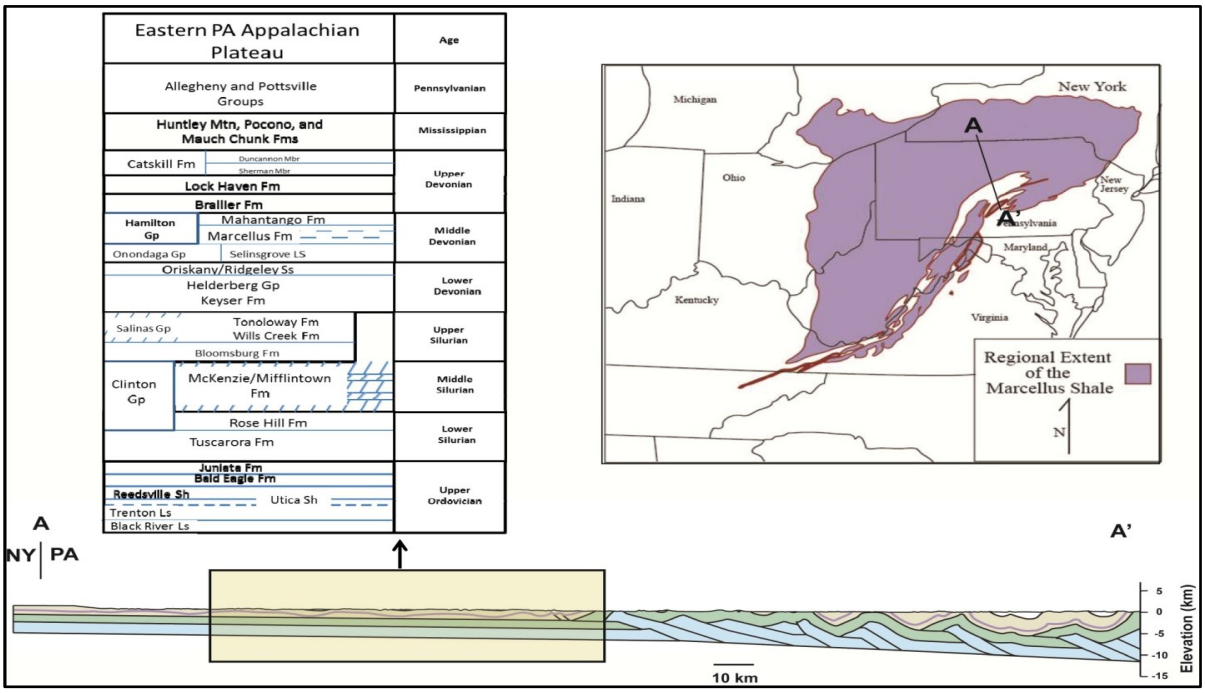

Figure 1.1: Aerial view of the extent of the Marcellus formation showing variability in thickness across A to A' (Walsh, 2011).

The Marcellus formation is Middle Devonian in age and is quite extensive, covering states such as Ohio, West Virginia, Virginia, Maryland, Pennsylvania, and New York (Figure 1.1). It is well-known within the petroleum industry as it has been deemed a valuable shale play area; in particular, it has been evaluated to be an enriched source of natural gas. This more unconventional recovery scenario entails that the shale not only acts as the source rock, but also the reservoir rock. Increasing reliance on natural gas over more traditional fuel sources such as coal may have the advantageous consequence of curbing current greenhouse gas emissions. Natural gas burns more "cleanly" than coal, contributing only about half as much carbon dioxide per unit of energy (Zielinski, 2014). The United States possesses multiple shale plays across the country which is a beneficial attribute that allows the country to remain more independent of foreign petroleum resources (Figure 1.2). The Marcellus formation specifically, has the fortuitous advantage of close proximity to some of the nation's most highly populated cities, making transportation and servicing of these areas easier (Energy Information Administration, 2010).

For the Marcellus in particular, it has been observed that the formation possesses vertical fractures running through it (Energy Information Administration, 2010). Depth zones where this formation is likely to be in the optimal oil and gas-generating window are more likely to be prime targets for the petroleum industry looking to employ horizontal drilling to extract petroleum. Horizontal drilling has been receiving more attention due to its potential for greater recovery over more conventional vertical drilling techniques. In the Marcellus, this technique is more productive and cost-effective as it simultaneously intersects as many vertical fractures as possible while drawing out petroleum. In addition to horizontal drilling, hydraulic fracturing may be incorporated to enhance recovery.

Figure 1.2: Shale plays across the contiguous United States (Vengosh, Warner, Jackson, & Darrah, 2013).

From oldest to youngest, the Devonian-aged formation consists of three members: the Union Springs, Cherry Valley, and Oatka Creek. The end members, the Oatka Creak and Union Springs, are composed of black shale while the middle member is limestone (Figure 1.3). The dark colored mudrocks of the Marcellus formation, despite the commonly held opinion regarding basic black shale traits, do not exhibit fine, even laminations throughout the entirety of the formation. Rather, the formation often appears massive in the absence of bioturbation or large particles such as calcareous bioclasts (Werne, Sageman, Lyons, & Hollander, 2002). Laminations are typically only present when organic matter formed distinctive laminae (Werne et al., 2002). Laminae are not readily observable in this study's field site.

The composition of the Marcellus mudrocks range in calcareous content from less than 10% and up to 50% $CaCO_3$, with some disparity in coloration from black to gray (Werne et al.,

2002). Black shales of the Union Springs member contain C_{org} values ranging from 4-16% (Werne et al., 2002). Depending on the site where the Oatka Creek member is under inspection, C_{org} content typically ranges from 1-4%, with some outliers reaching as much as 7.5% (Werne et al., 2002). The presence of styliolinids is not prevalent in the Oatka Creek although this pelagic organism appears to have hit an abundance peak sometime during the deposition of the Union Springs (Werne et al., 2002). The limestone member of the Marcellus formation is classified as having greater than 70% $CaCO_3$ (Werne et al., 2002). The Cherry Valley limestone ranges from medium to light gray in color and shows ample bioturbation and occurrence of fossils; its texture ranges from wackestone to packstone to grainstone (Werne et al., 2002).

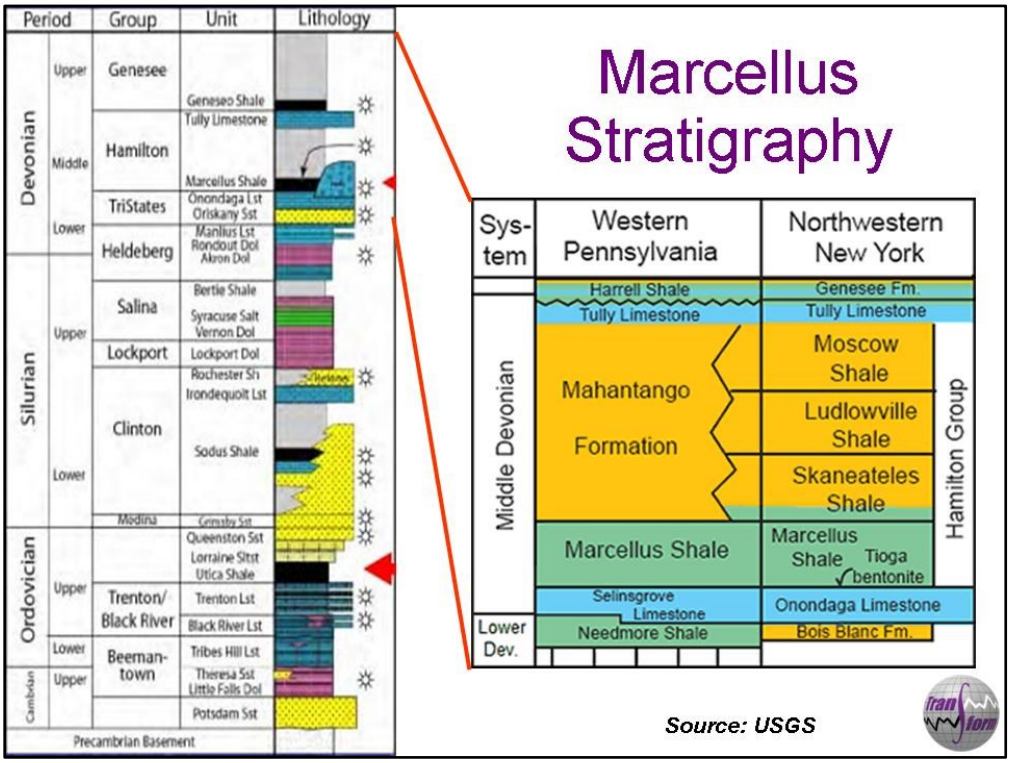

Figure 1.3: Stratigraphic column including the Marcellus shale (Transform and USGS).

Overall, the Marcellus is not considered a particularly level, blanketing formation; rather, its depth varies across its extent. Around one mile below the surface, the depth of the formation dips dramatically around southwestern Pennsylvania due to proximity with the Appalachian Mountains and their associated tectonic deformation with folding and faulting, before rising back to shallower depths approaching eastern Ohio (Energy Information Administration, 2010). Areas with related shallowing in depth of this formation are particularly fortunate as this is beneficial for drilling operations and improves the potential to recover petroleum as it is more likely that the rock has not been subjected to such great temperatures and pressures that would leave the reservoir barren of hydrocarbons due to thermal overmaturation (Energy Information Administration, 2010).

The paleogeography and large-scale tectonic activity of the Devonian were likely important controls on the accumulation of this formation, although these factors have led to widely varying conclusions as to the extent of their influence and have led to questioning if other variables were at work. The central Appalachian Basin that the Marcellus formation occupies was stationed around the southern subtropics (15-30°S) during deposition of the Oatka Creek in the Middle Devonian (Werne et al., 2002). Although the basin may have been in the path of easterly trade winds laden with moisture, it is likely that the Acadian Orogen produced a rain shadow, resulting in an arid to semi-arid environment that was susceptible to intense storm events (Werne et al., 2002). Some researchers have interpreted three, possibly four, phases of southward migrating deformation in the Acadian Orogen that involved cyclic subsidence in the foreland basin with subsequent infilling of sediments as the uplifted mountains were eroded (Werne et al., 2002). Each phase featured anoxic conditions and the presence of a pycnocline under which were deposited shallow water carbonate rocks overlain by transgressive black shales

(Werne et al., 2002). The shales were then overlain by more clastic-rich lithologies ranging from sandstone in proximal locations and gray mudrocks in more distant areas, which were themselves overlain by more carbonates (Werne et al., 2002). Such characteristics are present in the Oatka Creek, according to these studies. However, debate has arisen over the fact that there is no direct observational evidence on hand that confirms the presence of a nearly permanent pycnocline, although assumptions of water stratification have persisted throughout the literature as a dominant interpretation of the Devonian in the northeastern American continent (Werne et al., 2002). Additionally, some have speculated that the Oatka Creek was not formed due to the subsidence involved in the Acadian Orogen, but that eustatic sea level rise played a role in accommodating the Oatka Creek (Werne et al., 2002).

This research will encompass several geochemical analyses in order to discern the paleoenvironment conditions that made deposition of black shale favorable in the Marcellus formation. In particular, this study will propose an explanation for why the upper Oatka Creek shale is purportedly less rich in organic matter than the lower Union Springs shale to test whether this difference is a result of differences in oxygen deficiency, preservation capability, changes in the basin's maturity, or some yet to be determined factor(s).

1.2 Goals and Objectives

The outcome of this research is intended to refine our understanding of which favorable combination of environmental characteristics must be present to allow for black shale deposition. To answer such a large-scale question, a wide array of parameters will be tested and compared for correlation. The deposition and preservation of organic matter is influenced by multiple variables such as: sedimentation rate, anoxia, biota richness, paleoclimate, continental

configuration, and depth of the water column. With so many factors to account for, it is clear that a robust methodology is needed in this analysis.

For this analysis, I present the following objectives:

1. Understand the environmental conditions expressed by the relationships between the abundances of carbon, sulfur, and iron.

Carbon Analysis:

At the foundation of this project is the intent to explain the mechanism behind why it can be observed that a disparity in organic matter richness exists between the two black shale members of the Marcellus formation, with the Oatka Creek being less organic-rich than the Union Springs.

Carbon provides information on the level of primary productivity in the environment at the time sediments accumulated. The stable isotope signature for carbon, $\delta^{13}C$, expresses the ratio between ^{13}C:^{12}C. This signature can be affected by several variables such as clathrate release, organic burial, and primary productivity (Selley & Sonnenberg, 2015). Thus, it is common to see cyclic reversals in this signature with the changing of the seasons. As biochemical reactions in photosynthesizing organisms fractionate for lighter ^{12}C for metabolic purposes, it is expected that a rise in $\delta^{13}C$ will follow as productivity picks up and more ^{12}C is being utilized by plants and more is being buried in sediments (O'Leary, 1988). Reversals in this trend occur when less CO_2 is being withdrawn from the atmosphere by plants, meaning that more ^{12}C is available (O'Leary, 1988).

Thus, when $\delta^{13}C$ values are high, it reflects greater activity and proliferation of photosynthesizers, which in turn allows for greater potential of higher-level taxa to be present in the environment. Decreasing values would indicate that organic carbon is being released into the

oceans and atmosphere and may be indicative of times of enhanced preservation, which would favor black shale deposition.

These carbon isotopes may also be useful in distinguishing the source of the organic content, whether it is of terrigenous, marine, or mixed composition. The source expressed by these $\delta^{13}C$ values must be carefully interpreted as they may be influenced by the preservational quality affected by the activity of living organisms and temperature variation (Wignall, 1994).

However, enhanced primary productivity leading to greater supplies of organic matter is not the only purported cause for black shale formation. Preservation of organic matter is also a significant factor and the efficiency of this is dependent on oxygen levels in the environment (Wignall, 1994). Interestingly, despite the common misconception that high productivity and preservation is necessary to allow for black shale formation, these two variables are rarely found in combination within the same closed basin (Wignall, 1994). This is often because the preservation model would require stratification of the water column which would produce a pycnocline restricting the upward advection of nutrients (Wignall, 1994) (Figure 1.4). While this would create the desired anoxic bottom waters to improve preservation, this would adversely affect productivity (or at the very least not enhance it) as nutrients from lower depths could not be recycled upward to the surface due to density layering within the water column (Wignall, 1994). Thus, productivity models rely on more vigorous circulation than what would be assumed for the preservation model of black shale formation. Still, it should be noted that some productivity is essential in the preservation model as this produces the decaying organic matter that eventually passes down through the water column and consumes oxygen (Wignall, 1994).

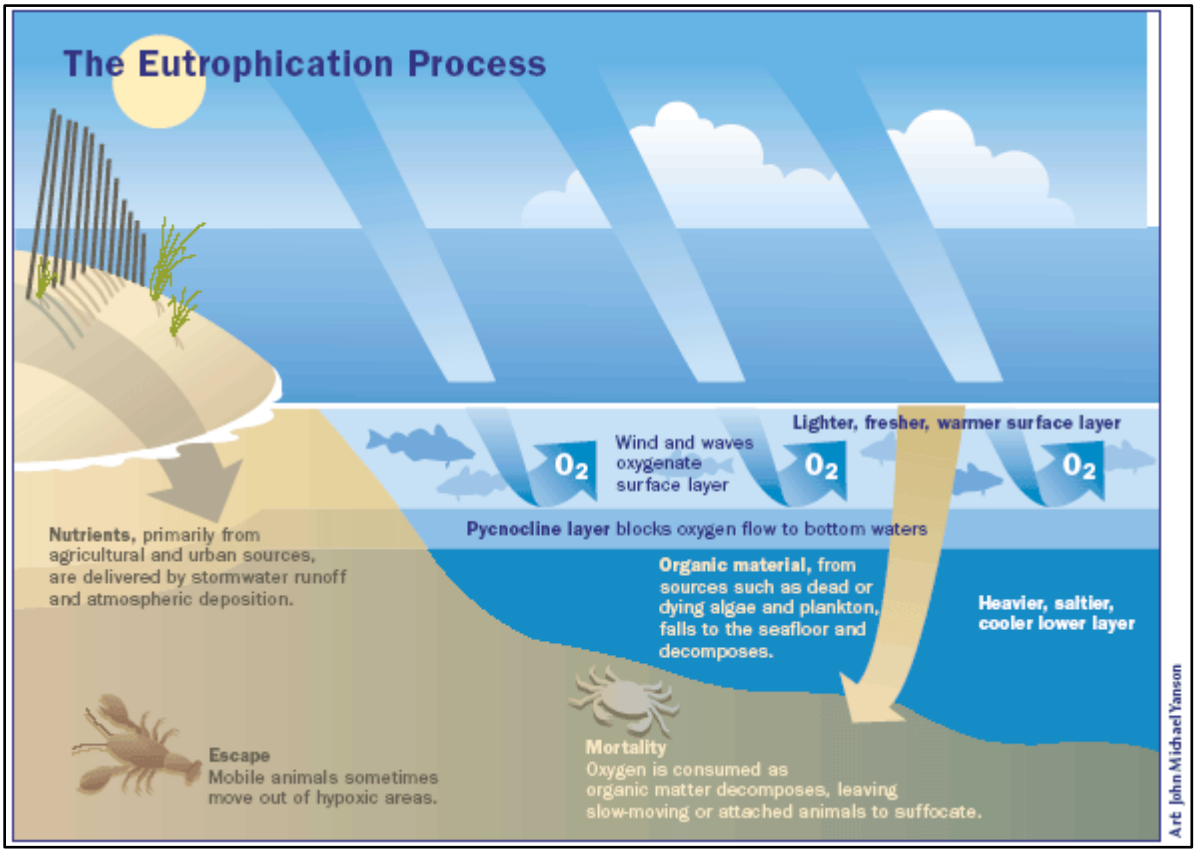

Figure 1.4: Effects of a pycnocline in a modern marine environment (Pew Trusts, 2003).

In order to assess the preservational differences between the Union Springs and Oatka Creek of the Marcellus formation, it is necessary to designate each as either oxic, dysoxic, anoxic, or euxinic (note that euxinia is like anoxia but with the addition of free hydrogen sulfide in the water column). Except for the oxic zone, all sediments pass through the same stages of diagenesis beneath oxygenated to anoxic/euxinic waters. Under anoxic waters, most organic matter is degraded within the sulfate reduction zone which leads to the creation of hydrogen sulfide as a byproduct of the anaerobic bacteria decomposing the organic material (Wignall, 1994). Organic matter is oxidized to a lesser extent in this zone under anoxic conditions which could be due to several reasons: the activity of sulfate-reducing bacteria may be hindered as they

rely on organic acids supplied by heterotrophic bacteria in the oxic zone, bacterial lipids may preferentially survive under anoxic conditions, or the sulfate-reducing bacteria may be inhibited by their own poisonous byproduct (H_2S) (Wignall, 1994). While H_2S is typically removed from solution by reacting with available iron to form pyrite, this reaction largely depends on the amount of available iron (Wignall, 1994). Compared to anoxic settings which should reveal well-preserved pyrite (including microscopic framboids) in shale samples, oxic settings will reveal no pyrite as sedimentary iron sulfides are re-oxidized at the redox boundary (Wignall, 1994). Dysoxic settings involve the continuous oxidation and re-precipitation of pyrite (Wignall, 1994). Thus, pyrite may only escape this cycle if it forms within voids like the internal chambers of ammonites (Wignall, 1994), or in particular microenvironments such as within a concretion in which a microbial film forms around decaying organic matter (Feldmann et el., 2012). Otherwise, pyrite may be found in sediments as H_2S is generated (Wignall, 1994).

In addition to bacteria in the sulfate reduction zone not being as efficient at breaking down organic matter under anoxic conditions compared to their aerobic counterparts in oxic settings, preservation is further enhanced by the presence of anoxia due to its limitations on the fauna capable of surviving in such environments. By preventing benthic organisms or infaunal burrowers, particularly macrofauna types, from colonizing on the sediment-water interface or at a shallow depth below it, preservation can be better assured as bioturbation tends to be destructive to sedimentary structures like laminations and, more importantly, to organic matter. By tunneling through the sediments, these organisms prevent alkalinity from building up in the pore waters and their activity allows for the oxidation of sulfates (Wignall, 1994). Bacterial respiration has the consequence of lowering the pH of the water as organic matter is destroyed,

thereby leading to the dissolution of carbonate fossils and removal of organic carbon (Wignall, 1994).

Burial rates may play some part in enhancing organic matter preservation under anoxic conditions as well. The presence of stratification in anoxic basins causes sedimentation rates to be slow, with most deposition occurring in distinct events involving a detached turbid layer which produces a suspended layer of well-sorted, fine sediments that settle through the water column in a blanket-like distribution (Wignall, 1994). Typically, black shales are found as condensed units located within basin centers, thickening around the shallower margin of the basin (Wignall, 1994). This type of slow sedimentation rate and particular mechanism can be assumed for many black shale deposits, although not all. Canfield (1993) conducted a study on the burial efficiency (taken to be the greatest direct measure of preservation) for a range of oxic, dysoxic, and euxinic environments, concluding that while high sedimentation rates in oxic conditions favor organic carbon accumulation, slow sedimentation rates in dysoxic to anoxic settings lead to much greater preservation (Wignall, 1994). This latter observation is again related back to the absence or extreme reduction in the occurrence of bioturbation in oxygen-restricted environments. Organic carbon has a longer residence time at the sediment surface where most oxidation occurs when bioturbation is present (Wignall, 1994).

In order to separate inorganic carbon from solid shale samples so that organic carbon content can be measured against total carbon, a method using acid fumigation will be administered to all samples to remove carbonates. This requires that the samples are thoroughly crushed with first mortar and pestle and then a five minute stint in a ball mill to achieve a very fine powder. Powder from each sample will be portioned into its own slot within a well tray that is placed within a desiccator cabinet (sans desiccant) along with an exposed beaker three quarters

full of bulk hydrochloric acid (12.1 N). The entire desiccator cabinet will be placed within an Isotemp furnace at 60°C for twenty-four hours. Exposure to HCl vapor over an extended period of time leads to any inorganic carbon in the samples being released as CO_2. This method has the advantage over other acid treatment techniques that involve washing the samples in highly concentrated acid, in that water soluble carbon will not be lost from the samples (Harris, Horwáth, & van Kessel, 2001). After baking in the furnace, the sample tray will be removed from the desiccator cabinet and samples will be weighed to fall in a target range between five and seven milligrams. These weighed samples will be balled up in tin capsules in preparation for combustion analysis using an Elemental Analyzer.

Sulfur Analysis:

The abundance of sulfur in black shale is due to the activity of sulfate-reducing bacteria during diagenesis as organic matter is broken down. At this stage, anaerobic bacteria utilize sulfate as the major oxidant and they are typically active below the sediment-water interface or in anoxic bottom waters. Their activity will lead to the production of hydrogen sulfide (H_2S) in the pore waters and anoxic bottom waters, leading to a decrease in pH. This production is typically unlimited, and while a significant portion of H_2S may be oxidized at the redox boundary, some will be fixed with iron. The formation of iron sulfides will initially go through unstable early forms such as mackinawite and greigite, but can eventually stabilize as framboidal pyrite (Wignall, 1994). The formation of pyrite and the other iron sulfides depends on the destruction of organic matter and is therefore limited by its availability as well as that of iron.

The sulfur isotopes within the pyrite are mediated in a manner similar to how the light carbon isotopes are selected for by photosynthesizers. Bacteria preferentially incorporate the lighter sulfur isotope (^{32}S) during reduction (Wignall, 1994). The lighter isotopes can also be

found in proximity to the redox boundary as they are produced from the repeated oxidation and recrystallization of iron sulfides (Wignall, 1994). In an environment free from the threat of bioturbation disturbing accumulated sediments in either anoxic/euxinic or dysoxic bottom waters, pyrite formation is likely to incorporate progressively more of the heavier sulfur isotope (^{34}S) in this relatively closed system at the sulfate reduction zone (Wignall, 1994).

Free hydrogen sulfide is present in the water column in euxinic environments (this is what differentiates it from anoxic conditions). Iron sulfides form in the water column and settle out of it if iron is available to react with the sulfur in the H_2S bacterial byproduct. The presence of iron sulfides will help verify that the shale was deposited in an environment severely lacking or completely absent of oxygen – to what extent the paleoenvironment was oxygen-deficient will be determined through degree of pyritization (DOP) analysis in which reactive iron concentrations are taken into account.

Iron Analysis:

Iron is derived from detrital iron minerals in the environment. Its presence attributes a darker coloration to black shales, along with other possible factors including thermal maturity (Wignall, 1994). Iron sulfides will form under anoxic or euxinic conditions, with the amount of available iron typically being the limiting factor in pyrite formation. Thus, analyzing the shale samples for pyrite will determine the level of oxygen deficiency at the time of deposition as the clear presence of pyrite framboids would indicate anoxic to euxinic conditions compared to dysoxic conditions which may show some pyrite in the sediments, and oxic conditions which would completely lack any pyrite. This severe disparity in pyrite formation under oxic or anoxic conditions is related to the affinity with which iron has to bond with either oxygen or sulfur.

With a preference for oxygen, iron will form iron oxides rather than iron sulfides provided conditions are oxic.

Degree of Pyritization:

Degree of pyritization (DOP) is the measurement taken as the ratio between reactive iron and nonreactive iron. Using DOP value ranges already established by Raiswell, Buckley, Berner, & Anderson (1988), the depositional environment of the Marcellus formation can be categorized as either oxic, dysoxic, or anoxic/euxinic. If all reactive iron is used up in the formation of pyrite, the environment is interpreted to be at least anoxic if not euxinic, and will be assigned a DOP value exceeding 0.75. If the black shale samples contain significant quantities of pyrite, euxinia would be the likely condition at the time of deposition. The DOP index can also readily lend itself to useful comparisons with biofacies, being applied to a similar scheme of either aerobic, restricted, or inhospitable as pyrite formation can be correlated with oxygen levels.

$$\text{DOP} = \frac{\text{pyritic Fe}}{\text{pyritic Fe} + \text{acid soluble Fe}}$$

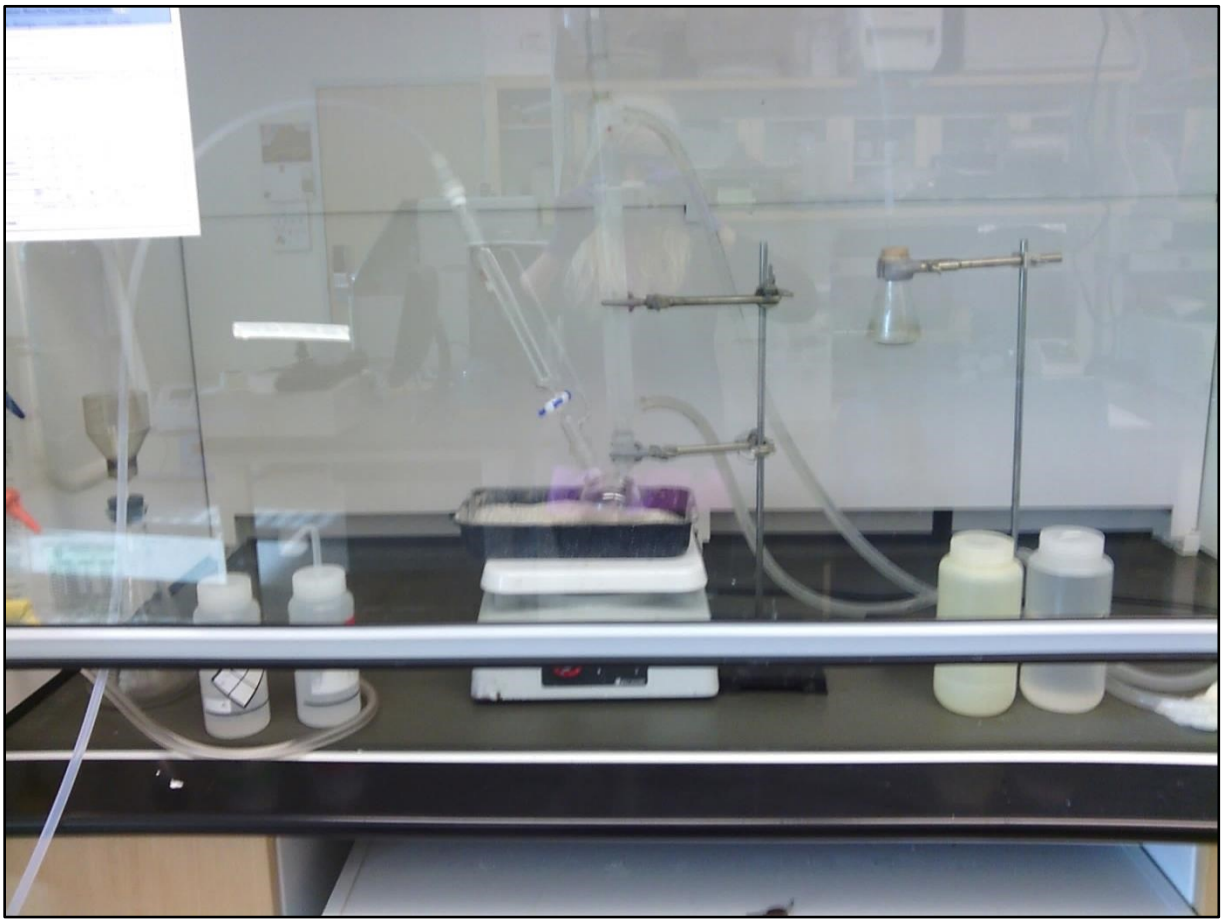

Figure 1.5: Experimental set-up for obtaining sulfur abundance from samples.

DOP analysis will require both sulfur and iron measurements which will involve a multi-step procedure to first obtain the abundance of pyritic sulfur from each sample (which is calculated from the final product of Ag_2S) as outlined in the method from Sullivan, Bush, & McConchie (2000) (see Figure 1.5 for basic laboratory set-up). From this, the sulfur concentration of the entire sample/rock will be calculated as a percentage. With the percentage of sulfur measured, the amount of pyritic iron will be calculated, keeping in mind that more sulfur than iron is needed to complete the chemical formula for pyrite, FeS_2. In order to complete the DOP calculations, the fraction of iron that had the potential to react with the dissolved sulfate to produce pyrite but did not do so, must be measured. This iron is termed the reactive iron, or the

HCl-extractable iron (Leventhal & Taylor, 1990). This percentage can be experimentally obtained by boiling approximately 0.1 g of sample with 5 mL of concentrated HCl in a test tube for one minute, and then rapidly quenching the solution and sample with distilled water to dilute the solution (Raiswell et al., 1988). The sample will then be transferred to a volumetric flask and allowed to stand so that the particulates can settle and the solute portion becomes distinct to the point that it can be extracted and quantified using ICP-OES (Raiswell et al., 1988). To capture total iron content, containing not only the pyritic and reactive iron abundances mentioned above, but also other iron phases of no interest for measuring DOP, samples must be homogenized in the ball mill into a finely ground powder before completing loss on ignition to remove volatiles. Afterward, each sample can be transformed into a glass bead using the LeNeo Fluxer. Once the sample has been prepped into glass bead form, it will be analyzed using XRF to obtain the percentage of total iron in the sample.

DOP calculations for each of the shale samples will aid in determining if there was a significant difference in the amount of iron or sulfur available at the time of black shale deposition that would have ultimately influenced the formation of pyrite. This can then be used to distinguish if there were differences in oxygen levels, or if some other factor was the cause for the disparity in organic matter richness. It should be noted that the DOP technique is best suited for samples of Devonian age or younger (Raiswell et al., 1988). Any sediments prior to this time period are affected by the lack of terrestrial plant matter and show greater sulfur fixation in the form of pyrite per unit of buried carbon compared to Devonian and post-Devonian sediments (Raiswell et al., 1988).

Preservation Analysis:

In total, these analyses will act as multiple parameters for the verification of the oxygen level in the paleoenvironment at the time of deposition for each of the black shales, with oxygen level correlating to the ability for preservation.

For preliminary working hypotheses, it will be useful to distinguish the potential for either of the following scenarios to explain why there is a discrepancy in the organic matter richness of two black shale members within the same formation:

Hypothesis 1 (syn-depositional oxygen changes): Both black shale members experienced different oxygen levels at their respective times of deposition. If this hypothesis is correct, the Union Springs member formed under either total anoxia or possibly euxinia while the Oatka Creek member formed under higher oxygen levels. This may have taken the form of dysoxic conditions or more complex, fluctuating conditions such as oxic/dysoxic or dysoxic/anoxic.

Hypothesis 2 (post-depositional changes due to iron availability): Both black shale members were deposited under the same oxygen conditions (anoxic or euxinic), but the amount of iron available to react with sulfur to form framboidal pyrite from the anaerobically-produced H_2S was limited in the Oatka Creek relative to the Union Springs. A sufficient amount of H_2S remained unreduced in the Oatka Creek, thereby reducing the amount of organic matter.

Hypothesis 3 (syn-depositional productivity changes): The initial amount of organic carbon present at the time of deposition was significantly different between the two black shale members due to differences in the overlying production or export production, with more organic matter delivered to the Union Springs than the Oatka Creek. However, this hypothesis is problematic and cannot be robustly addressed in the analyses proposed for evaluation of the oxygen levels which is the primary focus of this study. It is suggested that measurement of the

productivity during deposition of the Marcellus formation should be more thoroughly explored in future works.

To facilitate this analysis, it will be essential to have measurements for the degree of pyritization and knowledge of the presence of any fauna (and what type) in both members. Below, Table 1 summarizes the hypotheses that will be tested in this research as well as their expected responses.

Summary of Hypotheses

Hypothesis	Expected Response If Rejected	Expected Response If Failed to Reject
syn-depositional oxygen changes	DOP values will classify the two black shale members in the same oxygen level category.	DOP values for the two black shale members will be vastly different, placing the Union Springs in an anoxic/euxinic classification and the Oatka Creek will be categorized as less oxygen deficient.
post-depositional changes due to iron availability	Very similar amounts of available iron were present during deposition of the two black shale members.	Different amounts of available iron were present during deposition of the two black shale members.

Table 1: Summary of hypotheses tested to explain the differences in organic richness between the Union Springs and Oatka Creek.

2. Create a model for the accumulation and source of organic material in the paleoenvironment and see if a previously developed model can be applied, as well as if it can be discerned in which stage of maturity the basin was in.

Basin Model:

Three basic models have been proposed to explain the environments in which black shales are capable of being deposited. These include 1) the restricted circulation model, 2) the open ocean model, and 3) the continental shelf model. Tentatively, this project is operating on

the restricted circulation model, the most famous modern representative of which is the Black Sea. This is the type euxinic model, possessing enhanced preservation as the result of little to no circulation and low to moderate productivity that allows organic matter to accumulate. Oxygen depletion during the decay of organic matter is largely believed to be the result of the limitations on physical oxygen delivery rather than changes in organic carbon supply by variable export production (Tourtelot, 1979). The organic material eventually passes through the water column to settle on the sediment floor where it can only be destroyed by anaerobic bacteria which produce H_2S that diffuses into the overlying water (Tourtelot, 1979).

Wilson Cycle Stage:

It is worth examining the evolution of the basin in which the Marcellus formation was deposited to determine if it underwent dramatic changes in maturity between the time the Union Springs was deposited and the time the Oatka Creek was deposited. The maturity of a basin results from plate tectonic activity, thus any favorable conditions for organic matter preservation that may have existed locally within the basin during the time the Oatka Creek was deposited, may have been overridden by such large-scale factors. Of course, tectonic plate movement is not the only large-scale influencer of basin evolution as sea level and ocean circulation and, therefore, climate may affect deposition as well (Trabucho-Alexandre, Hay, & De Boer, 2012).

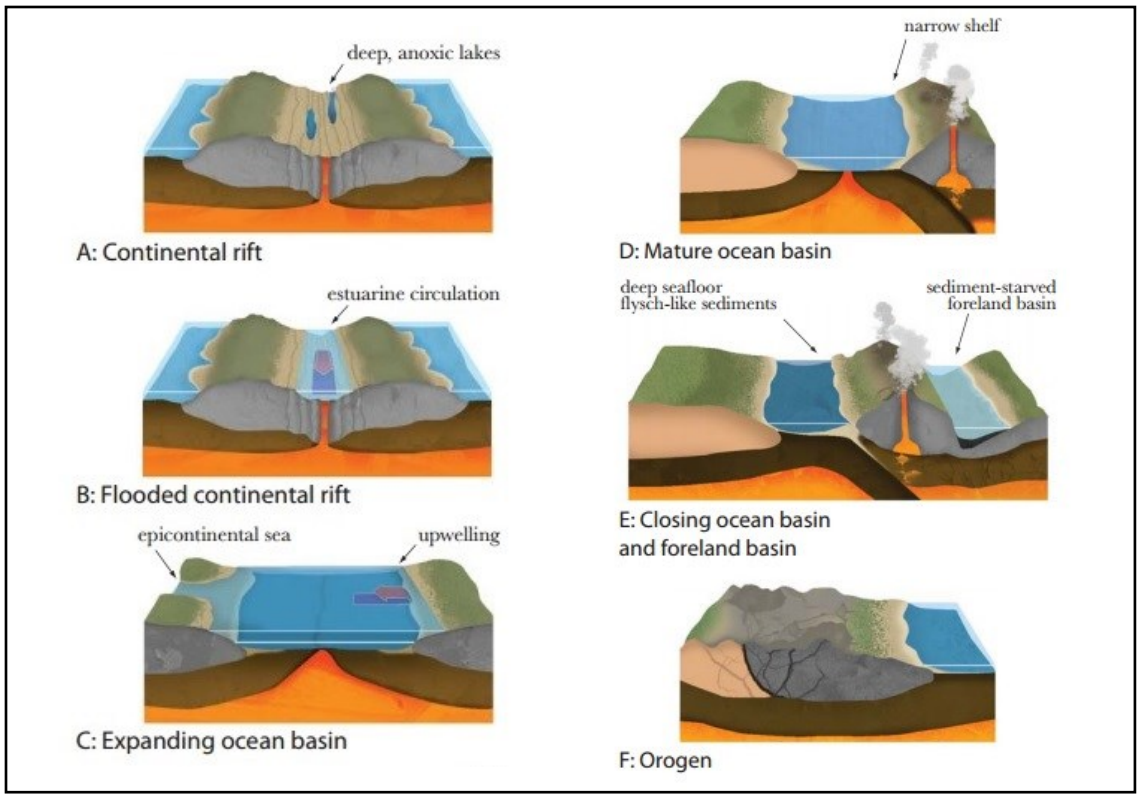

Figure 1.6: Stages of the Wilson Cycle (Trabucho-Alexandre et al., 2012).

Still, if it can be determined that the Oatka Creek was deposited at a later stage in the basin's development than the Union Springs, this may be worked into the overall explanation for why there is a difference in the composition of the two shale members. The beginning of the end of a basin is marked by the convergence of one plate subducting beneath another, thus reducing deposition in mature basins as they begin to close up. It could be that the Oatka Creek was deposited around the onset of this closing event during which deposition would have been discouraged due to increasing depth to the seafloor and the narrowing of the basin margins reducing potential for sediment accumulation. Additionally, these narrowing shelves would have the effect of increasing tidal energy dissipation, allowing for greater vertical mixing that may not have been present under formerly stratified waters (this would make it more difficult for organic-enriched sediments to accumulate) (Trabucho-Alexandre et al., 2012). In comparison, the Union

Springs may have accumulated while the basin was fairly young and still spreading; if the source of the organic matter can be traced, it may be possible to more accurately define the stage of maturity at the time of deposition. This is due to the fact that a young basin that is expanding, but still mostly landlocked, is acquiring most of its sediments from terrestrial origins, whereas a slightly later stage in which the basin is more open ocean-like, receives sources from pelagic algae (Trabucho-Alexandre et al., 2012). Therefore, once oxygen levels have been established for each black shale member, any discrepancies between the two in terms of organic matter preservation, should they exist, could potentially be explained by deposition during different stages in the Wilson Cycle (Figure 1.6) or differences in productivity.

1.3 Field Site and Proposed Sample Collection

The area of study is located in the Seneca Falls Quarry of Seneca County, New York, operated by an aggregate supplier primarily servicing the Finger Lakes Region (Seneca Stone Corporation) (Figure 1.7). The quarry, still active, provides easy access and many fresh exposures from which to collect without much concern over the potential for chemical weathering causing post-depositional alterations (Figure 1.8). The site offers access to all three members of the Marcellus formation, and this particular area of the formation has not endured hydraulic fracturing.

Figure 1.7: Location of field site (Sperling's Best Places).

Sample collection for the proposed project will begin in spring of 2017, requiring several days spent at the Seneca Stone Quarry in New York to obtain hand samples and to construct a complete stratigraphic column through all three members of the Marcellus formation. The perimeter of the quarry provides many freshly exposed outcrops from which collection will start at the base of the total formation (in the lowermost Union Springs member) and proceed to the top of the uppermost member, the Oatka Creek. Hand samples can easily be taken with a rock hammer and minimal effort, after which they will be sealed in individual Ziploc bags and marked on the outside of the bag according to the vertical profile they were sampled from and at which depth in the formation.

Figure 1.8: Image of the active quarry site (Seneca Stone Corporation).

1.4 Planned Work

I propose to collect samples from the black shale and interbedded limestone members of the Marcellus formation to have a complete vertical profile taken in 10 cm increments for better agreement and a comprehensive view of the geochemistry of the formation. Using elemental combustion analysis, degrees of pyritization, and elemental ratios that indicate redox conditions at the time sediments accumulated, I will create a model to explain the environmental conditions in the depositional basin and identify the source of the organic matter.

This work will be conducted within a time frame of two years to satisfy requirements for a Master's degree under the mentorship of Dr. Jeremy Williams.

1.5 Proposed Timeline

Time	Description
Year 1 – Semester 1 (Fall 2016)	• **Preparing lab room with supplies and setting up new instruments** • **Training on instrumentation: EA, XRF, LeNeo Fluxer, XRF** • **Readings: *Black Shales*; *Marine Black Shales*; *Mass Extinctions and Their Aftermath*** • **Applying for grants**
Year 1 – Semester 2 (Spring 2017)	• **Training at University of Massachusetts Boston for DOP**

	analysis • **Sample collection at Seneca Stone Quarry** • **Sample prep and running samples on instruments (EA, XRF, and DOP analysis; may run carbon isotopes at The Ohio State University)**
Year 1 – Summer 2017	• **Finish running samples**
Year 2 – Semester 3 (Fall 2017)	• **Analysis of sample results** • **Present at GSA in Seattle, Washington** • **Thesis writing**
Year 2 – Semester 4 (Spring 2018)	• **Thesis writing** • **Defend and submit thesis** • **Graduate from KSU**

Table 2: The proposed timeline for the completion of my M.S. degree.

Chapter 2: Discrepancy of Organic Richness within the Oatka Creek and Union Springs of the Marcellus Formation

2.1 Introduction

2.1.1 The Black Shale Controversy

While little debate surrounds what constitutes as a black shale, the same cannot be said as to the mechanisms that control black shale deposition. After Davidson and Lakin (1961) proposed that the United States might be ripe with both widespread and valuable metal-enriched black shales, enthusiasm took off in the search for commercially viable deposits laden with mobile trace elements such as copper, molybdenum, nickel, silver, and zinc, to name a few (Vine & Tourtelot, 1970). The search has continued into the present for these metal deposits as well as hydrocarbon source rocks, yet which conditions allow for the formation of these marine-deposited, organic-rich mudrocks remains unresolved.

The model of the black shale depositional basin itself is under scrutiny as to which provides the most suitable conditions for organic matter to accumulate. While oxygen-deficient levels ranging from anoxia to euxinia are typically agreed upon as a conventional condition as evidenced by the presence of pyrite in many black shales, the degree to which the basin is restricted from ocean circulation is contested (Arthur & Sageman, 1994). Various models have been constructed simulating completely enclosed, or landlocked, basins (restricted circulation model) as opposed to those that are only partly restricted (continental shelf model) or even completely open to the rest of the sea (open ocean model) (Tourtelot, 1979).

In this way, the particular Wilson Cycle stage for a given basin may shed some understanding as to how much potential the basin had for forming black shale. If a modern analogue type euxinic basin was to be named, many would consider the Black Sea to be the standard to which all others can be compared, and it can be used as a starting point for interpretations of ancient black shale environments (Arthur & Sageman, 1994).

The physical boundaries of a black shale basin are not where the argument ends. At the heart of much of the conflict are two controls: preservation vs. productivity. The organic matter in a black shale is sourced from photosynthesizing marine phytoplankton as well as terrestrial detritus transported into the oceans via rivers. In the near surface waters where productivity is highest, marine organic content is largely dependent on nutrient availability (Arthur & Sageman, 1994). Of this organic matter, less than 20% survives falling through the water column without being consumed or oxidized in the photic zone (Arthur & Sageman, 1994 and references therein). After escaping the first 100 m of the water column, an additional 75-85% of the organic matter is destroyed within the upper 500-1,000 m, and only 3-5% makes it past 1,000 m (Arthur & Sageman, 1994 and references therein). Of the organic matter that settles on the seafloor, 90% is decomposed, primarily by aerobic organisms (Arthur & Sageman, 1994 and references therein). The fact that any organic matter survives at all to form the globally widespread black shales we know of is rather incredible! Due to the varying stages of destruction and loss of organic matter through the water column, primary productivity levels are difficult to measure with certainty, but are typically reflected by burial rates (Arthur & Sageman, 1994 and references therein). While accurately measuring primary productivity can be difficult, it is intuitive that a greater supply of organic matter to begin with offers a greater chance for a portion of that

material to be buried on the sediment floor, having successfully avoided consumption and/or oxidation in what can be termed “organic overloading” (Wignall, 1994).

One possible explanation for the enhanced preservation observed in the Middle to Late Devonian involves the rapid diversification of terrestrial plants into various climates, ecological niches, and sizes (Algeo, Berner, Maynard, & Scheckler, 1995). It has been proposed that as plants began to adapt to drier, upland environments, terrestrial chemical weathering increased (Algeo et al., 1995,). This had a significant effect on marine environments as they were supplied with a greater influx of land-derived nutrients. Consequently, enhanced productivity would have occurred near the surface, driving a higher demand for oxygen at the sediment-water interface, ultimately leading to anoxia that would have aided in organic matter preservation (Algeo et al., 1995).

In terms of preservation, a common theme in all black shale models includes depleted, and oftentimes completely absent oxygen levels in bottom waters. Early studies revolving around black shale formation recognized that anoxia greatly reduced decomposition, permitting organic matter to accumulate – especially that which was lipid-derived, as these organic components seem more apt at resisting decay as opposed to proteins and carbohydrates (Wignall, 1994; Selley & Sonnenberg, 2015). The modern Black Sea is recognized as possessing anoxic bottom waters, thus providing an enclosed basin model as the analogue for comparison to ancient black shales (Wignall, 1994). The initial assumption that degradation rates between aerobic and anaerobic bacteria greatly differ has been contested since about 1970 (Wignall, 1994). Empirical evidence collected by Foree and McCarty (1970) suggested that reduction rates between the two bacteria types were not appreciable; however, they found that there is a notable drop in the efficiency of sulfate-reducing bacteria under low temperature or hypersaline conditions (Wignall,

1994). High salinity is noted in the Black Sea, thus strengthening the argument that depleted oxygen and thereby less effective bacteria make it suitable for high preservation potential and eventual black shale formation (Stewart, Kassakian, Krynytzky, DiJulio, & Murray, 2007).

Despite the effective reasoning for why either factor can amplify the amount of organic material deposited, the question remains: Does preservation potential or high primary productivity lead to the accumulation of organic-rich sediments that form black shales? Does one factor clearly exert greater influence? Enhanced preservation may result from water column stratification and particular chemical conditions near the sediment floor that allow for anaerobic respiration and less efficient breakdown of organic matter (Wignall, 1994). High primary productivity may be caused by the upwelling of deep ocean nutrients and could lead to a higher abundance of organic matter surviving the descent to the sediment floor in a scenario where burial rates outpace oxidation (Arthur & Sageman, 1994).

The two black shale members of the Marcellus have the potential to improve our understanding of the paleoenvironment and oxygen conditions that contribute to black shale formation. In this study, the paleoenvironment conditions at the time of deposition, specifically, the oxygen levels which would have influenced the decay or preservation of organic matter are evaluated for the Marcellus black shales.

The Marcellus formation is encompassed by the larger region of the Appalachian Basin (Lash & Engelder, 2011). Previous studies have attempted to create a model during this pivotal time in terrestrial plant evolution that explains the accumulation of marine organic matter while accounting for terrestrial input (Rimmer, Thompson, Goodnight, & Robl, 2004). Yet, my particular field site within the Marcellus formation has strangely not received much attention. This is odd given that this region of the formation offers favorable conditions for study such as:

1) fresh exposures of all Marcellus members, 2) little concern over alteration of geochemical signatures caused by hydraulic fracturing, and 3) a lack of complex fold and fault systems that are encountered in closer proximity to the Appalachian Mountains.

2.1.2 Previous Work in the Marcellus Formation

The Marcellus formation is Middle Devonian in age and consists of three members in stratigraphic order from oldest to youngest: Union Springs (black shale), Cherry Valley (limestone), and Oatka Creek (black shale). Despite commonly held opinions of basic black shale traits, the dark colored mudrocks of the Marcellus formation do not exhibit fine, even laminations throughout the entirety of the formation as might be expected. Rather, laminations are typically only present in the absence of bioturbation and when large particles such as calcareous bioclasts or organic matter formed distinctive laminae (Werne et al., 2002). Laminae or evidence of benthic fauna is not readily observable in the field at our chosen location for sample collection (Seneca Stone Corporation's quarry in Seneca Falls, NY).

The composition of the mudrocks range in calcareous content from less than 10% and up to 50% $CaCO_3$, with some disparity in coloration from black to gray (Werne et al., 2002). Black shales of the Union Springs member contain C_{org} values ranging from 4-16% (Werne et al., 2002). Depending on the site where the Oatka Creek member is under inspection, C_{org} content typically ranges from 1-4%, but can reach as much as 7.5% (Werne et al., 2002). Styliolinids are not prevalent in the Oatka Creek although this pelagic organism appears to have hit an abundance peak sometime during the deposition of the Union Springs (Werne et al., 2002). The limestone member of the Marcellus formation is classified as having greater than 70% $CaCO_3$ (Werne et al., 2002). The Cherry Valley limestone ranges from medium to light gray in color and shows ample bioturbation and occurrence of fossils; its texture ranges from wackestone to

packstone to grainstone (Werne et al., 2002).

Overall, the Marcellus is not considered a particularly level, blanketing formation. Rather, its depth varies across its extent. Around one mile below the surface, the depth of the formation dips dramatically around southwestern Pennsylvania, largely due to proximity with the Appalachian Mountains and their associated tectonic deformations (refer to Figure 1.1) (Energy Information Administration, 2010). The formation rises again to shallower depths approaching eastern Ohio (Energy Information Administration, 2010). Areas of shallower depth of this formation are particularly fortunate as this is beneficial for drilling operations and improves the potential to recover petroleum as it is more likely that the rock has not been subjected to such great temperatures and pressures that would leave the reservoir barren of hydrocarbons due to thermal overmaturation (Energy Information Administration, 2010).

The paleogeography and large-scale tectonic activity of the Devonian were likely important controls on the accumulation of this formation, although these factors have led to widely varying conclusions as to the extent of their influence and have led to questioning if other variables were at work. The central Appalachian Basin that the Marcellus formation occupies was stationed around the southern subtropics (15-30°S) during deposition of the Oatka Creek in the Middle Devonian (Werne et al., 2002). Although the basin may have been in the path of easterly trade winds laden with moisture, it is likely that the Acadian Orogen produced a rain shadow, resulting in an arid to semi-arid environment that was susceptible to intense storm events (Werne et al., 2002). Ettensohn (1985) and Ettensohn et al. (1988) have interpreted three, possibly four, phases of southward migrating deformation in the Acadian Orogen that involved cyclic subsidence in the foreland basin with subsequent infilling of sediments as the uplifted mountains were eroded (Werne et al., 2002). Each phase featured anoxic conditions and the

presence of a pycnocline under which shallow water carbonate rocks were deposited and overlain by transgressive black shales (Werne et al., 2002). The shales were then overlain by more clastic-rich lithologies ranging from sandstone in proximal locations and gray mudrocks in more distant areas, which were themselves overlain by more carbonates (Werne et al., 2002). Such characteristics are present in the Oatka Creek, according to these studies (Werne et al., 2002). However, debate has arisen over the fact that there is no direct observational evidence on hand that confirms the presence of a nearly permanent pycnocline, although assumptions of water stratification have persisted throughout the literature as a dominant interpretation of the Devonian in the northeastern American continent (Werne et al., 2002). Additionally, some have speculated that the Oatka Creek was not formed due to the subsidence involved in the Acadian Orogen, but that eustatic sea level rise played a role in accommodating its deposition (Werne et al., 2002).

This research will encompass several geochemical analyses in order to discern the paleoenvironment conditions that made deposition of black shales favorable in the Marcellus formation. In particular, this study will propose an explanation for why the upper Oatka Creek shale is less organic-rich than the lower Union Springs shale and if this is a result of differences in oxygen deficiency, preservation capability, changes in the basin's maturity, or some yet to be determined factor(s).

2.1.3 Broader Impacts

The Economic Value of the Marcellus Formation and Its Potential to Mitigate Rising Greenhouse Gas Emissions

The Marcellus formation is extensive, covering states such as West Virginia, Virginia, Maryland, Pennsylvania, New York, and Ohio. It is considered a valuable shale play area,

enriched in natural gas with the shale serving dual roles as source rock and reservoir. The United States possesses multiple shale plays across the country, a beneficial attribute that may lead to a decrease in dependence on costly foreign imports to meet our fuel needs. While the economic factor is significant, particularly when combined with horizontal drilling techniques to enhance recovery and make use of the many vertical fractures that exist throughout the formation, there is the additional factor of what this fuel source may mean for improving current anthropogenic effects on climate change.

Much is to be said about the promise of transitioning from coal to natural gas while renewable sources of energy are still gaining traction and undergoing further development to become an economically viable and widespread means of replacing current fossil fuel burning habits. Recent trends show an increase in reliance on natural gas over coal for generating electricity, demonstrating that the United States is capable of reducing its yearly greenhouse gas emissions by making this switch (Center for Climate and Energy Solutions, 2013). As of 2016, the transportation sector is the largest contributor of emissions in the U.S., making up nearly 28.5% of total emissions; electricity comes in as a close second at 28.4% (United States Environmental Protection Agency, 2018).

Natural gas, with its prime constituent being methane, offers at least a temporary solution to help improve emissions as its burning only contributes about half as much carbon dioxide per unit of energy as coal burning (Zielinski, 2014). Thus, if anthropogenic induced climate change is to be combatted, one of the initial steps will be to encourage the transition from coal to natural gas. The Marcellus formation has the fortuitous advantage of close proximity to some of the nation's most highly populated cities, making transportation and servicing of these areas easier (Energy Information Administration, 2010).

Depth zones where this formation is likely to be in the optimal oil and gas-generating window are probable targets for the petroleum industry aiming to employ horizontal drilling for extraction. More recently, horizontal drilling has received attention due to its potential for greater recovery of natural gas in productive shales in contrast to more conventional vertical drilling techniques. For the Marcellus in particular, it has been observed that the formation possesses vertical fractures running throughout it that can make horizontal drilling more cost-effective by simultaneously intersecting as many fractures as possible (Energy Information Administration, 2010; Lee, Herman, Elsworth, Kim, & Lee, 2011). In addition to horizontal drilling, hydraulic fracturing may be incorporated to enhance recovery.

It is possible that the geochemical analyses incorporated in this study to understand the depositional environment favorable for black shale creation, will also be instrumental in early identification of profitable natural gas reservoirs without the necessity of environmentally intrusive and expensive preliminary drilling.

Mass Extinctions and Tracking Climate Change with Black Shales

Black shales are a valuable asset in recording and reconstructing past mass extinction events as their globally widespread deposition is often timed around such events. It has been documented that certain mass extinctions are coeval with the presence of a large igneous province (LIP) which can often induce lethal environmental factors such as warming oceans and anoxia via carbon dioxide release and other greenhouse gas emissions (Bond & Wignall, 2014). Of the "Big 5" extinction events, four have been linked to the presence of a large igneous province and its associated large-scale volcanism, with the exception being the Ordovician-Silurian extinction (Bond & Wignall, 2014). While the influence of these eruptions may be

tempered or enhanced by the continental configuration, durability of existing biota, pre-existing climate, volume of the eruption, and a multitude of other factors, there is a strong correlation between volcanically induced marine warming and anoxia (Bond & Wignall, 2014). Anoxia is typically accompanied by a marine transgression in which these oxygen-deficient conditions may reach euxinic levels, invading continental shelves and poisoning these shallow water environments (Bond & Grasby, 2017). Widespread anoxia or euxinia may contribute to a decrease in access to fixed nitrogen, putting eutrophic organisms under stress (Bond & Grasby, 2017). This initial warming effect is subsequently followed by a cooling period in which photosynthesizers suffer after large volumes of sulfate aerosols are injected into the air during eruption and effectively produce a smog that blocks much needed sunlight (Bond & Wignall, 2014). Ultimately, this fatal disruption in the food chain can kickstart the accumulation of organic matter under anoxic marine conditions, providing the essential organic matter portion of a black shale's composition (Bond & Wignall, 2014). Thus, these LIPs and their associated volcanism may be the mechanism that propels globally widespread black shale deposition due to a biotic crisis.

By continuing to improve our interpretations of black shale formation, we can more realistically interpret mass extinction events and the geologic processes that were occurring at that time, and potentially look for those same conditions occurring in recent times in order to predict future mass extinctions.

Interpretation of Exceptionally Preserved Fossils

Since black shale deposition involves either oxygen-deficient or oxygen-free waters, valuable information about the paleoenvironment can be gleaned and interpreted. Considering

the lack of oxygen in many black shale-forming environments, it could be reasonably inferred that preservation potential would be high, and in fact, this can be observed in some of the exceptional fossils that come from black shale formations – for example, the famous Cambrian-aged Burgess Shale and its repository replete with soft-bodied imprints and tissues. High preservation potential may translate into an abundance of fossil material and/or highly complete and articulated specimens. If not for these environments and the black shales they form, there would be significantly less rare material preserved, such as soft parts, feathers, and chitin.

These deposits lead to some interesting interpretations of the lifestyles of these organisms that would presumably be unable to survive in the more toxic bottom waters where black shales form. Yet, their presence may indicate a specific stratification scheme in the water column and even more biodiversity than what may be originally expected from an oxygen-poor environment. Such assemblages may even lead to interpretations of a catastrophic kill event.

Productivity vs. Preservation

Ultimately, when it comes to determining the controlling factor of organic-rich sediments, two sides emerge: one that prefers organic matter input, and one that stresses more importance on organic matter preservation. The former contends that elevated primary productivity in the near surface waters is what leads to the high levels of organic matter available for preservation in the first place, while the latter claims that oxygen levels, specifically the presence of anoxia or euxinia, are what drive organic enrichment as organic carbon is less likely to mineralize in these conditions as opposed to oxic conditions (Tyson, 2005). While this research does not seek to take a stance on either side, the analyses used to evaluate the discrepancy in organic richness within the Marcellus are geared toward a more preservation-

oriented view. The methods employed aim to evaluate the abundance of organic content as it relates to oxygen levels – a key factor in determining the decomposition or preservation of organic matter. However, this study does not take the approach of attempting to suggest a plausible measurement for the amount of organic matter that existed in the environment prior to any kind of deposition and preservation. Establishing a paleoproductivity index is a difficult endeavor due to a lack of reliable biomarkers for very high or low productivity levels (Wignall, 1994).

In this on-going debate, either side paints an oversimplified picture when it comes to evaluating environmental controls on organic matter preservation. Likely, these are not the only factors that should be considered; for instance, dilution caused by other minerals in the sediment will affect organic carbon concentrations (Tyson, 2005) and sedimentation rate is often cited as a principle control (Wignall, 1994). Even more complicated is the likelihood that these controls are interrelated in the ways in which they affect organic matter content in black shales. Paradoxically, what would instinctively seem to be the most favorable combination of the two factors to produce accumulations of organic-rich sediments (high productivity coupled with enhanced preservation conditions) is simply not compatible based on actual stratification processes. In a high productivity model, a plentiful supply of nutrients is cycled into the environment either by upwelling or by the influx of terrestrial sediments (Wignall, 1994). Such conditions would generally be promoted by more robust water circulation rather than the calm stagnation ideal for anoxic bottom waters (Wignall, 1994). In contrast, a high preservation model is supported by water column stratification and reduced vertical advection so as to restrict nutrient-rich bottom waters from mixing with productive surface waters (Wignall, 1994). Likely, this restriction is caused by density stratification that maintains productivity at low to moderate

levels (Wignall, 1994). Yet, as Tyson (2005) eloquently digressed on the flawed thinking of this old productivity vs. preservation argument, "without production preservation is impossible, and without preservation production is irrelevant."

Clearly, no matter which side of the debate is taken, such research can lend itself to paleoclimate reconstruction, understanding current climate change, and planning for purposeful intervention in greenhouse gas emissions.

2.1.4 Outcomes of This Work

This study asks the question: Why is there a difference in the amount of organic matter preserved between two black shale members of the same formation, deposited in the same geologic time period? The answer was unexpected, yet perhaps it should have been anticipated when considering all the possible factors that can exert influence over preservation, and that sometimes only work in conjunction with one another in very precise combinations. To understand the history of a black shale environment is no easy task, and though conceptual models have been established to represent basin conditions favorable for organic matter accumulation, making comparisons between past and present environments is not straightforward for reasons such as climate change and continental reconfiguration, among others.

By measuring the concentrations of pyritic iron, acid soluble iron, pyritic sulfur, and total organic carbon (TOC) through degree of pyritization and combustion analysis, oxygen levels were assigned to each sample analyzed and an overall classification of each member was made as either oxic, dysoxic, or anoxic/euxinic. These oxygen levels were correlated with the abundance of organic matter present in the Union Springs and Oatka Creek black shales to determine if one member proved to have more favorable environmental conditions for black shale formation than the other.

2.2 Methods

2.2.1 Field Site and Sample Collection

The designated field site is located within an active quarry owned by the Seneca Stone Corporation operating out of Seneca Falls, New York (Figure 2.1). This company primarily services the Finger Lakes Region by supplying aggregate and is reasonable in granting permission for collection (Seneca Stone Corporation). Due to ongoing operations, this field site has the benefit of easy access to attain samples from fresh exposures that do not warrant concern over post-depositional alterations caused by chemical weathering. All three members of the Marcellus formation are present at various sections along the exposed perimeter of the quarry. This particular site was selected not only due to its easy access, but because this region of the Marcellus has not undergone hydraulic fracturing which would interfere with interpretations of chemical analyses.

Fieldwork consisted of a day trip to the quarry for sample collection. Samples were easily procured with a rock hammer and minimal effort, after which they were sealed in individually labeled Ziploc bags until sample preparation and analysis could commence. A total of 104 hand samples encompassing six stratigraphic profiles of the Union Springs were obtained in June 2017. Samples were taken from the base of the exposed member to the top of the exposure in increments of ten centimeters to ensure fine-scale resolution of any geochemical changes occurring throughout the formation, as well as within each member (Figure 2.2). This was done so that any marked chemical changes observed later in the laboratory could be classified as abrupt or episodic. Of the six columns collected, all were analyzed for their carbon content. Three columns were selected to measure iron and sulfur concentrations and are herein referred to

as Column RB (Union Springs 1), Column JD (Union Springs 2), and Column BD (Union Springs 3).

A previous expedition to the same quarry site conducted by The Ohio State University in the summer of 2014, supplied the Williams lab group with stratigraphic columns through the Cherry Valley limestone and Oatka Creek. Sampling methods were the same as those used in the 2017 collection trip. One column of the Oatka Creek totaling in 18 samples was used for comparative analysis; this column is herein referred to as Column D (Oatka Creek 1). A collaborative effort to pool samples from the two collection trips was necessary owing to the formation's variable levelness, even on such a localized scale. Exposures at the quarry that had once yielded access to all three members in a single stratigraphic column were no longer accessible by the 2017 expedition due to concerns for safety.

Figure 2.1: View of the Seneca Stone Quarry taken June 26, 2017, during sample collection (standing on limestone of the underlying Onondaga Formation; exposures of the Marcellus formation covered in vegetation can be seen in the background).

Figure 2.2: Collecting samples from the Union Springs.

2.2.2 Instrumentation and Analyses

Organic and Total Carbon

For the purpose of distinguishing between organic carbon and total carbon content in the black shales, samples were prepared for analysis on a Costech ECS 4010 Elemental Analyzer (EA) in the same manner, save for one critical step.

Regardless of final intent, all samples underwent powdering using a SPEX sample prep 8000M ball mill run at five minutes and five seconds per sample. For organic carbon analysis, powdered samples were transferred into a well tray that, in the presence of an uncovered 500 mL beaker filled approximately three quarters full of 12.1N hydrochloric acid (HCl), was placed inside a desiccator cabinet, sans desiccant. This set-up cooked inside an Isotemp Furnace adjusted to 60°C for twenty-four hours. By acid fumigating the samples using this procedure,

any inorganic carbon in the samples reacted with the HCl vapor and was released as carbon dioxide. After this baking period was completed, the well tray was covered with plastic wrap and stored in a desiccator cabinet until weighing. A duplicate set of samples was portioned into a separate well tray, but did not undergo acid fumigation for the purpose of capturing total carbon measurements.

Samples from each of the two sets were measured on a Sartorius microbalance for a target mass between 5 – 7 mg. These samples were collected in Costech 5x9 mm tin capsules and were carefully folded and balled up to ensure retention of the sample. Each set of samples was run on the EA which was periodically checked for precision and calibration using a series of blanks (empty tin capsules) to clean out the instrument and a series of checks (acetanilide) to create a 7-point calibration curve. To check for accuracy, two black shale standards were measured: USGS Green River Shale (SGR-1b) and USGS Brush Creek Shale (SBC-1).

Degree of Pyritization: Pyritic Sulfur, Pyritic Iron, and Acid Soluble Iron

Based on a procedure taken from Stebbins (2018), each sample underwent degree of pyritization (DOP) using a chromium-reducible sulfur method to determine the differences in oxygen levels at the time of deposition and to refine the resolution of any geochemical changes occurring throughout each collected stratigraphic column. Samples were powdered in the same manner as previous instrumentation preparation methods. A mass of approximately 0.05 g of sample was weighed on an analytical balance and transferred to a round-bottom flask, to which chromium powder weighing between 2.04 – 2.07 g and 10 mL of ethanol were added. This flask was connected to a purge and trap assembly as shown in Figure 2.3 below. This system produced an end product of zinc sulfide (ZnS) solution which, when 20 mL of silver nitrate ($AgNO_3$) were

added, resulted in a suspended precipitate that was filtered out using the vacuum pump and filtration system shown in Figure 2.4. By filtering the solution and doing several washes of 5% ammonia followed by a Milli-Q water rinse to dissolve any remaining unwanted solid, a final precipitate of Ag_2S was captured on a disk of filter paper. This filter was dried at 70°C for approximately twelve hours and then weighed to calculate the percentages of pyritic sulfur and pyritic iron by subtracting the initial weight of the filter and aluminum foil wrapping (used to protect and contain the filter) from the final weight of the sample, filter, and aluminum foil combined.

Figure 2.3: The DOP experimental set-up used for this study. (A) nitrogen gas tank, (B) funnel containing 60 mL HCl, (C) round-bottom flask containing sample, chromium powder, and 10 mL ethanol, (D) sand bath, (E) hot plate, (F) condenser, (G) Erlenmeyer flask containing 40 mL zinc acetate (more may be added according to sample). The nitrogen gas was constantly pushed through the system to flush out all oxygen, using < 1 psi to provide a sufficient stream of bubbling in the Erlenmeyer flask (Figure 2.3) (Stebbins, 2018). After allowing 60 mL of HCl to

drip into the round-bottom flask, the system was allowed to sit for one hour with the hot plate providing a light boil to the sample. During this time, hydrogen sulfide (H_2S) was purged from the sample by means of the N_2 gas, and trapped in the Erlenmeyer flask containing an initial amount of 40 mL of zinc acetate. Depending on the sample, more zinc acetate was added to the flask to counteract cloudiness; this necessitated an equal addition of extra $AgNO_3$ along with the required 20 mL.

Figure 2.4: Filtration system to obtain final product, Ag_2S.

Lastly, the percentage of acid soluble iron (also called HCl-extractable iron) was measured in order to obtain the portion of reactive iron present, referring to the iron not found in pyrite. To do this, approximately 0.1 g of sample was weighed on a semi-microbalance and added to 5 mL of HCl in a test tube. This solution was then boiled in a sand bath for one minute before rapidly being quenched with 10 mL of Milli-Q water to cool and dilute the solution. A

syringe filter was used on each of the samples to separate and discard particulate matter before a subsequent 1:50 dilution was completed. Samples were quantified for their iron content using inductively coupled plasma optical emission spectrometry (ICP-OES). USGS standards SGR-1b and SBC-1 were used as references with all unknowns calibrated to the more similar SGR-1b and corrected for dilution.

With the pyritic Fe and acid soluble Fe values experimentally obtained in the procedures described above, a final calculation was made using the following equation to assign a DOP value to which a corresponding oxygen level could be assigned (Figure 2.5):

$$DOP = \frac{\text{pyritic Fe}}{\text{pyritic Fe + acid soluble Fe}}$$

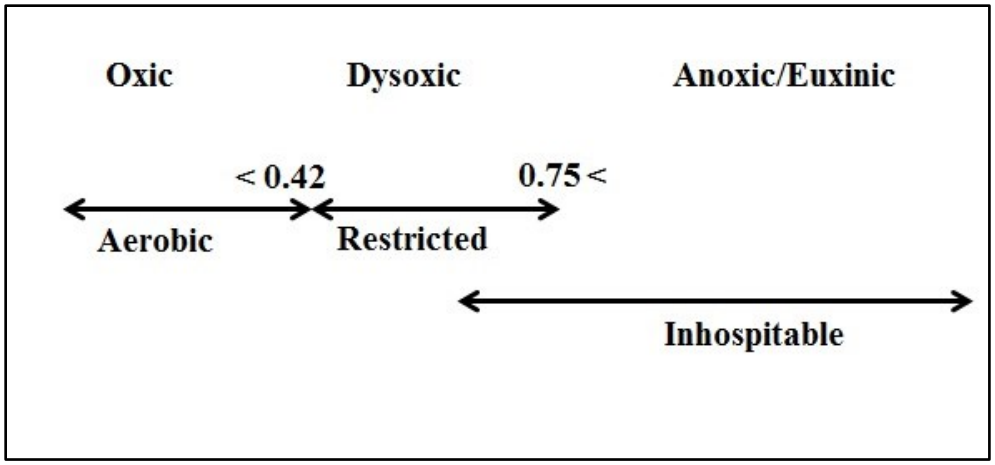

Figure 2.5: Oxygen level scale based on DOP value ranges. Modified from Rimmer (2004), referencing Raiswell et al. (1988) and Hatch & Leventhal (1992).

2.3 Results

2.3.1 Normality

Using IBM SPSS Statistics 25, each member was tested for normality (at the significance level of 0.05) based on data collected for TOC, pyritic iron, pyritic sulfur, and DOP values. For each category, the Union Springs possessed non-normal data. The Oatka Creek data was normal except for the DOP values.

2.3.2 S-TOC Relationships

Organic carbon-sulfur relationships were plotted for three of the six columns collected from the Union Springs and one column from the Oatka Creek (Figure 2.6). The normal marine regression line is provided to demonstrate values for sediments deposited in an environment that can range from oxic to dysoxic (Leventhal, 1995). The vast majority of the Union Springs samples were characterized by pyritic sulfur values that place them well outside oxygenated conditions, with sulfur values that did not correlate strongly with the organic carbon values. Pyritic sulfur values were high with a few anomalies; values ranged from 0.48-17.91 %. In comparison, the Oatka Creek was characterized by a similarly widespread range of pyritic sulfur values from 1.44-27.64%. The Oatka Creek also displayed greater scatter that can most likely be attributed to the smaller sampling size. Like the Union Springs, the high pyritic sulfur concentrations did not correlate strongly with the organic carbon content, with most samples clustering in the more ambiguous region of weakly euxinic to strongly anoxic (Figure 2.6). Both Marcellus shales grouped primarily in the range of 2-6% organic carbon. The median TOC value of the Oatka Creek (5.48%) was higher than the median TOC value of the Union Springs (4.38%).

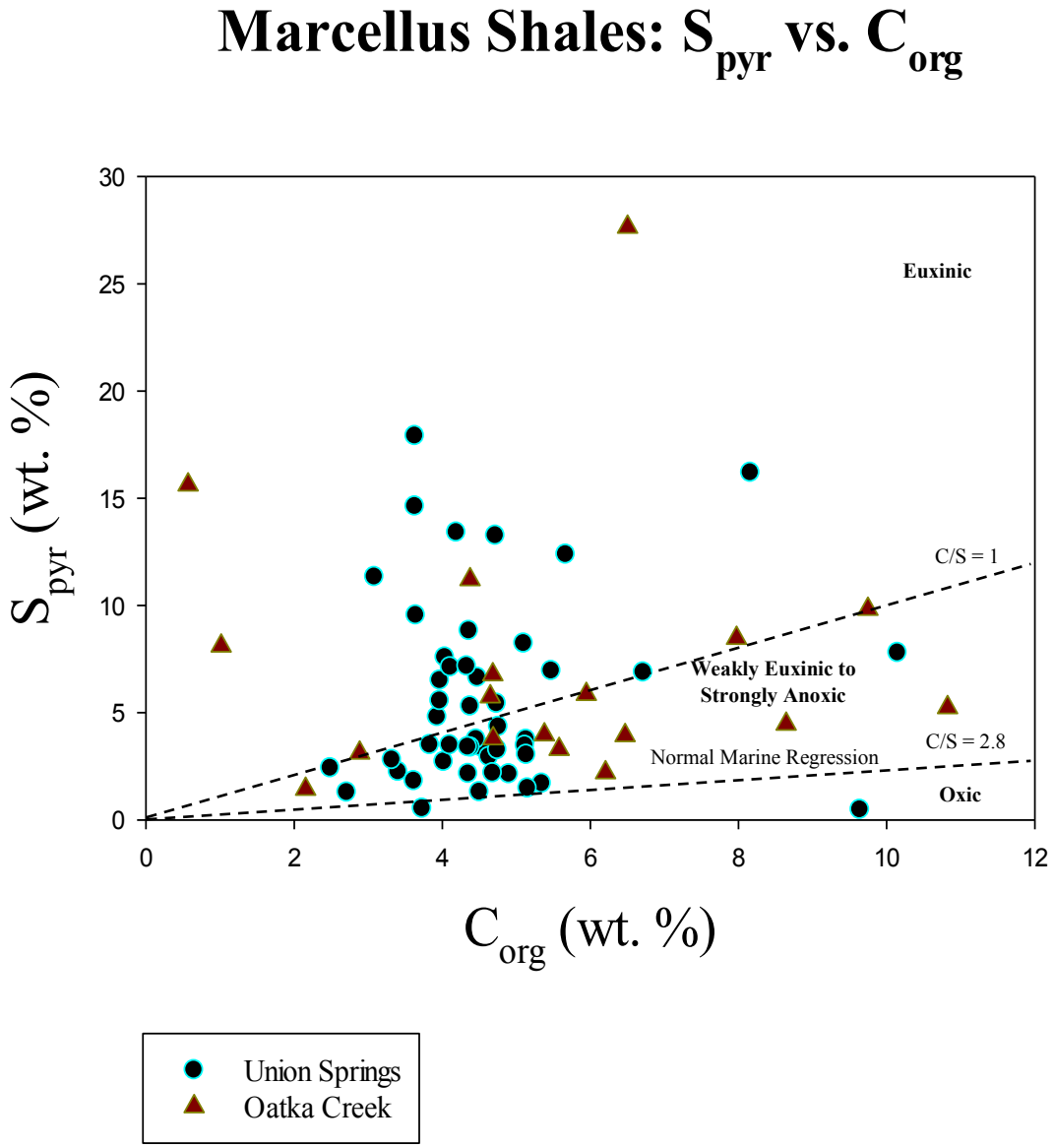

Figure 2.6: S-TOC cross-plot for the Union Springs and Oatka Creek. The upper trend line exhibits the weight percentages of organic carbon and pyritic sulfur in a 1:1 ratio. The lower trend line exhibits a 2.8 ratio and is representative of normal marine conditions which can entail oxygen levels ranging from dysoxic to oxic. Trend lines are taken from Leventhal (1995) and Berner (1984).

2.3.3 Fe-S-TOC Relationships

To further expound upon the trend indicated in the S-TOC plots, Fe-S-TOC ternary diagrams were constructed to emphasize the oxygenation level in the basin at the time of deposition for each of the black shale members. The same three columns used to generate the S-TOC plot of the Union Springs were selected for their pyritic sulfur and pyritic iron (the unreactive fraction of iron stabilized in the form of pyrite) values. The pyritic iron, pyritic sulfur, and TOC values were combined to create a single data point for each of the selected samples and plotted as shown in Figure 2.7. Without exception, samples plotted along the sulfidized iron trend line, indicating that depositional conditions were oxygen depleted. Pyritic iron content ranged from 0.42-15.59%. Unlike the S-TOC plot, the Fe-S-TOC diagram more distinctly grouped the samples of the Union Springs into two categories: 1) euxinic and 2) weakly euxinic to anoxic, and eliminated the characterization of any samples as dysoxic or oxic.

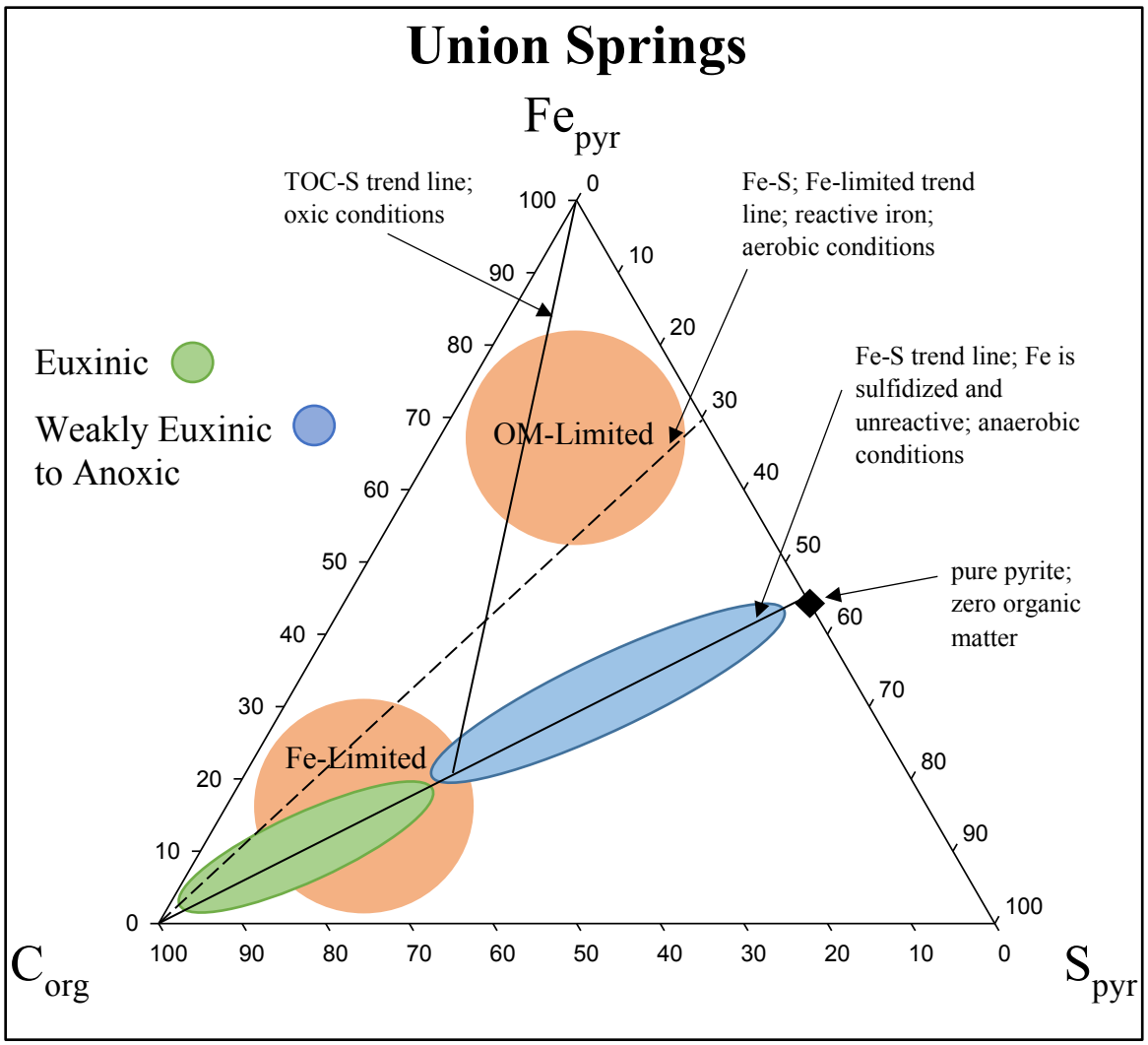

Figure 2.7: Fe-S-TOC ternary diagram for the Union Springs showing that the system is iron-limited and enriched in organic matter. Samples consistently plot along the Fe-S sulfidized trend line, indicating anaerobic conditions. Colored ovoids are drawn around the plotted data to approximate cut-offs between distinctly euxinic conditions (green) and less severe conditions ranging from weakly euxinic to anoxic (blue). Orange circles denote regions within the diagram referring to variables which may be a limiting factor in a given system. Note that a sulfur-limited region does not exist in its own designated corner as it would not be theoretically plausible for these samples. This is due to the inherent composition of a black shale being organic-rich; to plot near the S_{pyr} corner of the diagram would mean that the sample is essentially pure sulfur and

does not contain TOC. Trend lines are taken from Hofmann, Ricken, Schwark, & Leythaeuser (2000).

A ternary diagram was also constructed for the Oatka Creek based on the same samples used to create the S-TOC plot (Figure 2.8). The Oatka Creek plots along the sulfidized iron trend line similar to the Union Springs, but with a more prominent grouping of samples in the weakly euxinic to anoxic range. Only a singular sample can be considered euxinic. Pyritic iron concentrations range from 1.25-24.07%.

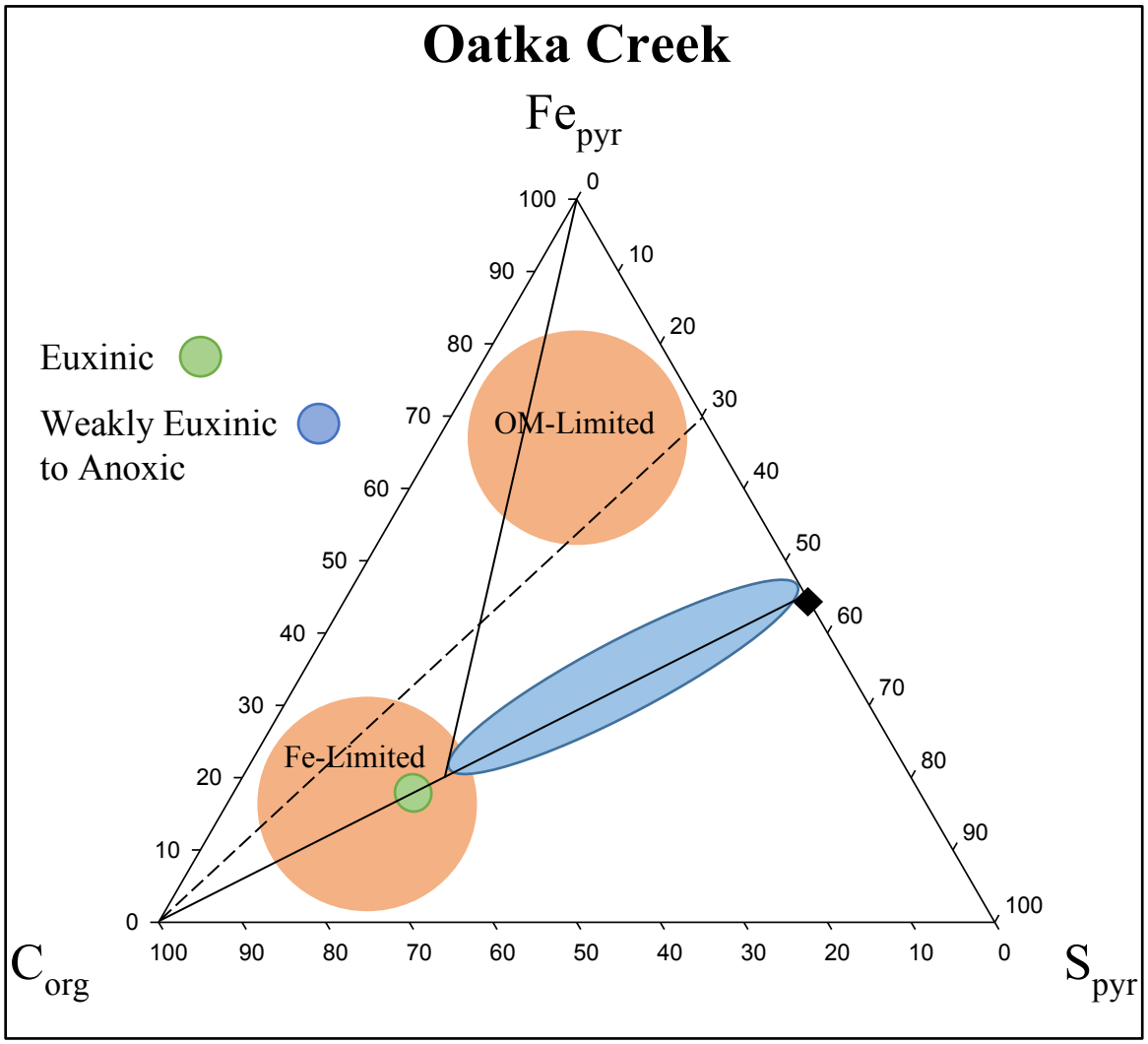

Figure 2.8: Fe-S-TOC ternary diagram for the Oatka Creek.

2.3.4 DOP

Calculations were made for each of the samples used in the S-TOC plots and Fe-S-TOC ternary diagrams in order to assign a DOP value and associated oxygen level. For a complete table of values, refer to Appendix 1. Of the forty-eight Union Springs samples analyzed for their pyritic iron and acid soluble iron concentrations, all but one (sample RB-10 of Union Springs 1) were classified as anoxic/euxinic based on DOP values greater than 0.75, with a median value of 0.96. However, despite these high values, a distinction between anoxic and euxinic cannot be made based on DOP values alone. The single sample classified as dysoxic had a DOP value of 0.74, placing it at the critical boundary between oxygen classifications. It is possible that repeated measurements may have yielded a value in the anoxic/euxinic range.

The overwhelming majority of Oatka Creek DOP values also point to deposition under anoxic/euxinic conditions, with a median value of 0.95. A single sample had a DOP value of 0.59 that placed it well within the dysoxic range. Taking each of the dysoxic outliers into consideration for the two black shale members, the Oatka Creek had a greater range of DOP values despite its smaller sample size.

2.3.5 DOP and Depth Relationships

Depth profiles were created for each of the stratigraphic columns that underwent degree of pyritization analysis in order to determine if any cyclical patterns or abrupt changes could be observed at the sampling resolution of every 10 cm (Figures 2.9-2.12). Any anomalies in a given profile could indicate changes in oxygen level throughout the duration of a given member's deposition, therefore affecting the preservation of organic matter.

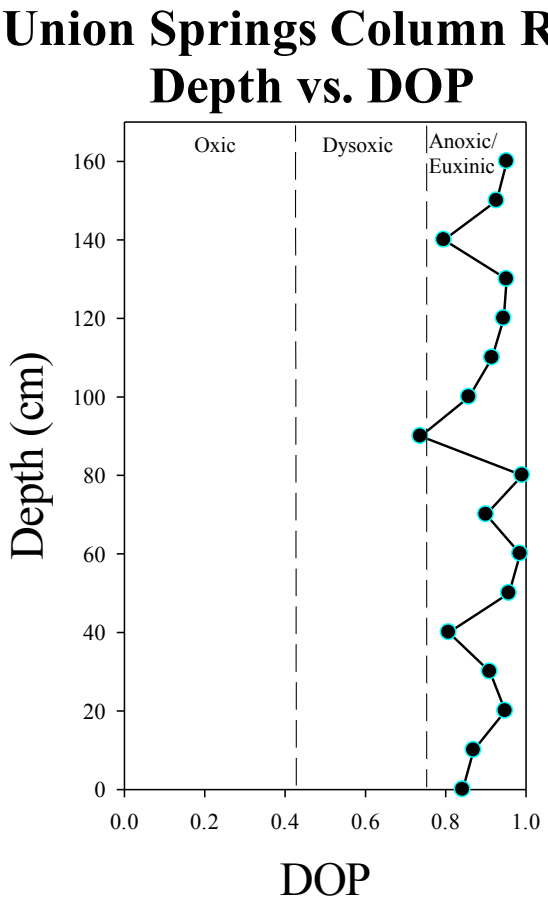

Figure 2.9: Depth vs. DOP profile of Union Springs 1.

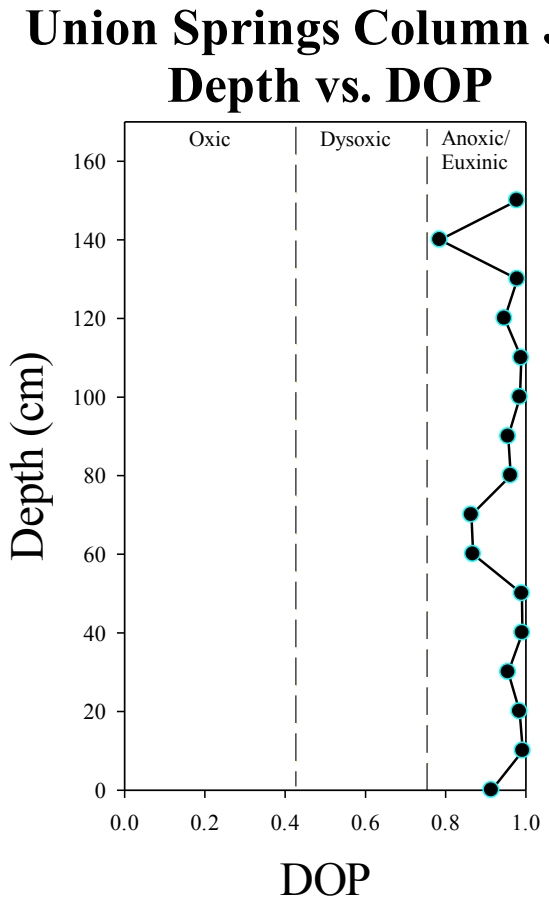

Figure 2.10: Depth vs. DOP profile of Union Springs 2.

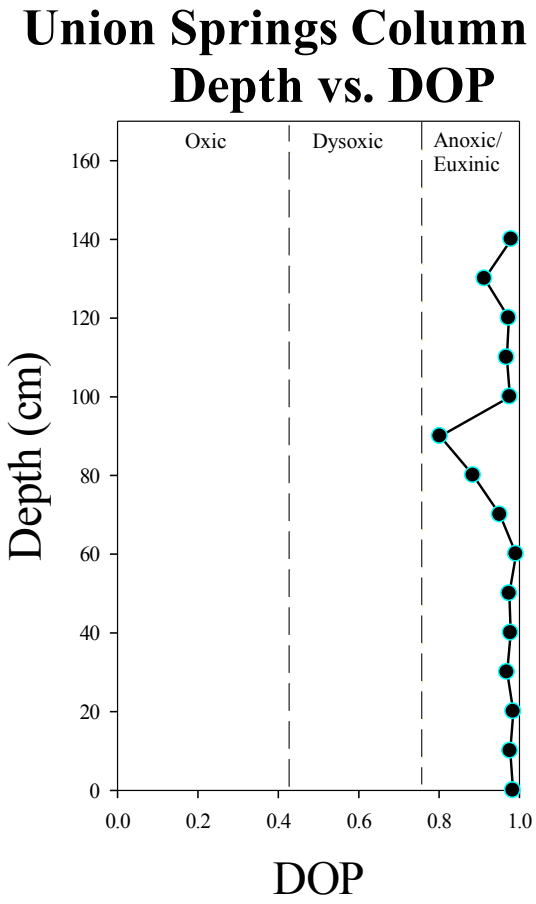

Figure 2.11: Depth vs. DOP profile of Union Springs 3.

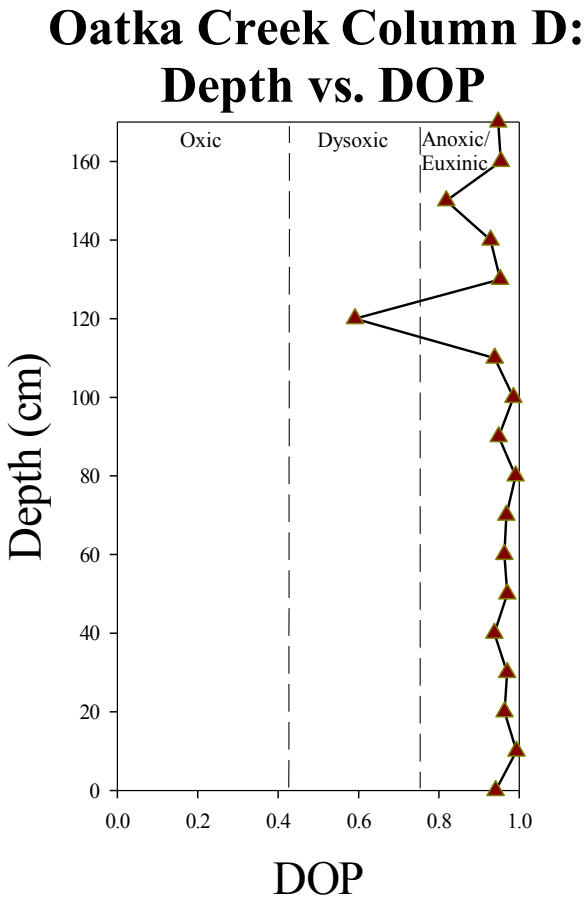

Figure 2.12: Depth vs. DOP profile of Oatka Creek 1.

Take note that each column was collected starting at the base of the exposed member and working upward, so that greater depths correlate with younger stratigraphic position. The three Union Springs columns were laterally adjacent and separated by a distance of approximately 3 m. Discrepancies in DOP values at like depths for this member could be attributed to variations in sampling technique as well as subtle changes in levelness of the formation across the exposure. Barring these possibilities, microenvironment conditions or spatial heterogeneity may have contributed to noted differences. Columns RB and JD each displayed a relatively pronounced decrease in DOP value around 140 cm while RB and BD shared a similar decrease at 90 cm. Of significance, it is at the 90 cm depth that the RB column possessed the singular

instance in the Union Springs that a sample was placed in the dysoxic category of the DOP classification scheme. However, the other columns at this depth placed their samples within the anoxic/euxinic category. The JD column witnessed a similar drop in DOP value as the RB and BD columns at 90 cm, but this occurred earlier in the JD profile at 60-70 cm.

Though the Oatka Creek displayed relatively consistent DOP values for over half of its total thickness (from 0-110 cm), it had a sharp drop at 120 cm that placed deposition conditions in the dysoxic range for that single instance before returning into the anoxic/euxinic range for the remainder of the column.

Overall, while the columns investigated displayed some spikes that contrasted against the baseline for the depositional duration, these abrupt increases in oxygen level were minor and no clear cyclic fluctuations appear to be preserved.

2.3.6 DOP-S Relationships

The DOP-S plot (Figure 2.13) showed that while the majority of samples from either black shale member fell in the upper range of the anoxic/euxinic DOP classification scheme, there was a much greater scatter of pyritic sulfur values associated with them.

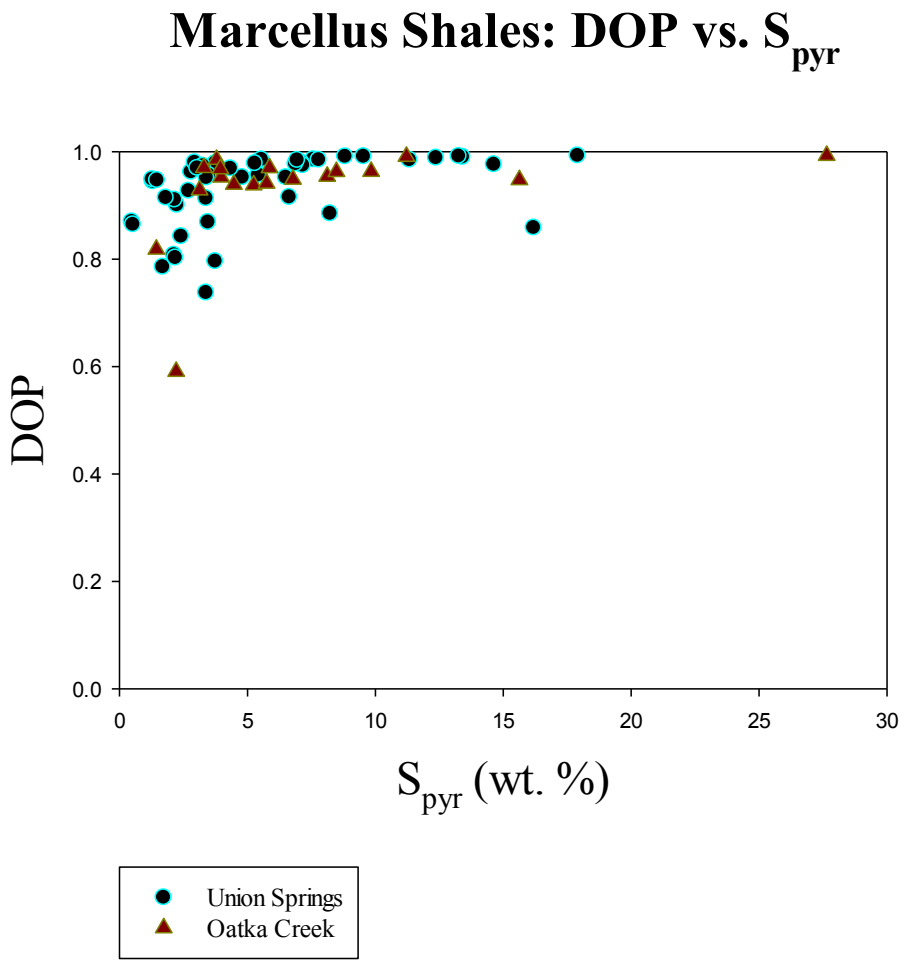

Figure 2.13: DOP-S cross-plot for the Union Springs and Oatka Creek.

2.3.7 TOC and Sedimentation Relationships

To analyze the impact of sedimentation rate on the preservation of TOC, Al_2O_3 was used as a proxy for sedimentation rate, owing to its abundance and conservative, immobile nature. The data corresponding to the Union Springs and Oatka Creek is shown in Figure 2.14. A distinct trend was not apparent in the Union Springs; as Al_2O_3 content increased, there was no discernable pattern for an associated increase in organic carbon. Similarly, for the Oatka Creek, there was no striking correlation in the data, though it did appear to divide into two distinct

groupings of samples – those that plotted at low C_{org} values coupled with low Al_2O_3 values, and those that plotted at high C_{org} values coupled with high Al_2O_3 values.

A linear regression analysis performed in SigmaPlot suggested that sedimentation rate did affect organic matter preservation in the Union Springs at the significance level of 0.05 at which P = 0.0089 and $r^2 = 0.0658$. For the Oatka Creek at the significance level of 0.05, P = 0.0007 and $r^2 = 0.5215$. While this sedimentation factor was present and significant, it was not powerful. This was by no means a thorough test to explain how much control sedimentation rate exerted on preservation, but it did imply that this variable can have an impact and that oxygen level was not the only actor in preservation quality.

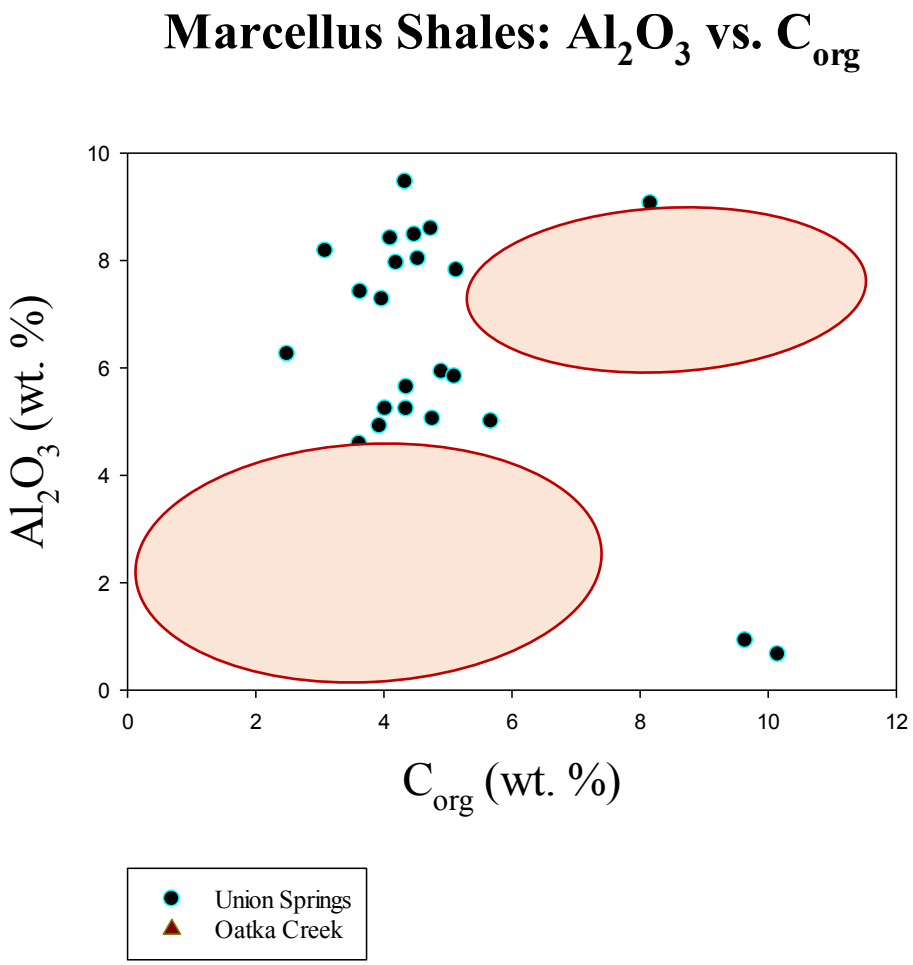

Figure 2.14: Al_2O_3-C_{org} cross-plot for the Union Springs and Oatka Creek. Colored ovoids are drawn to call attention to the two distinct clusters of Oatka Creek samples.

2.4 Discussion

2.4.1 The Interrelationships of Fe, S, and TOC

The S-TOC plot (Figure 2.6) offered a quick analysis to observe into which oxygen level categories the black shale samples fall. Wignall (1994) remarked that S-TOC plots for oxic environments most often reveal a positive correlation between the abundances of organic carbon and pyritic sulfur. Despite the counterintuitive nature of this claim – for organic matter must be destroyed for iron sulfides to precipitate – Wignall posited that this trend most likely exists because a constant fraction of the organic matter (rather than the total amount) was involved in pyrite production. The C/S ratios of the Union Springs and Oatka Creek did not indicate a strong trend that positively correlated pyritic sulfur concentrations with organic carbon concentrations. Rather, pyritic sulfur concentrations were high relative to the low to moderate concentrations of organic matter, suggesting that euxinia was a prevalent characteristic of the environment for a significant portion of the material deposited. This lack of distinct positive correlation but distinguished occurrence of high pyritic sulfur values at low to moderate organic carbon values has been noted for other euxinic environments such as the Black Sea (Wignall, 1994 and references therein). Sulfur values were not constant, but appeared to separate samples into two main clusters. The first group was distinguished by plotting above the C/S = 1 trend line, expressing pyritic sulfur values that greatly surpassed the amount of organic matter present in the samples. Likely, such conditions involved a limited amount of iron readily available for pyrite formation, thereby leading to an excess amount of sulfur to remain in solution as sulfate

reduction continued. Therefore, any samples that plotted above this line can definitively be classified as euxinic, with some very strongly so as they approached sulfur values > 10%. The second group of samples clustered in the vague territory lying between the C/S = 1 trend line and the normal marine regression line of C/S = 2.8. This area is ambiguous as the S-TOC plot lacks the robustness to clearly delineate distinctions between euxinia and anoxia. Thus, the samples that plotted in this area may range from weakly euxinic to anoxic and even dysoxic in the case of samples near the normal marine trend line. Both members had claimed a majority of samples in the weakly euxinic to strongly anoxic region, though the Oatka Creek possessed fewer samples bordering on dysoxia.

In order to parse out the boundaries between these oxygen conditions, a more quantitative proxy such as DOP was incorporated to accurately classify the oxygen level any of these individual samples were deposited under. Nevertheless, a strong case for anoxia/euxinia can be made for much of the depositional history of the Union Springs and Oatka Creek based on the S-TOC plot alone, with the need to resolve discrepancies between weakly euxinic and strongly anoxic conditions through other means. Due to the lower resolution of this cross-plot, samples indicated as approximately dysoxic or even oxic became more well-established within the anoxic region of the corresponding ternary diagram for each of the black shales.

The ternary diagram has the distinct advantage over its S-TOC plot counterpart because it visually signals which factor is the limiting control on pyrite formation. Additionally, it eliminates the effects of biogenic and siliciclastic minerals (Hofmann et al., 2000). Under anoxic to euxinic conditions, pyrite production is limited by the abundance of available iron in the system (Berner, 1970). Thus, precipitation of pyrite ceases once the iron reservoir is depleted even though sulfate reduction may continue provided that organic matter remains for anaerobic

bacteria to thrive upon (Berner, 1970). Figures 2.7 and 2.8 clearly demonstrate that the Union Springs and Oatka Creek environments were iron-limited, with all samples distinctively plotting along the constant sulfidized iron (or pyrite) trend line, ranging from the TOC corner where organic matter content is exceptionally high and continuing out to conditions that would produce more pure pyrite samples with decreasing concentrations of organic matter in their composition. This indicates that the iron in these samples is in the unreactive form of pyrite, having been sulfidized. Data from the Union Springs and Oatka Creek suggested that all or nearly all of the available iron went into the formation of pyrite. Had this not been the case and a lesser portion of the available iron reacted with sulfur to precipitate pyrite, then the ternary diagram would express a shift in the intercept of the Fe-S line with the TOC-S line toward the Fe corner (Hofmann et al., 2000). However, this was not demonstrated in the Union Springs or Oatka Creek, therefore the samples do not appear to have been deposited in oxic or dysoxic conditions in which organic matter is more likely to be the limiting agent. Furthermore, acid soluble iron concentrations obtained through ICP-OES support this assessment as samples contained extremely low levels of this iron fraction (< 1 wt. %) compared to that found in pyrite.

While iron ultimately limits the amount of pyrite that can form, from a big picture perspective, it is organic matter that is the driving force behind the establishment of euxinic conditions. Without organic matter available in an oxygen depleted environment, anaerobic bacteria could not respire and the production of hydrogen sulfide would not occur (Berner, 1970). The samples that plotted closest to the TOC corner along the Fe-S line exemplified strongly euxinic conditions in which organic carbon was by far the highest constituent between the three variables, followed by sulfur, and containing a more limited amount of iron. Continuing along this line and away from the TOC corner, the conditions gradually changed from strongly

euxinic to anoxic upon approaching the pyrite point. This procession still reflected strongly depleted oxygen levels even when reaching the pyrite point. Overall, both black shale members exhibited minimal fluctuations in oxygen level, demonstrating an organic matter dominated environment that provided adequate material for sulfate reduction throughout the duration of deposition.

2.4.2 The Influence of Sedimentation Rate

While it is apparent that productivity ultimately controls the total amount of organic material potentially available for preservation, and oxygen levels greatly influence the favorability of preservation, another factor may have an influential role: sedimentation rate. Trends comparing sedimentation rate to organic carbon abundances have exhibited a similar trend and degree of counterintuitive-ness to that of the positive correlation displayed in S-TOC plots for oxic environments. Generally, as sedimentation rates increase, organic carbon values do as well. However, this may seem unexpected because high sedimentation rates can lead to higher rates of hydrogen sulfide production as organic remains are quickly buried, providing anaerobic bacteria the ideal environment to oxidize available organic carbon (Wignall, 1994). This positive correlation could be explained by an increase in organic matter accumulation at the sediment-water interface coinciding with an increase in sedimentation rate (Wignall, 1994). As sulfate reduction continues to be fueled by this flux of organic matter, the proportion of organic carbon mineralized ultimately decreases because of its shorter residence time in surface sediments (Wignall, 1994).

The source of any high sediment influxes to the Marcellus formation can be attributed to the weathering of the Acadian Mountains and differences in erosion rates could explain why the Union Springs is reportedly more organic-rich than the Oatka Creek. Still, it is important to note

that this comparison is relative. While the Union Springs was likely deposited under higher sedimentation rates that contributed a grittier texture to its deposits as well as a lack of laminations, black shales are most often associated with slow sedimentation rates. It is extremely difficult if not impossible to calculate absolute sedimentation rates and such a feat is outside the scope of this research. However, it should be said that the influence of sedimentation rate, especially high rates, can be overemphasized. High sedimentation rates can eventually have deleterious effects after a certain point. Primary productivity can be disrupted by especially high rates of fine-grained sediment influx which increase turbidity and ultimately dilute the organic carbon content settling on the ocean floor by ushering in clastic terrestrial material (Aller & Mackin, 1984). So, while the Union Springs may have had higher sedimentation rates that effectively buried organic matter more quickly for preservation, both black shale members may have still had what would be considered low to moderate sedimentation rates.

The larger grouping of samples in the euxinic category for the Fe-S-TOC plot of the Union Springs further supports the argument that the depositional history of this member witnessed higher sedimentation rates and may suggest a time of increased erosion from the weathering of the Acadian Mountains and the invasion of that material into the basin. Additionally, the coincident timing of this increased erosion coupled with an ample abundance of organic matter at the sediment-water interface may explain the higher organic content found in this member in some localized areas.

The Oatka Creek data showed a weaker correlation between the sedimentation rate proxy and organic matter preservation and, interestingly, grouped samples into two clusters. Initially, it was thought this may be evidence of a sharp change in the amount of weathered material entering the Marcellus at some point during the Oatka Creek's depositional history. Closer

inspection of the chronological order of each Oatka Creek sample revealed that the two distinct clusters did not coincide with a singular point in time during the member's deposition. Rather, there appeared to be fluctuation in sedimentation rate, though in no clear cyclical pattern. Overall, the Oatka Creek data presented in Figure 2.14 illustrates that preservation will typically be enhanced by higher sedimentation rates. Nevertheless, based on the Al_2O_3-C_{org} plot, sedimentation rate or supply exerted some influence, but was not the dominant control on organic matter preservation in either black shale member.

2.4.3 Oxygen Levels and Preservation

By examining environmental proxies for oxygen conditions at the time of deposition, this Marcellus site further asserts the notion that oxygen deficiency and its relationship with the amount of available organic matter is a controlling factor in the formation of black shales (Tourtelot, 1979). That this formation was established in a geographically restricted basin rather than in a less restricted continental shelf setting, suggests that anoxia/euxinia was a response to the accumulation and decomposition of organic matter rather than a precursor to it. This would be in contrast to a continental shelf setting in which an overabundance of organic matter is needed to overwhelm the rate of oxidation in an upwelling zone (Selley & Sonnenberg, 2015). In such a setting, anoxia may already be established at or near the sea floor, therefore it is the input of an exceptional amount of organic matter that may lead to preservation and eventual formation of black shales.

In a restricted or silled basin, paleoproductivity is generally low as a consequence of poor vertical advection caused by density stratification (Wignall, 1994). Therefore, it is likely that high primary productivity was not present during the deposition of the Marcellus formation. This further points to oxygen levels and their influence over preservation as the deciding factor in the

abundance of organic content found in the black shales from this location. So, while the means by which oxygen deficient conditions were established in the Marcellus formation may reflect that anoxia is not a prerequisite, it does point to it being a beneficial factor so that organic content is not diminished after accumulation.

2.4.4 Comparing the Marcellus Formation to Modern Black Shale Environments

It is difficult to make comparisons between ancient and modern black shale environments, partly because those expressed in the geologic record were formed in epicontinental seas that were greatly restricted in connectivity to the rest of the world's oceans (Wignall, 1994 and references therein). Today, epicontinental seas are a less common feature. Still, there are some present day examples: the Swiss lake, Lake Greifen, that experiences seasonal stratification and nutrient input supplied through anthropogenic and agricultural activities; hypersaline lagoons, of which the Mediterranean Sea is a silled basin with a negative water balance and weak density stratification; upwelling zones with a well-established oxygen minimum zone (i.e. the California Borderland); shallow shelf seas that endure seasonal stratification and temporal oxygen deficiency in the bottom waters; and a restricted basin, such as the Black Sea, which receives a mixture of freshwater and marine water inputs that have produced a halocline and poor circulation (Wignall, 1994).

The Black Sea is often cited as the type euxinic environment and has been useful in comparisons of black shale paleoenvironments (Tourtelot, 1979; Wignall, 1994; Stewart et al., 2007). Due to its source waters of differing salinities, a distinct halocline was produced that severely limited the vertical circulation of oxygen-rich surface waters to greater depths (Wignall, 1994). Lateral advection is also hindered due to the relatively small amount of water entering the basin compared to its total volume (Wignall, 1994). As a result, circulation is so restricted

beneath the halocline that complete mixing in the lower water column requires approximately one thousand years (Brumsack, 1989). It is in the lower portion of the water column, beneath the halocline, that descending organic matter places an added demand on the choked oxygen supply. Thanks to the halocline and decomposition of organic matter, the lower anoxic waters contain free hydrogen sulfide, making the Black Sea truly euxinic.

Three different scenarios for the deposition of black shales have been transformed into basin models known as 1) the restricted circulation model, 2) the open ocean model, and 3) the continental shelf model. Each model is based on the abundance of organic matter present in relation to the oxygen level. Of the three, the Marcellus formation most closely resembles the restricted circulation model for which the Black Sea is a prime example.

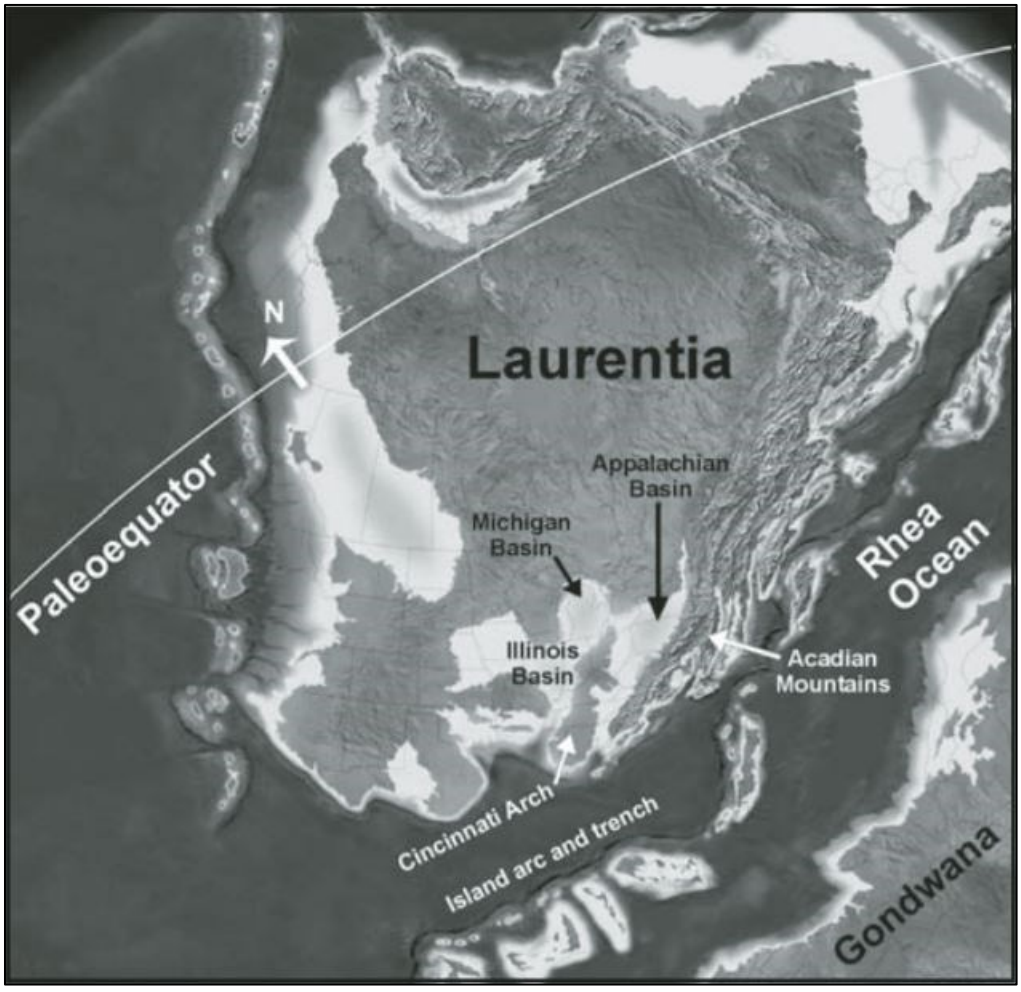

Figure 2.15: Paleomap reconstruction of the Appalachian Basin during the Middle Devonian (Soeder, Enomoto, & Chermak, 2014 and references therein).

During the Middle Devonian, the Rhea Ocean was closing along a subduction zone as Laurentia and Gondwana approached one another to eventually coalesce into Pangea (Soeder et al., 2014). Highlands and mountain belts were produced through the collision of continental plates and transpressional faulting (Soeder et al., 2014). While the highlands served as the dominant supplier of sediments to the Acadian foreland basin, the Marcellus formation was deposited at the toe of a westward prograding clastic wedge (Soeder et al., 2014). Residing within the Appalachian Basin (Figure 2.15), the Marcellus had highly limited connectivity to the ocean, partly due to the positioning of the Cincinnati Arch (Figure 2.15), thereby hindering circulation of colder, denser currents which are a significant factor in supplying the oxygenated waters present in an open ocean model (Tourtelot, 1979). However, less restriction to ocean circulation may have had little effect anyway in establishing basin stratification given the low equatorial latitude at the time. The continental shelf model also seems to be a poor fit for this particular paleoenvironment because of the lack of potential for upwelling based on its geographic position. This study also lacks evidence of high productivity which is a characteristic feature in the continental shelf model thanks to the nutrient-rich waters carried into an unrestricted environment (Selley & Sonnenberg, 2015; Tourtelot, 1979).

In the restricted basin model, circulation is poor or absent, thereby allowing organic matter to accumulate even if productivity is low (Tourtelot, 1979). In this case, the oxygen deficiency was brought about after the accumulation and degradation of organic matter, rather than existing prior to the introduction of the material into the basin (Tourtelot, 1979). In this type

of basin environment, oxygen may be present in the photic zone where photosynthesizers thrive at or near the surface and additional organic matter may be supplied from terrestrial sources (Tourtelot, 1979). Any organic matter that endures the descent to reach below the level of zero oxygen can only be decomposed by anaerobic bacteria and leads to the production of hydrogen sulfide, which further promotes the type of anoxic/euxinic environment that allows organic-rich sediments to accumulate.

By the time of the Oatka Creek's deposition, the Appalachian Basin was positioned in the southern subtropics, putting it in the path of moisture-laden winds coming off of the Iapetus Ocean (Werne et al., 2002). With the Acadian Orogen bordering its eastern side, a rain shadow was produced that created a temporal climate with arid to semi-arid conditions that may have even experienced intense, monsoon-like storms (Werne et al., 2002 and references therein). Like the Black Sea, it is possible that the Marcellus formation was stratified because of a halocline – though one produced by different means. Rather than a stratified water column resulting from the mixing of two widely differing water sources into a silled basin (Brumsack, 1989), the Marcellus was situated in an evaporitic environment on the leeward side of the mountains that left the basin hypersaline (Werne et al., 2002). Any water entering the restricted basin from the open ocean would have been less dense, causing it to float on top of the indigenous basin water, leading to greater distinction in density layers when acting in combination with the evaporation effect of the rain shadow (Selley & Sonnenberg, 2015). Combined with seasonal variability that may have resulted in further stratification during the hotter summer months, any organic matter that managed the journey to the sediment floor had a good chance for preservation (Werne et al., 2002). In such a well-stratified environment, neither high productivity nor high sedimentation

rate may have been needed to ensure a significant abundance of organic matter was preserved in the Marcellus shales.

Regarding the maturity of the basin at the time of deposition, it is likely that the Marcellus formation was deposited at a later stage of the Wilson Cycle, such as stages E or F in Figure 1.6. Of course, there can be a significant difference in the environment between the two stages, such as sea level which can have an effect on the accommodation space available for collecting organic matter as well as the length of its trip to the sediment floor in the first place (Trabucho-Alexandre et al., 2012). However, based on the striking similarity in both the abundance of organic matter and the oxygen levels for the Union Springs and Oatka Creek, it would seem that at this location, differences in depth and sea level were either not significant between the two members, or these variables did not account for the greatest influence on preservation.

I propose that Stage E most accurately reflects the Marcellus formation, for at this point the larger, all-encompassing Appalachian Basin was highly constricted by land and nearly cut off from the Iapetus and Rheic oceans (Trabucho-Alexandre et al., 2012). In such a phase, black shale deposition is largely a result of the location within the basin and the zonal climate belt it resides in (Trabucho-Alexandre et al., 2012). During the closing of a basin and the subsequent orogeny and subduction, a foreland basin forms and can be invaded by a shallow transgressive sea. Without a major subaerial source of sediment, the basin becomes starved of siliciclastics and is filled primarily with mud and organic matter that lithifies into black shales (Trabucho-Alexandre et al., 2012). With increasing aerial relief, organic content becomes diluted with siliciclastic material, thus putting an end to the formation of black shales. This final stage must have occurred sometime after the Oatka Creek was deposited.

The presence of the Cherry Valley limestone member and even the inorganic carbon abundances within the black shale members, demonstrates that there is a considerable amount of carbonate content within the Marcellus. This could be further indication that the Marcellus formed in a mature basin in which the growing mountains were steadily supplying more siliciclastic material to eventually overwhelm the amount of organic matter in the basin.

Future analysis may have the ability to more definitively state whether or not maturity in a restricted basin is a key component of black shale formation regardless of other environmental factors, or if it simply has a beneficial additive effect in combination with favorable oxygen-depleted conditions.

2.4.5 Future Work

To further corroborate with the oxygen level distinctions made in this study through DOP and Fe-S-TOC relationships, an additional proxy such as measuring pyrite framboids both in terms of abundance and diameter, could be used to further confirm current anoxic/euxinic classifications. These framboid sizes can correspond to oxygen restricted biofacies and paleoredox conditions (Wignall & Newton, 1998).

More thorough sampling will be needed in the Oatka Creek from the Seneca Falls site to check for precision in measurements and to confirm that this distinct grouping in sedimentation rates truly exists and is representative of the member at this locale, rather than an artifact of the small sampling size. It would also be advised that more samples per member be sampled to check for cyclicity at levels finer than 10 cm resolution. Once consistency can be established, the timing for any large-scale tectonic events may be correlated with changes in either weathering rates or transportation of sediments into the basin. Future sample collection trips should make use of distinct marker beds when creating accurate stratigraphic profiles throughout each

member. This will aid in eliminating some of the ambiguity that exists within the depth profiles caused by human error and the unevenness of the formation's depth.

Establishing the existence of either a singular, abrupt change in sedimentation rate or multiple reversals during the deposition of the Oatka Creek specifically, and the Marcellus formation as a whole, could have an impact on characterizing the paleoenvironment and maturity of the basin. One of the initial objectives of this research was to present a basin model and propose which stage(s) of the Wilson Cycle the Marcellus was deposited in. While it is accepted that anoxic bottom waters, slow sedimentation rates, and low productivity seem to be the combination responsible for the deposition of many ancient black shales, recent environments suggest high sedimentation rates and high productivity could also produce black shales (Wignall, 1994). To create a depositional model for any given black shale basin, it is vital that the distinction between these two scenarios can be made. Yet, this can be critically hindered by the difficulty in measuring paleoproductivity. I propose that a similar project should analyze the same samples within this research for their organic compounds in order to identify the source. Doing so will be advantageous both in providing a more informed understanding to the extent of sedimentation rate's influence on organic carbon burial and preservation, as well as early identification of potential oil- and gas-generating shales based on the maturity and type of kerogen present.

Conclusions

- Contrary to reports in other areas within the Marcellus formation, this site did not display a sharp contrast in organic richness between the Union Springs and Oatka Creek; in fact the median TOC concentration was unexpectedly higher for the Oatka Creek than the Union Springs. The Oatka Creek even reported a higher maximum TOC value than the Union Springs. This suggests the variability of organic richness within the same member can result from differences in geographic location and associated, complex relationships with other factors such as climate zones.
- Based on relationships expressed between Fe, S, and TOC concentrations, the oxygen conditions that prevailed during the deposition of both black shale members can be classified as anoxic/euxinic. Iron was the limiting factor in the formation of pyrite for each of these black shale members. The dominant majority of available iron reacted to form pyrite as evidenced visually in the ternary diagrams and agreed upon by the concentration of acid soluble iron measured using ICP-OES.
- There were some minor fluctuations in oxygen levels throughout the deposition of each black shale member, but these changes do not reflect strong cyclical patterns.
- Sedimentation rate exerted some influence on organic matter preservation in each black shale member, but its effect was slight and by no means the dominant control.
- The basin model for the Marcellus formation can be likened to that of the Black Sea in that it was heavily restricted from connectivity to the oceans and became highly stratified. Stratification in the Marcellus can likely be attributed to the arid conditions produced in this region due to the rain shadow effect cast by the Acadian Orogen. As a result,

anoxic/euxinic conditions were likely established after the development of the halocline and further assisted in accumulating and preserving organic matter.

- Deposition of the formation likely occurred in a later, mature stage of the Wilson Cycle when the foreland basin was forming.

References

Algeo, T. J., Berner, R. A., Maynard, J. B., & Scheckler, S. E. (1995). Late Devonian oceanic anoxic events and biotic crises: "rooted" in the evolution of vascular land plants. GSA today, 5(3), 45-66.

Aller, R. C., & Mackin, J. E. (1984). Preservation of reactive organic matter in marine sediments. Earth and planetary science letters, 70(2), 260-266.

Arthur, M. A., & Sageman, B. B. (1994). Marine Black Shales: Depositional Mechanisms and Environments of Ancient Deposits. Annual Review of Earth and Planetary Sciences, 22(1), 499-551. doi:10.1146/annurev.ea.22.050194.002435

Berner, R. A. (1970). Sedimentary pyrite formation. American journal of science, 268(1), 1-23.

Berner, R. A. (1984). Sedimentary pyrite formation: an update. Geochimica et cosmochimica Acta, 48(4), 605-615.

Bond, D. P., & Grasby, S. E. (2017). Editorial: Mass extinction causality. Palaeogeography, Palaeoclimatology, Palaeoecology, 478, 1-2. doi:10.1016/j.palaeo.2017.05.011

Bond, D. P., & Wignall, P. B. (2014). Large igneous provinces and mass extinctions: An update. Geological Society of America Special Papers, 29-55. doi:10.1130/2014.2505(02)

Brumsack, H. J. (1989). Geochemistry of recent TOC-rich sediments from the Gulf of California and the Black Sea. Geologische Rundschau, 78(3), 851-882.

Canfield, D. E. (1993). Organic matter oxidation in marine sediments. In Interactions of C, N, P and S biogeochemical Cycles and Global Change (pp. 333-363). Springer Berlin Heidelberg.

Center for Climate and Energy Solutions. (2013). Leveraging Natural Gas to Reduce Greenhouse Gas Emissions. Retrieved from https://www.c2es.org/site/assets/uploads/2013/06/leveraging-natural-gas-reduce-ghg-emissions.pdf

Davidson, D. F., & Lakin, H. W. (1961). Metal content of some black shales of the western United States [Pb, Mn, Cu, Zn, Ni, V, Mo, Ag, Cr, Fe, and Se]. US, Geol. Surv., Prof. Pap. (United States), 424.

Energy Information Administration. (2010, December 20). EIA's Energy in Brief: What is shale gas and why is it important?. Retrieved from http://www.dnr.louisiana.gov/assets/TAD/reports/about_shale_gas.pdf

Ettensohn, F. R. (1985). Controls on development of Catskill Delta complex basin-facies. The Catskill Delta: Geological Society of America Special Paper, 201, 65-77.

Ettensohn, F. R., Miller, M. L., Dillman, S. B., Elam, T. D., Geller, K. L., Swager, D. R., Markowitz, G., Woock, R.D., & Barron, L. S. (1988). Characterization and implications of the Devonian-Mississippian black shale sequence, eastern and central Kentucky, USA: Pycnoclines, transgression, regression, and tectonism.

Feldmann, R. M., Franţescu, A., Franţescu, O. D., Klompmaker, A. A., Logan Jr, G., Robins, C. M., Schweitzer, C. E., & Waugh, D. A. (2012). Formation of lobster-bearing concretions in the Late Cretaceous Bearpaw Shale, Montana, United States, in a complex geochemical environment. Palaios, 27(12), 842-856.

Foree, E. G., & McCarty, P. L. (1970). Anaerobic decomposition of algae. Environmental science & technology, 4(10), 842-849.

Harris, D., Horwáth, W. R., & van Kessel, C. (2001). Acid fumigation of soils to remove carbonates prior to total organic carbon or carbon-13 isotopic analysis. Soil Science Society of America Journal, 65(6), 1853-1856.

Hatch, J. R., & Leventhal, J. S. (1992). Relationship between inferred redox potential of the depositional environment and geochemistry of the Upper Pennsylvanian (Missourian) Stark Shale Member of the Dennis Limestone, Wabaunsee County, Kansas, USA. Chemical Geology, 99(1-3), 65-82.

Hofmann, P., Ricken, W., Schwark, L., & Leythaeuser, D. (2000). Carbon–sulfur–iron relationships and δ13C of organic matter for late Albian sedimentary rocks from the North Atlantic Ocean: paleoceanographic implications. Palaeogeography, Palaeoclimatology, Palaeoecology, 163(3-4), 97-113.

Lash, G. G., & Engelder, T. (2011). Thickness trends and sequence stratigraphy of the Middle Devonian Marcellus Formation, Appalachian Basin: Implications for Acadian foreland basin evolution. AAPG Bulletin, 95(1), 61-103. doi:10.1306/06301009150

Lee, D. S., Herman, J. D., Elsworth, D., Kim, H. T., & Lee, H. S. (2011). A critical evaluation of unconventional gas recovery from the Marcellus shale, northeastern United States. KSCE Journal of Civil Engineering, 15(4), 679.

Leventhal, J., & Taylor, C. (1990). Comparison of methods to determine degree of pyritization. Geochimica et Cosmochimica Acta, 54(9), 2621-2625.

Leventhal, J. S. (1995). Carbon-sulfur plots to show diagenetic and epigenetic sulfidation in sediments. Geochimica et Cosmochimica Acta, 59(6), 1207-1211.

O'Leary, M. H. (1988). Carbon isotopes in photosynthesis. Bioscience, 38(5), 328-336.

Pew Trusts. (2003, May). America's Living Oceans: Charting a Course for Sea Change. Retrieved from http://www.pewtrusts.org/~/media/assets/2003/06/02/poc_summary.pdf

Raiswell, R., Buckley, F., Berner, R. A., & Anderson, T. F. (1988). Degree of pyritization of iron as a paleoenvironmental indicator of bottom-water oxygenation. Journal of Sedimentary Research, 58(5), 812-819.

Rimmer, S. M. (2004). Geochemical paleoredox indicators in Devonian–Mississippian black shales, central Appalachian Basin (USA). Chemical Geology, 206(3), 373-391.

Rimmer, S. M., Thompson, J. A., Goodnight, S. A., & Robl, T. L. (2004). Multiple controls on the preservation of organic matter in Devonian–Mississippian marine black shales: geochemical and petrographic evidence. Palaeogeography, Palaeoclimatology, Palaeoecology, 215(1-2), 125-154.

Selley, R. C., & Sonnenberg, S. A. (2015). Elements of petroleum geology (3rd ed.). Academic Press.

Seneca Stone Corporation. About Seneca Stone. Retrieved from http://senecastone.com/

Soeder, D. J., Enomoto, C. B., & Chermak, J. A. (2014). The Devonian Marcellus Shale and Millboro Shale. Field Guides, 35, 129-160.

Sperling's Best Places. Best Places to Live in Seneca Falls, New York. Retrieved from http://www.bestplaces.net/city/new_york/seneca_falls

Stebbins, A. G. (2018). Understanding the Permian-Triassic Extinction and Recovery through the Sulfur Cycle: A Multiproxy Approach Using Pyrite and Carbonate-Associated Sulfate. Graduate Doctoral Dissertations. 395. https://scholarworks.umb.edu/doctoral_dissertations/395

Stewart, K., Kassakian, S., Krynytzky, M., DiJulio, D., & Murray, J. W. (2007). Oxic, suboxic, and anoxic conditions in the Black Sea. In The Black Sea flood question: Changes in coastline, climate, and human settlement (pp. 1-21). Springer, Dordrecht.

Sullivan, L. A., Bush, R. T., & McConchie, D. M. (2000). A modified chromium-reducible sulfur method for reduced inorganic sulfur: optimum reaction time for acid sulfate soil. Australian Journal of Soil Research, 38(3), 729. doi:10.1071/sr99088

Tourtelot, H. A. (1979). Black shale—its deposition and diagenesis. Clays and Clay Minerals, 27(5), 313-321.

Trabucho-Alexandre, J., Hay, W. W., & De Boer, P. L. (2012). Phanerozoic environments of black shale deposition and the Wilson Cycle. Solid Earth, 3(1), 29-42. doi:10.5194/se-3-29-2012

Transform. A Comparative Study of North America's Largest Shale Gas Reservoirs. Retrieved from https://www.transformsw.com/joomla/index.php?option=com_content&view=article&id=67&Itemid=82

Tyson, R. V. (2005). The" productivity versus preservation" controversy: cause, flaws, and

resolution. Special Publication-SEPM, 82, 17.

United States Environmental Protection Agency. (2018, April 12). Sources of Greenhouse Gas Emissions. Retrieved July 27, 2018, from https://www.epa.gov/ghgemissions/sources-greenhouse-gas-emissions

Vengosh, A., Warner, N., Jackson, R., & Darrah, T. (2013). The effects of shale gas exploration and hydraulic fracturing on the quality of water resources in the United States. Procedia Earth and Planetary Science, 7, 863-866.

Vine, J. D., & Tourtelot, E. B. (1970). Geochemistry of black shale deposits; a summary report. Economic Geology, 65(3), 253-272.

Walsh, T. (2011). Microscale Fluid Flow Properties of the Marcellus Shale. Retrieved from http://www.optics.rochester.edu/workgroups/cml/opt307/spr11/talor/Intro.html

Werne, J. P., Sageman, B. B., Lyons, T. W., & Hollander, D. J. (2002). An integrated assessment of a "type euxinic" deposit: evidence for multiple controls on black shale deposition in the Middle Devonian Oatka Creek Formation. American Journal of Science, 302(2), 110-143.

Wignall, P. B. (1994). Black shales (Vol. 30, p. 144). Oxford: Clarendon Press.

Wignall, P. B., & Newton, R. (1998). Pyrite framboid diameter as a measure of oxygen deficiency in ancient mudrocks. American Journal of Science, 298(7), 537-552.

Zielinski, S. (2014, February 13). Natural Gas Really Is Better Than Coal. Retrieved from Smithsonian website: https://www.smithsonianmag.com/science-nature/natural-gas-really-better-coal-180949739/

Appendix 1: Data Summary Tables

Summary of Union Springs

Column/ Sample ID	Depth (cm)	Acid Soluble Iron (wt. %)	Pyritic Iron (wt. %)	Pyritic Sulfur (wt. %)	DOP	Organic Carbon (wt. %)
RB-17	160	0.21	4.18	4.80	0.95	3.93
RB-16	150	0.19	2.35	2.70	0.93	4.02
RB-15	140	0.83	3.26	3.74	0.80	5.13
RB-14	130	0.29	5.66	6.50	0.95	3.97
RB-13	120	0.07	1.13	1.30	0.94	4.50
RB-12	110	0.53	5.78	6.63	0.92	4.48
RB-11	100	2.33	14.11	16.20	0.86	8.16
RB-10	90	1.05	2.94	3.38	0.74	4.53
RB-9	80	0.07	7.68	8.82	0.99	4.36
RB-8	70	0.22	1.95	2.24	0.90	3.41
RB-7	60	0.10	6.60	7.58	0.99	4.04
RB-6	50	0.13	3.04	3.49	0.96	3.83
RB-5	40	0.44	1.85	2.13	0.81	4.90
RB-4	30	0.18	1.87	2.15	0.91	4.35
RB-3	20	0.06	1.12	1.28	0.95	2.71
RB-2	10	0.06	0.42	0.48	0.87	9.64
RB-1	0	0.39	2.10	2.41	0.84	2.49
JD-17	150	0.07	3.27	3.75	0.98	4.46
JD-16	140	0.40	1.47	1.69	0.79	5.35
JD-15	130	0.13	6.20	7.12	0.98	4.11
JD-14	120	0.07	1.28	1.47	0.95	5.15
JD-13	110	0.12	10.77	12.37	0.99	5.67
JD-12	100	0.07	4.83	5.55	0.99	3.97
JD-11	90	0.22	4.72	5.43	0.96	4.74
JD-10	80	0.10	2.44	2.80	0.96	3.32
JD-8	70	0.07	0.46	0.52	0.86	3.73
JD-7	60	0.46	3.01	3.46	0.87	5.12
JD-6	50	0.12	11.68	13.41	0.99	4.19
JD-5	40	0.07	8.30	9.53	0.99	3.64
JD-4	30	0.14	3.04	3.49	0.96	4.10
JD-3	20	0.15	9.86	11.33	0.98	3.09
JD-2	10	0.12	15.59	17.91	0.99	3.63
JD-1	0	0.15	1.58	1.81	0.91	3.62

BD-16	140	0.05	2.56	2.94	0.98	4.63
BD-15	130	0.28	2.98	3.39	0.91	4.38
BD-14	120	0.08	2.84	3.26	0.97	4.75
BD-12	110	0.12	3.78	4.34	0.97	4.76
BD-11	100	0.31	12.74	14.63	0.98	3.63
BD-10	90	0.47	1.90	2.18	0.80	4.68
BD-9	80	0.93	7.16	8.23	0.89	5.10
BD-8	70	0.15	2.96	3.40	0.95	4.34
BD-7	60	0.10	11.55	13.26	0.99	4.72
BD-6	50	0.16	6.24	7.16	0.97	4.33
BD-5	40	0.10	4.61	5.29	0.98	4.38
BD-4	30	0.08	2.65	3.04	0.97	5.14
BD-3	20	0.10	6.78	7.78	0.98	10.15
BD-2	10	0.14	5.99	6.88	0.98	6.72
BD-1	0	0.10	6.05	6.95	0.98	5.48

Table A1-1: Summary of all data utilized in Chapter 2 pertaining to Union Springs 1 – 3.

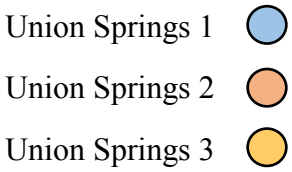

*Collection of each column started at the base of the exposed member and was assigned a starting depth of 0 cm.

**Indicates a DOP value below the anoxic/euxinic boundary of 0.75.

Summary of Oatka Creek						
Column/ Sample ID	**Depth (cm)**	**Acid Soluble Iron (wt. %)**	**Pyritic Iron (wt. %)**	**Pyritic Sulfur (wt. %)**	**DOP**	**Organic Carbon (wt. %)**
D-17	170	0.75	13.61	15.63	0.95	0.57
D-16	160	0.34	7.07	8.12	0.95	1.02
D-15	150	0.28	1.25	1.44	0.82	2.15
D-14	140	0.21	2.72	3.13	0.93	2.88
D-13	130	0.17	3.46	3.97	0.95	5.38
D-12	120	1.33	1.92	2.21	0.59	6.21
D-11	110	0.25	3.89	4.47	0.94	8.64
D-10	100	0.05	3.30	3.79	0.99	4.69
D-9	90	0.32	5.90	6.78	0.95	4.68
D-8	80	0.09	9.76	11.21	0.99	4.38
D-7	70	0.11	3.43	3.94	0.97	6.47
D-6	60	0.28	7.38	8.47	0.96	7.98
D-5	50	0.09	2.87	3.30	0.97	5.58
D-4	40	0.30	4.56	5.24	0.94	10.82
D-3	30	0.16	5.10	5.86	0.97	5.95
D-2	20	0.33	8.56	9.83	0.96	9.75
D-1	10	0.17	24.07	27.64	0.99	6.50
D-BP	0	0.31	5.01	5.75	0.94	4.65

Table A1-2: Summary of all data utilized in Chapter 2 pertaining to Oatka Creek 1.

*Collection of the column started at the base of the exposed member and was assigned a starting depth of 0 cm.

**Indicates a DOP value below the anoxic/euxinic boundary of 0.75.

Supplementary Data of the Union Springs		
Column/Sample ID	**Depth (cm)**	**Organic Carbon (wt. %)**
CK-19	160	4.535
CK-18	150	5.785
CK-16	140	5.950
CK-15	130	10.544
CK-14	120	3.974
CK-13	110	4.942
CK-12	100	4.938
CK-10	90	4.892
CK-9	80	3.939
CK-8	70	4.537
CK-7	60	5.901
CK-6	50	4.004
CK-5	40	4.626
CK-4	30	5.282
CK-3	20	4.128
CK-2	10	5.525
CK-1	0	4.882
DB-17	170	4.684
DB-16	160	4.425
DB-15	150	5.112
DB-14	140	6.078
DB-13b	130	5.623
DB-13a	120	5.955
DB-12	110	5.048
DB-11	100	5.001
DB-10	90	5.535
DB-9	80	5.792
DB-8	70	5.576
DB-7	60	4.808
DB-6	50	4.797
DB-5	40	5.508
DB-4	30	10.084
DB-3	20	5.311
DB-2	10	5.633
DB-1	0	4.895
DJ-20	190	4.414
DJ-19	180	4.369

DJ-18	170	4.035
DJ-17	160	3.968
DJ-16	150	4.139
DJ-15	140	4.809
DJ-14	130	4.426
DJ-13	120	3.713
DJ-12	110	4.131
DJ-11	100	3.889
DJ-10	90	4.609
DJ-9	80	4.115
DJ-8	70	4.388
DJ-7	60	5.022
DJ-6	50	3.844
DJ-5	40	3.536
DJ-4	30	4.087
DJ-3	20	3.639
DJ-2	10	3.311
DJ-1	0	3.943

Table A1-3: Additional depth and TOC data for three columns of the Union Springs otherwise not utilized in the thesis.

*Collection of the column started at the base of the exposed member and was assigned a starting depth of 0 cm.

Additional Depth Profiles

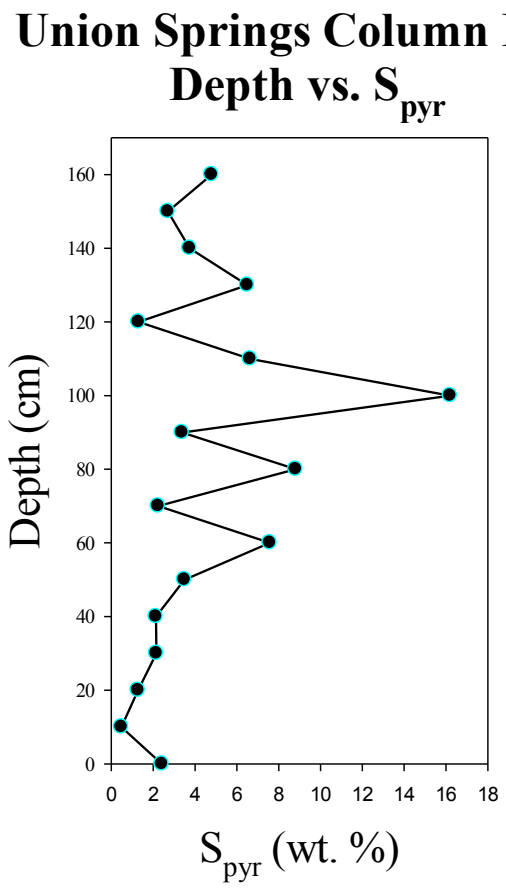

Figure A1-1: Depth vs. S_{pyr} profile of Union Springs 1.

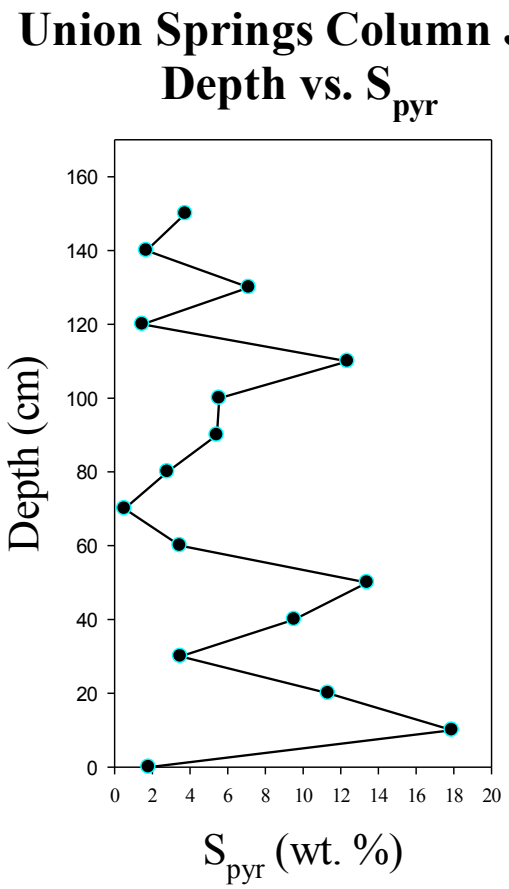

Figure A1-2: Depth vs. S_{pyr} profile of Union Springs 2.

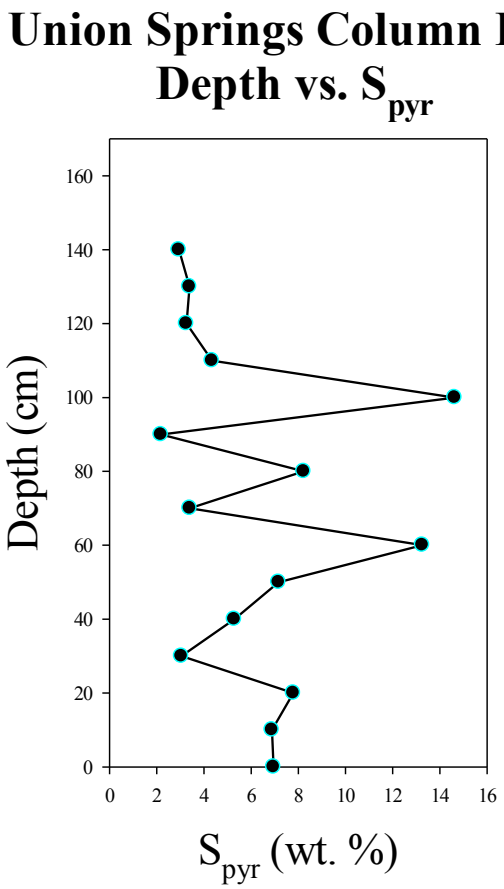

Figure A1-3: Depth vs. S_{pyr} profile of Union Springs 3.

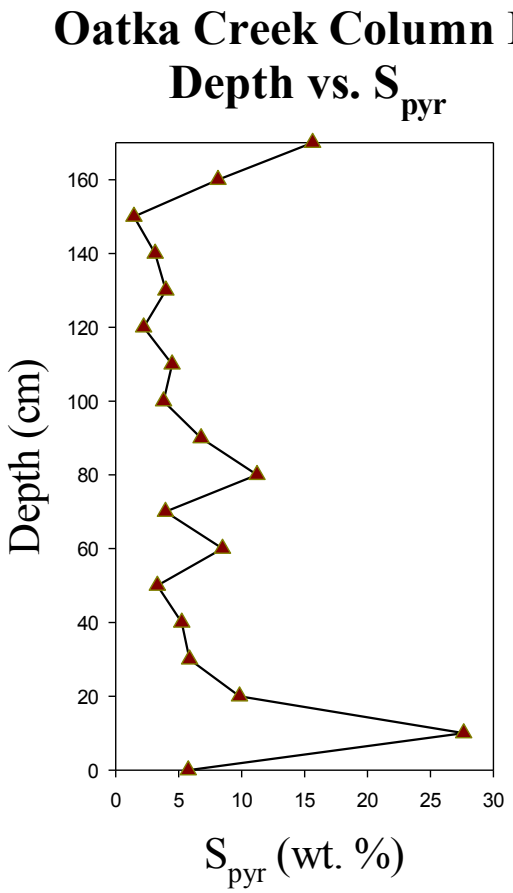

Figure A1-4: Depth vs. S_{pyr} profile of Oatka Creek 1.

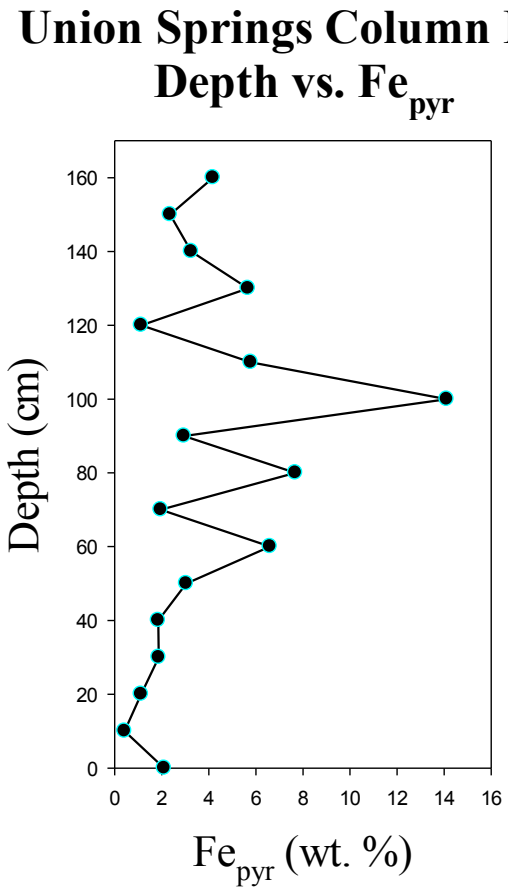

Figure A1-5: Depth vs. Fe_{pyr} profile of Union Springs 1.

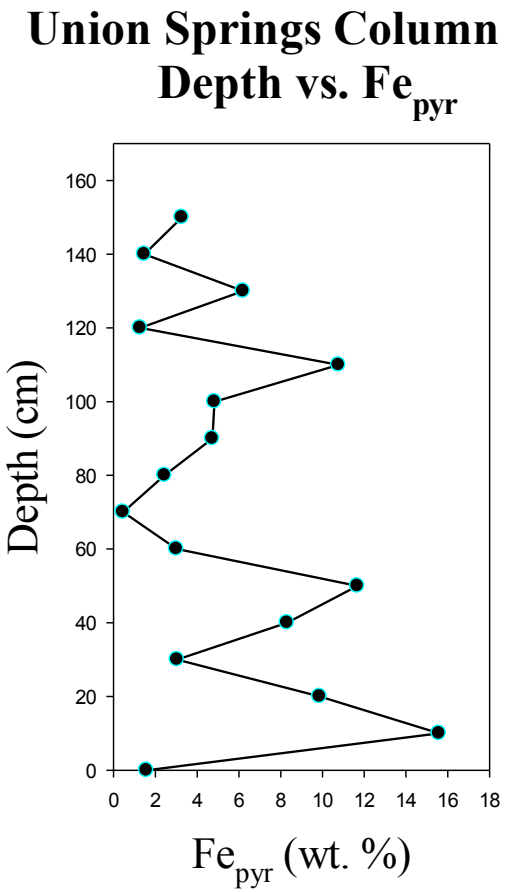

Figure A1-6: Depth vs. Fe_{pyr} profile of Union Springs 2.

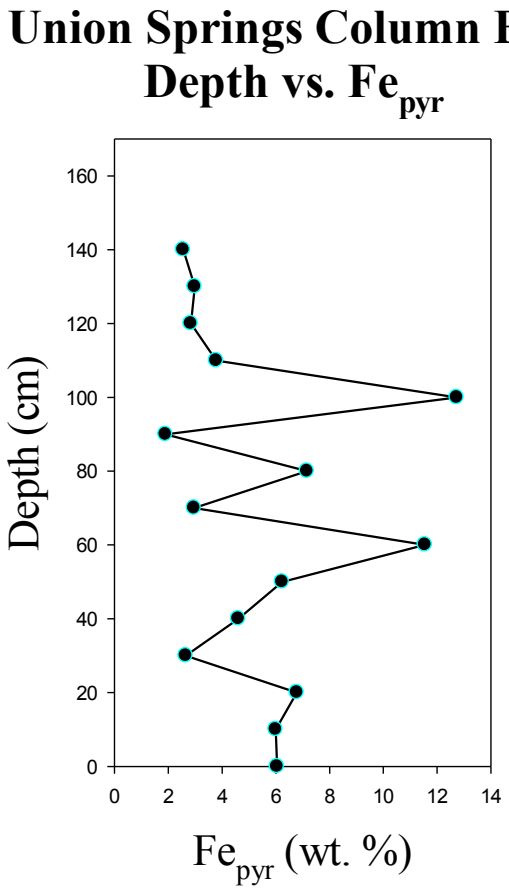

Figure A1-7: Depth vs. Fe_{pyr} profile of Union Springs 3.

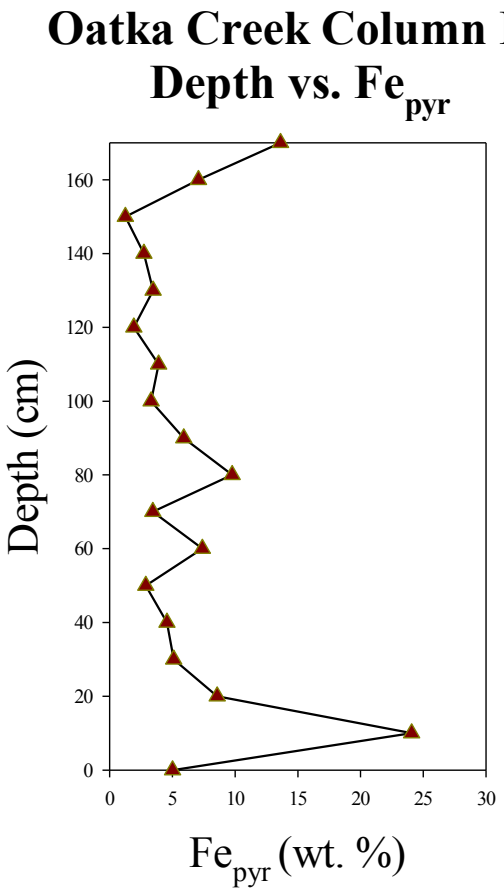

Figure A1-8: Depth vs. Fe_{pyr} profile of Oatka Creek 1.

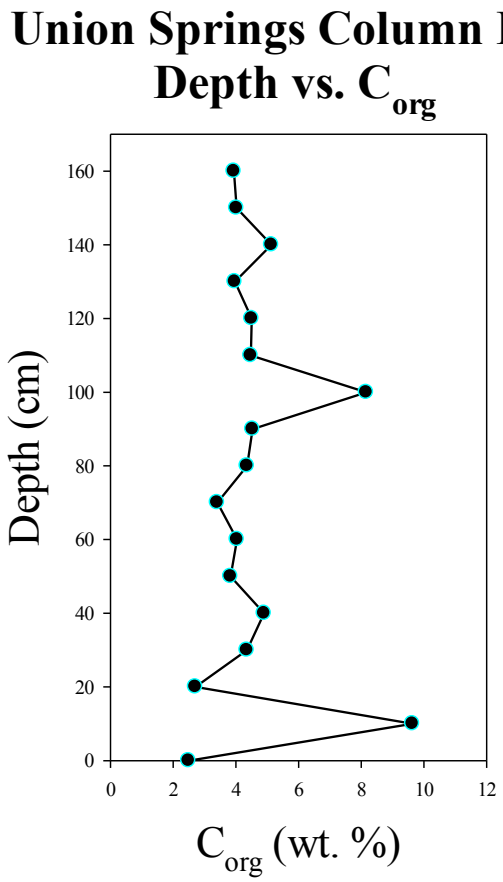

Figure A1-9: Depth vs. C_{org} profile of Union Springs 1.

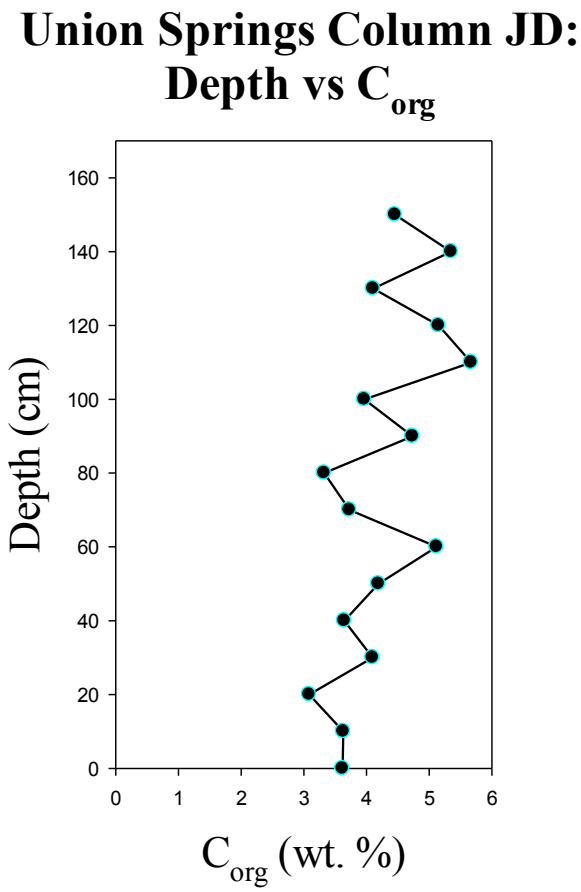

Figure A1-10: Depth vs. C_{org} profile of Union Springs 2.

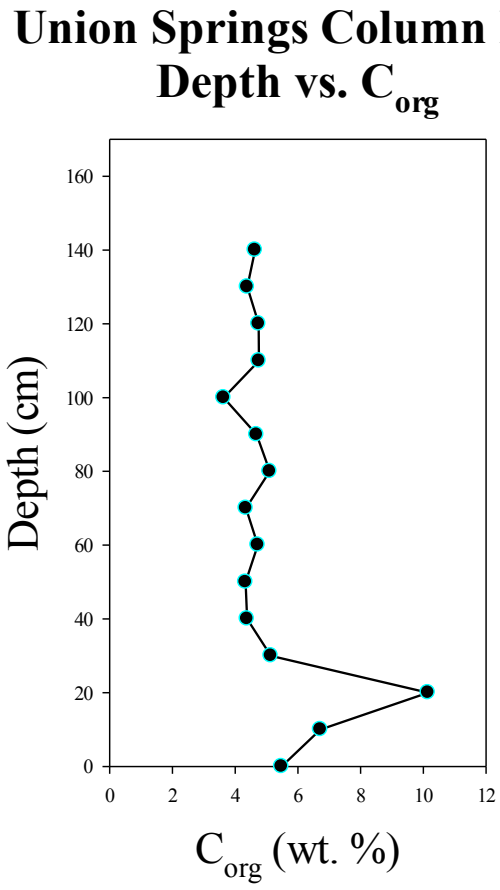

Figure A1-11: Depth vs. C_{org} profile of Union Springs 3.

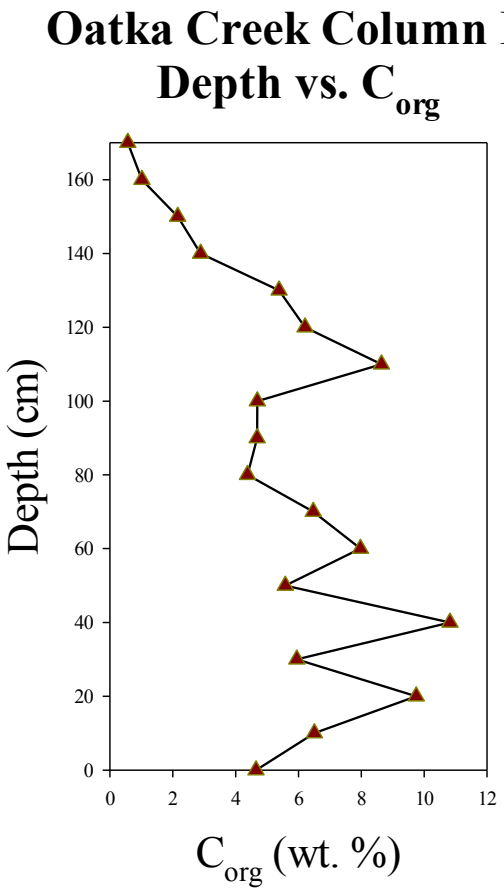

Figure A1-12: Depth vs. C_{org} profile of Oatka Creek 1.

Appendix 2: Standard Operating Procedures

Standard Operating Procedure:

Elemental Analyzer

Table of Contents

Introduction: Standard Operating Procedure for the Elemental Analyzer

The purpose of using the Elemental Analyzer (EA) is to measure (in weight percent) the differences between organic carbon and inorganic carbon values in solid phase samples. For this research, the total organic carbon (TOC) concentration serves as a proxy for evaluating oxygen levels at the time of deposition, particularly when considering its abundance in relation to other proxies such as pyritic sulfur and pyritic iron.

However, because the instrument cannot discern the difference between organic and inorganic carbon, each sample must be prepared in duplicate for separate runs in which one set is acid fumigated for organic carbon analysis and a second set is untreated in order to measure total carbon. Inorganic carbon can be calculated by taking the difference between these results.

Part 1: Acid Fumigation

Samples must be treated using this procedure in order to remove the inorganic carbon fraction of the samples so that the EA only records the isolated organic carbon concentration.

- Use nitrile gloves to avoid contamination of samples and contact with chemicals.
- Samples must be finely powdered to ensure homogeny before proceeding with this process.
- To measure total carbon values on the EA, acid fumigation is not used. Inorganic carbon can be calculated by subtracting the measured organic carbon value from the total carbon value obtained from the EA. For preparation of total carbon samples, finely powder the samples and proceed to Part 2.

➢ Wear safety glasses while working with chemicals to avoid splashes and eye irritation.

1. Scoop the finely powdered samples into their own individual holes within a well tray; fill approximately ¾ full.
    - Rinse the spatula with Milli-Q water and wipe clean with a Kimwipe between each sample.
    - Create a chart that details the positions of each sample if the well tray is not clearly marked.
    - You may choose to fill every other hole in order to prevent cross-contamination of samples in the event of overflow during the acid fumigation process. This can occur in samples with high volatile/inorganic carbon content.

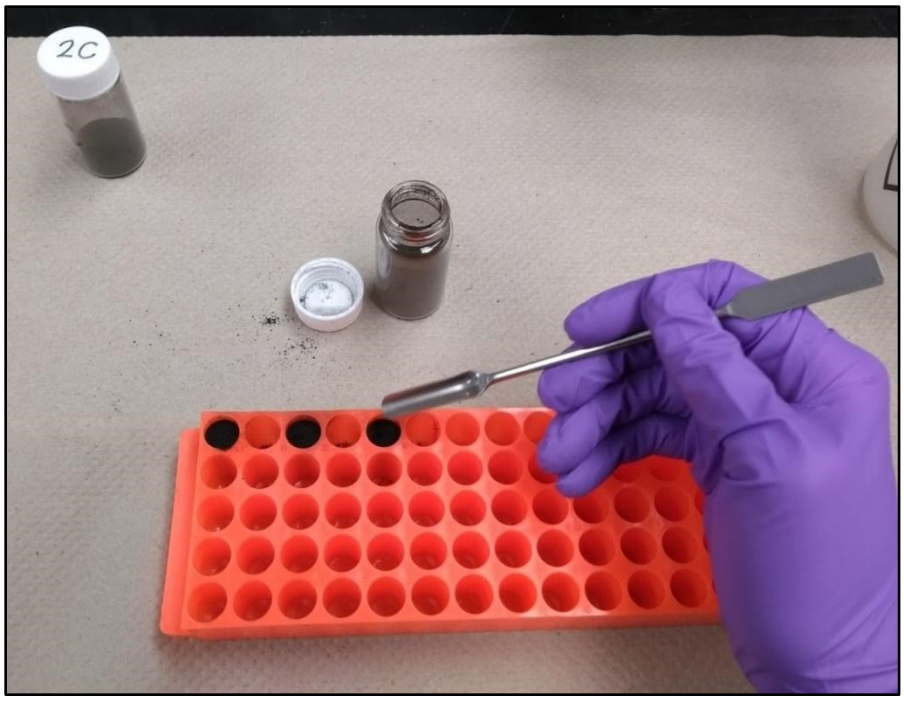

Figure A2-1: Portioning samples into a well tray for acid fumigation.

2. Fill a 500 mL beaker approximately ¾ full (375 mL) with bulk concentrated HCl (12.1 N). Place the beaker and well tray inside a desiccator cabinet sans desiccant.

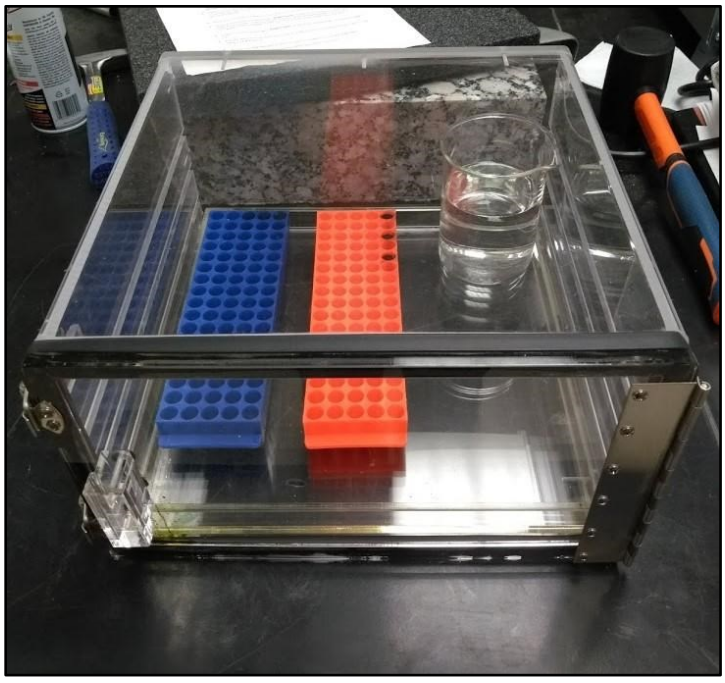

Figure A2-2: Desiccator cabinet readied for acid fumigation with filled sample well trays and beaker of HCl inside.

3. Place the entire cabinet inside a furnace adjusted to 60°C for 24 hours.

- This temperature is necessary to release the inorganic carbon in the form of carbonates such as $CaCO_3$, $FeCO_3$, and $Mg(Ca)CO_3$. In particular, dolomites must be freshly powdered and heated in order to react with the acid vapor.
- Inorganic carbon is released from the samples as CO_2.
- It is fine to allow the sample to heat for as much as 48 hours to ensure all inorganic carbon has cooked off, but 24 hours is typically sufficient.

Figure A2-3: Placing the acid fumigation set-up inside the furnace at 60°C for 24 hours.

4. After the 24 hours, remove the cabinet from the oven using heat resistant gloves and transport it to a fume hood. Once inside the fume hood, open the cabinet door to allow the contents to cool down and for fumes to disperse.
    - Save the HCl for future re-use and store it in a labeled container.
    - ➢ Without proper ventilation provided by the fume hood, the dispersed vapors and gases sealed within the cabinet could lead to eye and lung irritation. Thus, it is important to wait until the cabinet is inside the fume hood before opening the door.

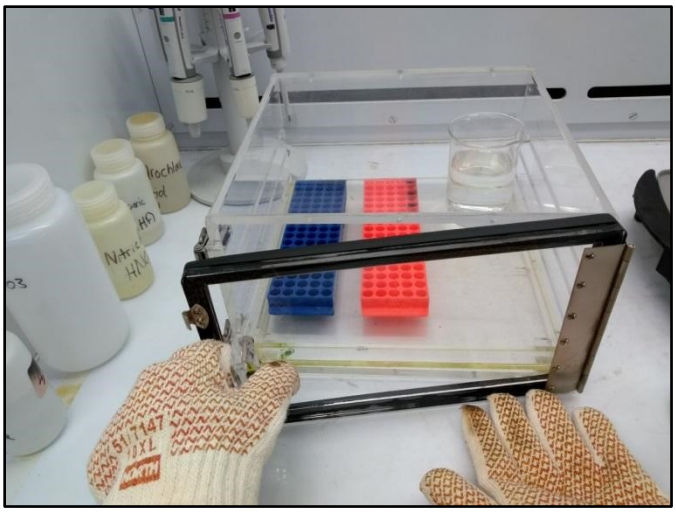

Figure A2-4: Using heat resistant gloves to handle the heated desiccator cabinet and open it within a fume hood.

5. Once the samples have cooled, wrap the well tray in plastic wrap if not yet prepared to weigh them out. Place the wrapped and labeled well tray in a desiccator cabinet (with desiccant) to prevent moisture from entering the samples.

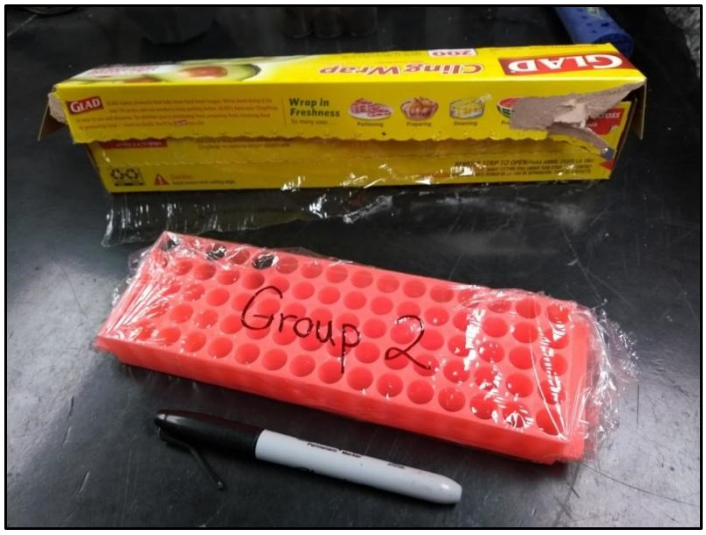

Figure A2-5: Well tray wrapped in plastic wrap and ready for sample weighing.

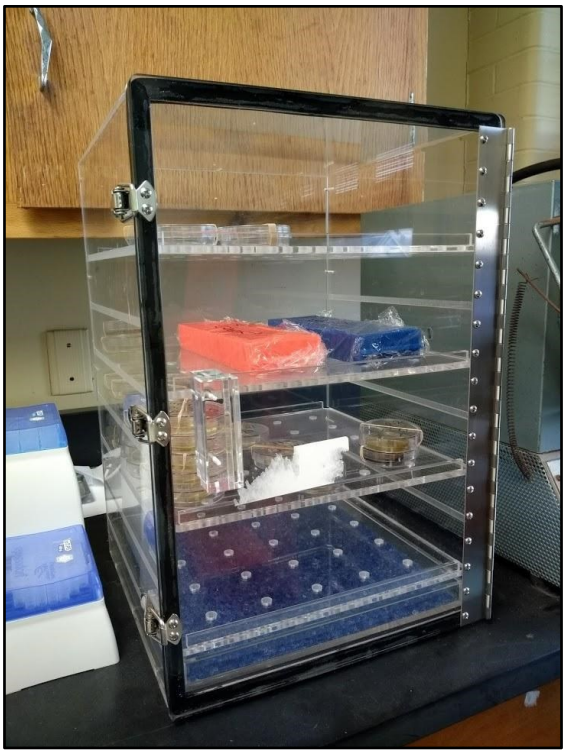

Figure A2-6: Well trays that have undergone acid fumigation and are awaiting weighing. Well trays are stored in a desiccator cabinet to prevent the invasion of moisture.

Part 2: Weighing Acid Fumigated and Non-Acid Fumigated Samples

Once the organic carbon samples have been prepared using acid fumigation, both they and the untreated finely powdered samples meant for total carbon analysis can be weighed on a microbalance.

- Wear nitrile gloves rinsed with acetone to avoid contamination of samples.
- The balance can be highly sensitive to static electricity; an anti-static gun may be useful prior to and during weighing. The anti-static gun only needs to be used as needed, such as when the scale continues to count up or down by 0.001 mg without settling on a final weight.
- Ensure that the bubble on the microbalance is centered so that the scale is leveled before weighing commences. Scales can be moved incremental distances through use even while remaining on the same work surface so it is important to periodically check the level. If the surface is not level, the calibration of the scale can be affected.
- The weighing area will need to be covered in aluminum foil to reduce contamination from the working surface.

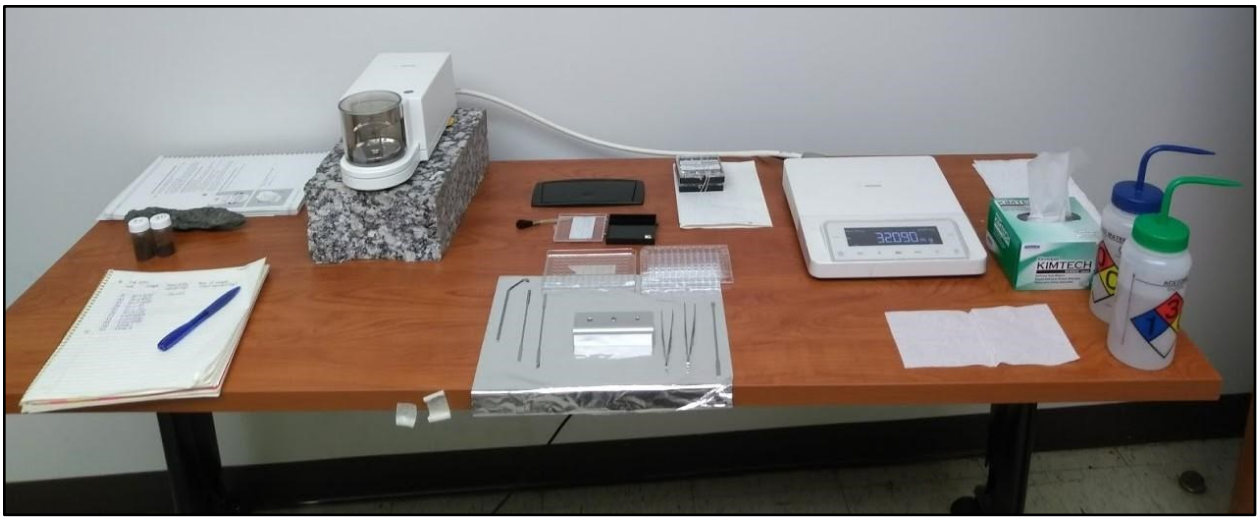

Figure A2-7: Weighing room set-up for measuring EA samples on the microbalance.

1. Set up a lab notebook to record the well tray number prepared samples will be placed into once completed, the sample I.D., the weight of the tin capsule (mg), and the weight of the sample (mg).

2. Using forceps, place an empty tin capsule on the balance and record the weight. With the capsule still on the scale, tare the balance and remove the tin capsule.

Figure A2-8: Using forceps to place an empty tin capsule on the scale.

3. Place the weighed tin capsule into the appropriate sized slot in the capsule plate. Then, using a spatula, transfer 5-7 mg of sample into the capsule. Place the capsule back on the tared balance and record the weight of just the sample.

- Use a small brush to wipe the balance clean of any spilled sample. At the end of the weighing process, or if the scale is in need of cleaning, wipe the weighing platform with acetone and a Kimwipe.

Figure A2-9: Adding sample to the tin capsule held within a slot in the capsule plate.

Figure A2-10: Using a small brush to dust off spilled sample from the scale.

4. Remove the tin capsule with sample from the scale. Next, while holding the capsule with a pair of forceps, take up another pair of forceps in your free hand and begin to close off the capsule to carefully seal the contents inside. This can be done by first clamping shut each end of the capsule and then proceeding to fold it over lengthwise and widthwise before balling it up.
    - This step must be done gently as the tin capsule can be easily pierced by the forceps and the sample can spill free. If this occurs, obtain a new capsule and re-weigh the sample.
    - A nicely compacted ball is needed to ensure a consistent burn during the combustion analysis in the EA.
    - Clean all spatulas, forceps, and the well plate (if needed) between samples by rinsing with Milli-Q water and wiping clean with a Kimwipe.

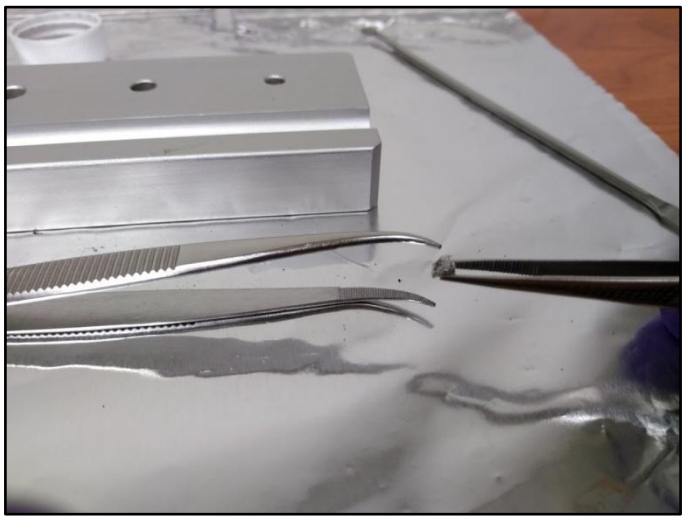

Figure A2-11: Carefully balling up the tin capsule containing the weighed sample.

5. Transfer the balled up sample into a well tray for collection of all prepared EA samples.

Figure A2-12: Placing the completed sample in a well tray.

6. In addition to the unknown samples prepared for analysis, weigh out any available standards of similar composition as well as blanks (empty tin capsules used to periodically clean out the combustion chamber in the EA), checks (acetanilides used to periodically monitor any drift of the instrument during each run), and a calibration curve (a series of acetanilides increasing in weight with known concentrations that can be compared against the concentrations of unknown samples).
    - A linear calibration curve is used to account for how much carbon or nitrogen is in each sample and to check for the precision and accuracy of the instrument. A 7-point calibration curve is typical, including acetanilide samples weighed out in the following increments: 0.250, 0.500. 0.750, 1.000, 1.300, 1.500, and 1.700 (all +/- 0.050 mg).
    - Acetanilides not used in the calibration curve, but used as periodic checks can range between 0.500 – 0.700 mg.
    - The acetanilide standard should be kept in the desiccator cabinet at all times when not in use to prevent contamination and moisture invasion.
    - ➢ Acetanilide can cause skin irritation.

Figure A2-13: The acetanilide standard used for the calibration curve and as periodic check samples throughout the run.

7. Label the well tray and tape up the sides to avoid accidental spills. If not yet prepared to run the samples on the EA, place the sealed well tray inside a desiccator cabinet to keep the samples dry.

Figure A2-14: A completed well tray with weighed out samples, acetanilide standards, and blanks. Well tray is labeled and taped closed.

Part 3: Preparing the Elemental Analyzer

After the samples, acetanilide standards, and blanks have been weighed and placed into a well tray with the appropriate labels, it is now possible to begin testing with the Elemental Analyzer. To begin, the instrument will need to be prepared correctly. Become familiar with the instrument's basic components as shown in Figure A2-15 below.

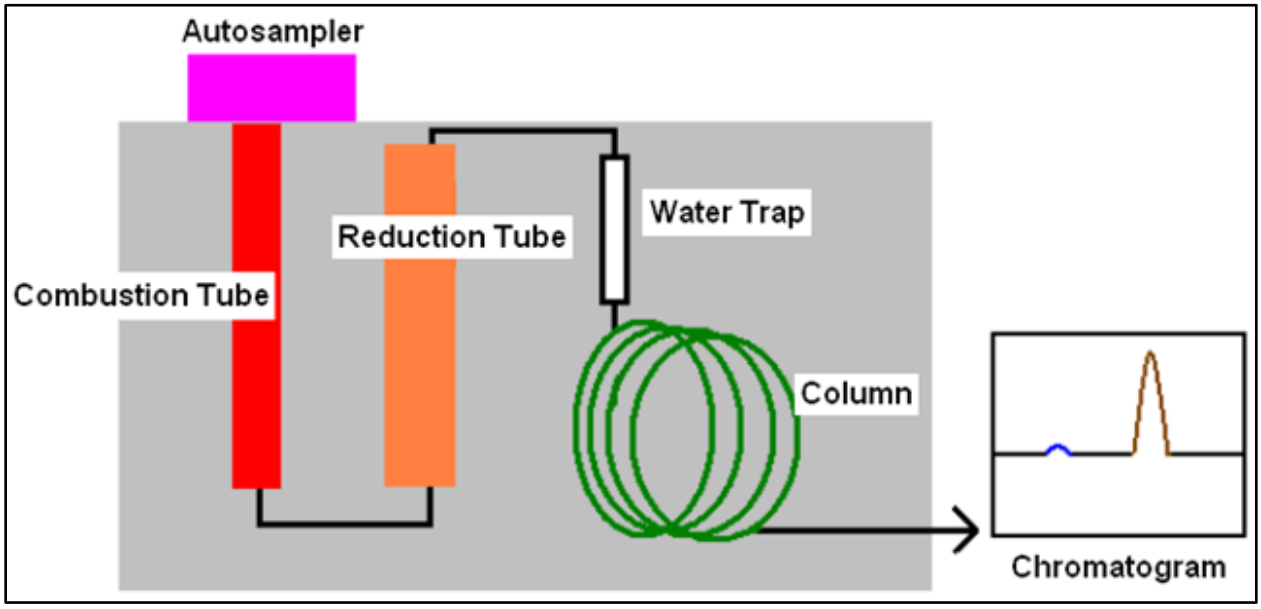

Figure A2-15: A basic schematic showing the position of the EA's various components (credit: Shannon Joseph).

Some of these components must be replaced after running varying numbers of samples:

- Quartz insert (within the combustion column): after every 200 samples
- Combustion column: after every 1,000 samples
- Reduction column: after every 800 samples
- Water trap: after every 300 samples

Figure A2-16: The EA hooked up to the helium, oxygen, and air tanks, as well as the computer.

The autosampler drops the sample into the combustion tube, where the tin-oxygen reaction combusts the sample at a very high temperature. Once the sample has been converted to a gas, helium gas that moves through the system transports the combusted sample to the reaction tube. The reaction tube removes excess oxygen to avoid errors in the reading. Gases then move to the column at different rates, which are recorded as peaks on the chromatogram. Nitrogen will

generate the first peak (shown in blue) and carbon will generate the next peak (the taller peak, shown in brown) as shown in Figure A2-15.

1. Before beginning any runs, the EA will need to be placed into "Work" mode. Press the "work" button on the EA's touchpad and then press "enter." It may take a while for the instrument to warm up. A set of red, blinking lights will turn on, indicating that the columns are starting to heat up. The left oven = 980°C, the right oven = 650°C, and the oven column = 55°C.

Figure A2-17: Touchpad located on the front of the EA.

2. Turn on all three gases: hydrogen, oxygen, and air.
    - To do this, turn the knob at the top of the tank until it is completely open, then turn back 1/4th of a turn. Repeat for all tanks.
    - The helium keeps the other gases circulating through the system. The oxygen is used to combust the samples. The air is used to rotate the autosampler.

- Be sure to turn down the He tank when not in use. Typically, this is the only tank that will need to be opened and closed to operate the instrument.

3. Leak Checks
   It is important to check for leaks as these will prevent the EA from operating effectively.

   - Leaks will be found around the autosampler and inside the EA wherever there are removable parts. There may also be leaks in the water trap.
   - To check for leaks, take a small cap and screw it onto the helium vent (labeled "VHe" and located on the bottom right of the machine). Only screw until finger-tight; do not screw too tightly or this may damage the seal on the inside of the cap.

Figure A2-18: Putting a cap on the helium vent to begin the leak check.

   - Wait 15 seconds or so until the pressure has stabilized then turn the helium gauge down by turning it counter clockwise. Check the pressure reading. If the pressure level remains fixed for at least 30 seconds, then no leaks are present. Turn the helium gauge clockwise until the needle twitches. Remove the cap from the vent and return to a designated location to avoid losing it.

Figure A2-19: Side of the EA with all gas control knobs and gauges.

- If there is a leak, it will need to be fixed.
    - Use a leak detector or, alternatively, a mixture of soap/water to discover where the leak is. For the latter method, if an area bubbles, it is indicative of a leak.
    - To fix, put the Elemental Analyzer into “Standby" mode (st-by-> enter). Tighten any loose connector with a pair of soft-pliers or by hand.
    - Confirm that the connectors on the reduction column, combustion column, and water trap are all secure.
    - Repeat leak-checking procedure above to confirm there is no longer a leak in the system.

4. It is suggested that periodic check-in calls are made to the Costech representatives to check on the most up-to-date maintenance and setting recommendations. For instance, current settings have the “gain” dial to 3 and low.

5. Return to the EA’s touchpad. Select “O_2” and select “semi” for both N and C.

6. Flow Checks

The gases will need to be at a certain level to ensure the EA is back to a good running condition. Checking the flow of the gases will require a flowmeter.

- Begin by turning on the flowmeter.
- Attach the long plastic tube to the helium vent labeled "VHe."
- Twist the He gauge until the Flowmeter screen shows a reading of 100 mL/min (+/-5 mL/min). Remove the long plastic tube.
- Attach the long plastic tube to the oxygen vent labeled "VO_2."
- Twist the unmarked knob that lies directly above the two vents. This controls the flow of oxygen. Adjust the knob until the flowmeter screen shows a reading of 20 mL/min. Remove the long plastic tube from the vent.

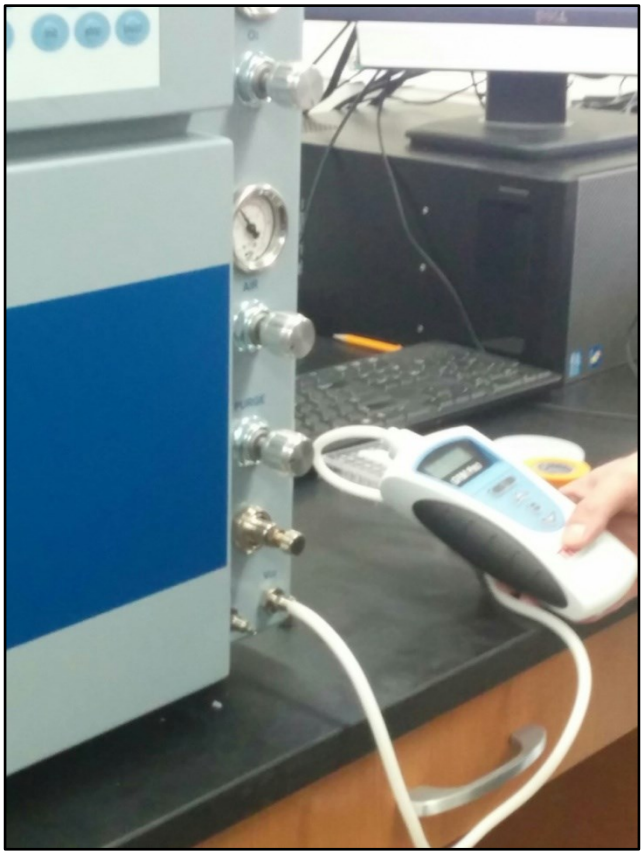

Figure A2-20: Using the Flowmeter to check the flow of gases as described in Step 6 of Part 3.

7. Preparing the Computer Software

- Open the EAS Clarity software by selecting its icon on the computer desktop.
- In the window for Instrument 1, select "Method" then "Measurement" then "NC."

- Select “Analysis” then “Sample Run Time” and input “6 minutes.” This is a standard run time but may be adjusted as needed. For example, samples that are predicted to produce high carbon peaks may require more run time.
- Create a sample table similar to Figure A2-21. It is possible to upload an Excel file or input data directly into the EAS Clarity software.

Sample	**Sample Weight (mg)**	**Well ID**	**Position**
Bypass1	0.0000	A1	1
Bypass2	0.0000	A2	2
Standard1	0.4000	A3	3

Figure A2-21: An example sample table with appropriate headings. Position refers to the sample’s designated position when placed in the autosampler.

Part 4: Performing the Analysis

Once all the necessary preparations have been completed, it is time to run the EA.

1. Load the Autosampler
    - Remove the plastic cover of the autosampler. Do not touch the surface that is in contact with the autosampler so that the cover remains clean.
    - With a pair of clean forceps (wipe with ethanol), position samples into the autosampler according to the sample table in the file.
    - Once all samples have been loaded, replace the clear plastic cover to reduce atmospheric exposure to the samples and combustion tube.
    - Well trays can be cleaned in a 10% HCl bath and re-used.
    - ➢ Always wear gloves when loading samples into the Autosampler to prevent contamination.

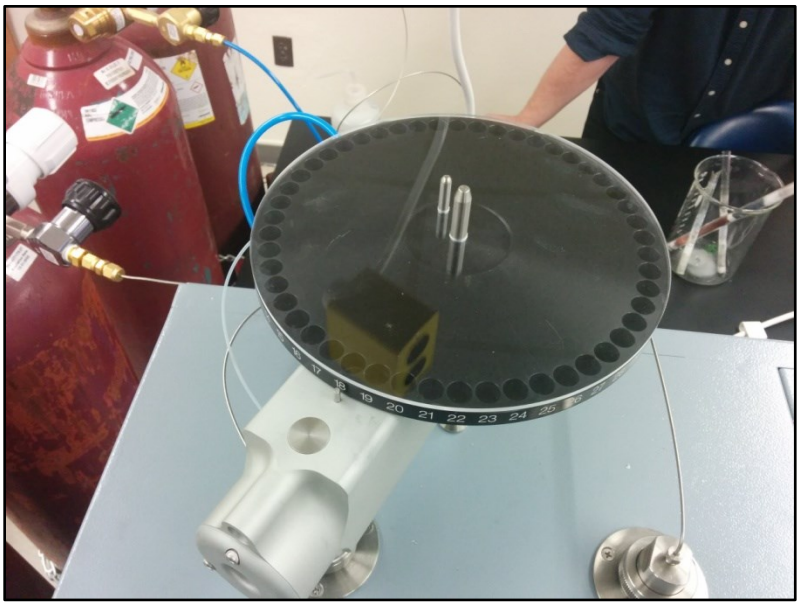

Figure A2-22: The autosampler. The numbers below the holes correspond to the "Position" number from the sample table in Figure A2-21.

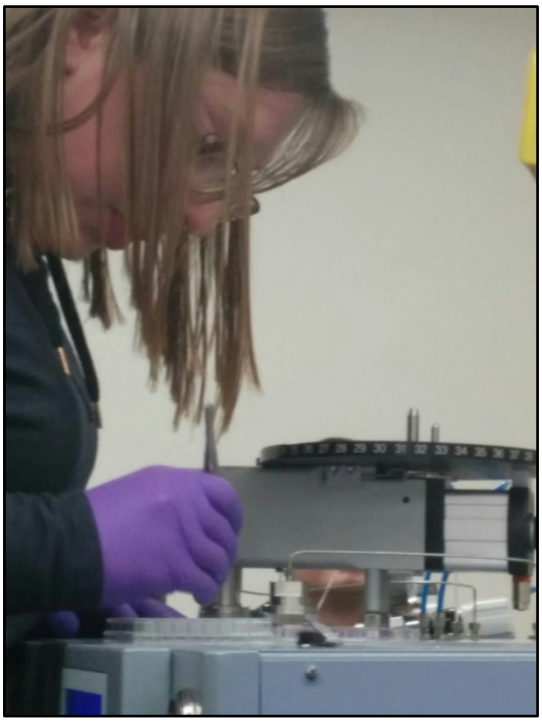

Figure A2-23: Loading samples from the well tray into the autosampler using a pair of clean forceps.

8. Check Detector signal

- Select the "Detector Signal" button to open the data window.
- Make sure the baseline is above zero mV.

- If the mV baseline is negative, turn the dial labeled “Zero” in the upper right hand corner to increase the baseline mV.

9. Setting the Calibration

- Each EA run will consist of: 1) a series of blanks to periodically flush out the system of any lingering residue from previous samples, 2) a series of acetanilide checks to periodically check if the instrument experiences drift over the course of the run, 3) a calibration curve of acetanilides (if analyzing for C and N), 4) the unknown samples, and 5) standards of similar composition to the unknowns.
- The general input of samples into both the autosampler and the sample table should be as follows:
    - blank
    - blank
    - calibration curve samples
    - blank
    - 12 samples
    - blank
    - acetanilide check
    - blank
    - 12 samples
    - ...etc.
- The calibration curve is used to check for error and serves as a reference standard for the EA. These acetanilide samples should not undergo acid fumigation even when a run is meant to capture organic carbon values.
    - Typically, a calibration curve will consist of seven acetanilide standards weighed out in progressively increasing weights. The following may be an example of a 7-point acetanilide calibration curve (weighed in mg): 0.250, 0.500, 0.750, 1.000, 1.300, 1.500, and 1.700 (all +/- 0.050). Acetanilides that are not part of the calibration curve should be measured in the range of 0.500 - 0.700 mg.
    - In the sample table, the calibration curve acetanilides should be identified as acetanilide standards and assigned a level (1, 2, 3, etc.). The remaining acetanilide checks do not need to be identified with an EA standard name.
    - The EA will use the 7-point calibration curve to create a linear calibration to account for how much C and N are in the samples. Precision and accuracy should be strived for in measuring these acetanilides, however, if only one of these qualities is achieved, corrections can be made to the generated linear regression.

    - The linear regression line should be equal to or better than $r^2 = 0.9997$ to be acceptable in the Williams Lab. Most labs require at least $r^2 = 0.997$ and government standards require a minimum of $r^2 = 0.995$.
    - If the linear regression does not meet the minimum r^2 requirement, adjustments can be made to the fit of the line by eliminating points that lack accuracy. Typically, a minimum of three points is required for geochemical analyses, though more is better. In rare cases, such as for a standard, a 1-point curve can be created.
- In the sample table, the first two blanks should be identified as such, but all remaining blanks should be run as unknown samples to help check for instrumentation drift. The first two blanks should not have a weight inputted into the sample table. All other blanks can be assigned a weight of 1.000 mg regardless of actual weight.

10. Running the Elemental Analyzer

- Confirm that the EA is in "Work" mode.
- Lights in the top left hand corner of the touchpad should be green for "left," "right," and "oven." This means that the various EA components are heated to the proper temperature and ready for use. If these green lights do not come on, the EA cannot be used and requires maintenance.
- Press "Remote" then "Enter" to allow the EA to be operated from the computer. The computer does not control the temperature of the ovens, but does control the turning of the autosampler and timing.
- On the computer, confirm that all samples to be run have a check mark in the "Run" column of the sample table. These samples will be highlighted in green.
- Go to the Menu Bar and select "Sample Table" and "Run."
- Click the "Detector Signal" button and a window will appear with the chromatogram. This is the live data.

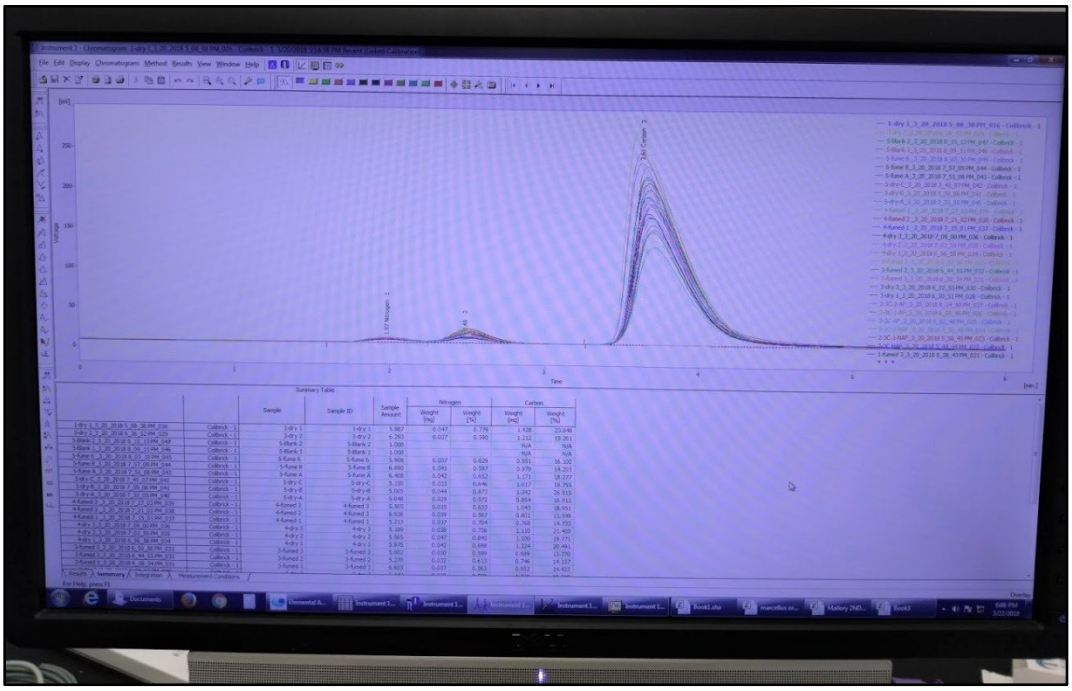

Figure A2-24: Example of a chromatogram showing the capture of nitrogen (first peak) and carbon (third peak). The middle peak was unexpected and likely unique to the set of samples or indicative of the need to change out the reduction column.

11. Summary Table

- Once all samples have been analyzed, a "Summary Table" will appear. Record the retention time information, % nitrogen and % carbon, and the C:N ratio into an Excel spreadsheet and SAVE. All samples in the instrument window should be highlighted in blue to show that they ran successfully.

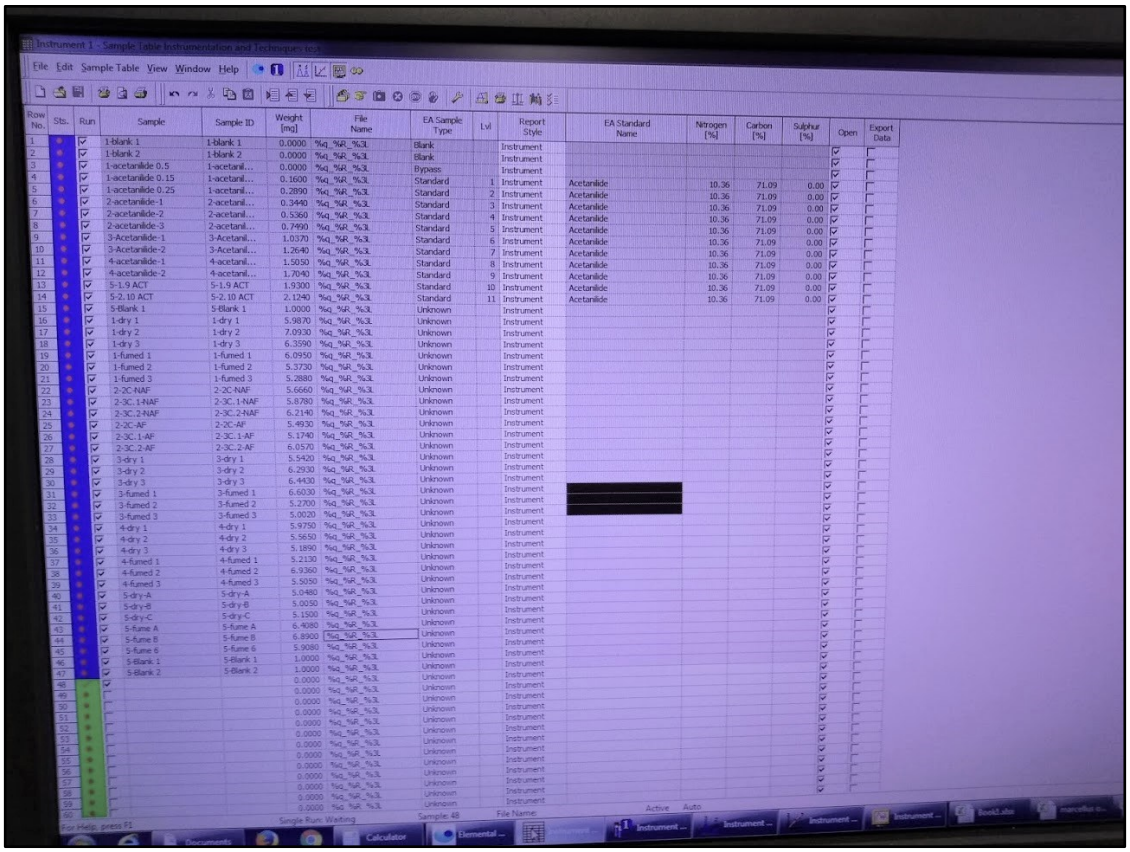

Figure A2-25: Completed EA run showing the sample table with blue boxes next to samples that were analyzed.

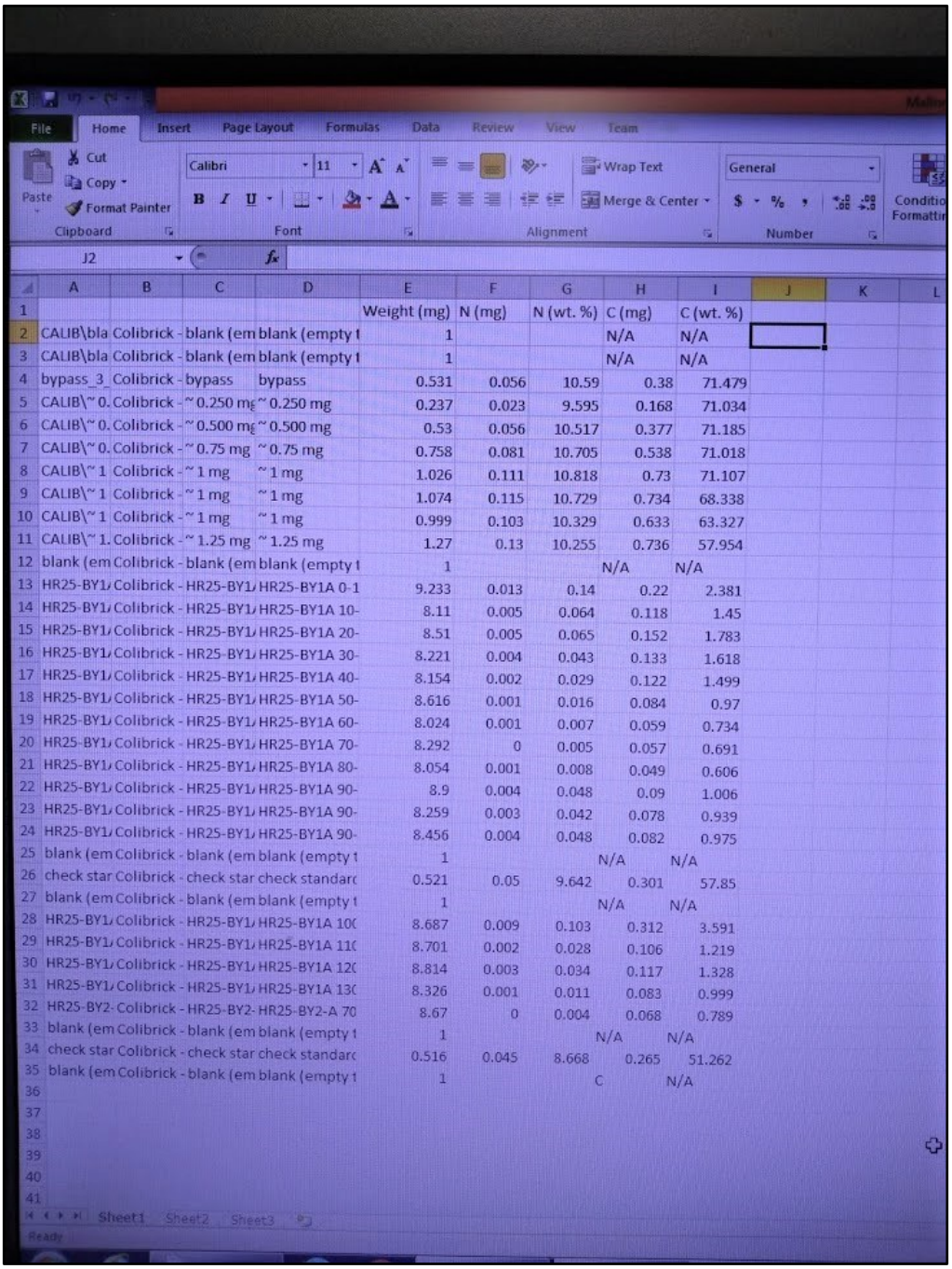

	A	B	C	D	E	F	G	H	I	J	K	L
1					Weight (mg)	N (mg)	N (wt. %)	C (mg)	C (wt. %)			
2	CALIB\bla	Colibrick -	blank (em	blank (empty t	1			N/A	N/A			
3	CALIB\bla	Colibrick -	blank (em	blank (empty t	1			N/A	N/A			
4	bypass_3	Colibrick -	bypass	bypass	0.531	0.056	10.59	0.38	71.479			
5	CALIB\~ 0.	Colibrick -	~ 0.250 mg	~ 0.250 mg	0.237	0.023	9.595	0.168	71.034			
6	CALIB\~ 0.	Colibrick -	~ 0.500 mg	~ 0.500 mg	0.53	0.056	10.517	0.377	71.185			
7	CALIB\~ 0.	Colibrick -	~ 0.75 mg	~ 0.75 mg	0.758	0.081	10.705	0.538	71.018			
8	CALIB\~ 1	Colibrick -	~ 1 mg	~ 1 mg	1.026	0.111	10.818	0.73	71.107			
9	CALIB\~ 1	Colibrick -	~ 1 mg	~ 1 mg	1.074	0.115	10.729	0.734	68.338			
10	CALIB\~ 1	Colibrick -	~ 1 mg	~ 1 mg	0.999	0.103	10.329	0.633	63.327			
11	CALIB\~ 1.	Colibrick -	~ 1.25 mg	~ 1.25 mg	1.27	0.13	10.255	0.736	57.954			
12	blank (em	Colibrick -	blank (em	blank (empty t	1			N/A	N/A			
13	HR25-BY1/	Colibrick -	HR25-BY1/	HR25-BY1A 0-1	9.233	0.013	0.14	0.22	2.381			
14	HR25-BY1/	Colibrick -	HR25-BY1/	HR25-BY1A 10-	8.11	0.005	0.064	0.118	1.45			
15	HR25-BY1/	Colibrick -	HR25-BY1/	HR25-BY1A 20-	8.51	0.005	0.065	0.152	1.783			
16	HR25-BY1/	Colibrick -	HR25-BY1/	HR25-BY1A 30-	8.221	0.004	0.043	0.133	1.618			
17	HR25-BY1/	Colibrick -	HR25-BY1/	HR25-BY1A 40-	8.154	0.002	0.029	0.122	1.499			
18	HR25-BY1/	Colibrick -	HR25-BY1/	HR25-BY1A 50-	8.616	0.001	0.016	0.084	0.97			
19	HR25-BY1/	Colibrick -	HR25-BY1/	HR25-BY1A 60-	8.024	0.001	0.007	0.059	0.734			
20	HR25-BY1/	Colibrick -	HR25-BY1/	HR25-BY1A 70-	8.292	0	0.005	0.057	0.691			
21	HR25-BY1/	Colibrick -	HR25-BY1/	HR25-BY1A 80-	8.054	0.001	0.008	0.049	0.606			
22	HR25-BY1/	Colibrick -	HR25-BY1/	HR25-BY1A 90-	8.9	0.004	0.048	0.09	1.006			
23	HR25-BY1/	Colibrick -	HR25-BY1/	HR25-BY1A 90-	8.259	0.003	0.042	0.078	0.939			
24	HR25-BY1/	Colibrick -	HR25-BY1/	HR25-BY1A 90-	8.456	0.004	0.048	0.082	0.975			
25	blank (em	Colibrick -	blank (em	blank (empty t	1			N/A	N/A			
26	check star	Colibrick -	check star	check standarc	0.521	0.05	9.642	0.301	57.85			
27	blank (em	Colibrick -	blank (em	blank (empty t	1			N/A	N/A			
28	HR25-BY1/	Colibrick -	HR25-BY1/	HR25-BY1A 10(	8.687	0.009	0.103	0.312	3.591			
29	HR25-BY1/	Colibrick -	HR25-BY1/	HR25-BY1A 11(	8.701	0.002	0.028	0.106	1.219			
30	HR25-BY1/	Colibrick -	HR25-BY1/	HR25-BY1A 12(	8.814	0.003	0.034	0.117	1.328			
31	HR25-BY1/	Colibrick -	HR25-BY1/	HR25-BY1A 13(	8.326	0.001	0.011	0.083	0.999			
32	HR25-BY2-	Colibrick -	HR25-BY2-	HR25-BY2-A 70	8.67	0	0.004	0.068	0.789			
33	blank (em	Colibrick -	blank (em	blank (empty t	1			N/A	N/A			
34	check star	Colibrick -	check star	check standarc	0.516	0.045	8.668	0.265	51.262			
35	blank (em	Colibrick -	blank (em	blank (empty t	1			C	N/A			
36												
37												
38												
39												
40												
41												

Figure A2-26: An example of an exported data file in Excel displaying carbon and nitrogen abundances.

12. Shutting Down the EA

- Close out of the EAS Clarity software.
- Return to the EA touchpad. Select “Abort” and “Enter” to exit “Remote” mode.
- Select “Local” then “Enter” then “St-by” (standby) then “Enter.”
- Return to the gas tanks and turn down the helium gas tank.

Standard Operating Procedure:
Degree of Pyritization

Table of Contents

Standard Operating Procedure for Degree of Pyritization

The purpose of this technique is to experimentally acquire the pyritic sulfur, pyritic iron, and reactive iron values for black shale samples. These values are used in the following DOP equation to establish a discrete value that correlates to oxygen conditions:

$$DOP = \frac{\text{pyritic Fe}}{\text{pyritic Fe + acid soluble Fe}}$$

Part 1: Powdering to Achieve a Homogenous Sample

A homogeneous sample is favorable to ensure that no matter which section of the sample is analyzed, the properties are the same throughout. Random selection of any portion of the sample would yield the same results, as would selecting the entire sample for analysis.

- Use nitrile gloves to avoid contamination of sample.

1. Crush the bulk sample with a rock hammer against a clean granite slab to produce small chips of rock. Hammer the sample into as fine of a powder as possible.
    - Use Milli-Q water and a Kimwipe to clean the slab as needed.
    - Use of the slab prevents damage to the tabletop.
    - Depending on the number and types of analyses used, varying quantities of powder will eventually be needed; aim for 20-30 g of sample to start with so that extra is on hand if needed.
    - ➢ Be mindful of finger placement when hammering.
    - ➢ Wear safety glasses to protect eyes from flying shards of rock and irritating rock dust.
    - ➢ Take advantage of any cleavage planes present when you strike to use less effort.

Figure A2-27: Hammering sample against granite slab.

2. Collect rock chips/powder into a mortar to further grind the sample into finer grain sizes with the pestle. This will improve the result the ball mill produces and can reduce the time spent on this step.
    - Use an agate mortar and pestle since a typical ceramic version is too breakable and would lead to contamination as ground particles of ceramic would mix with the sample.

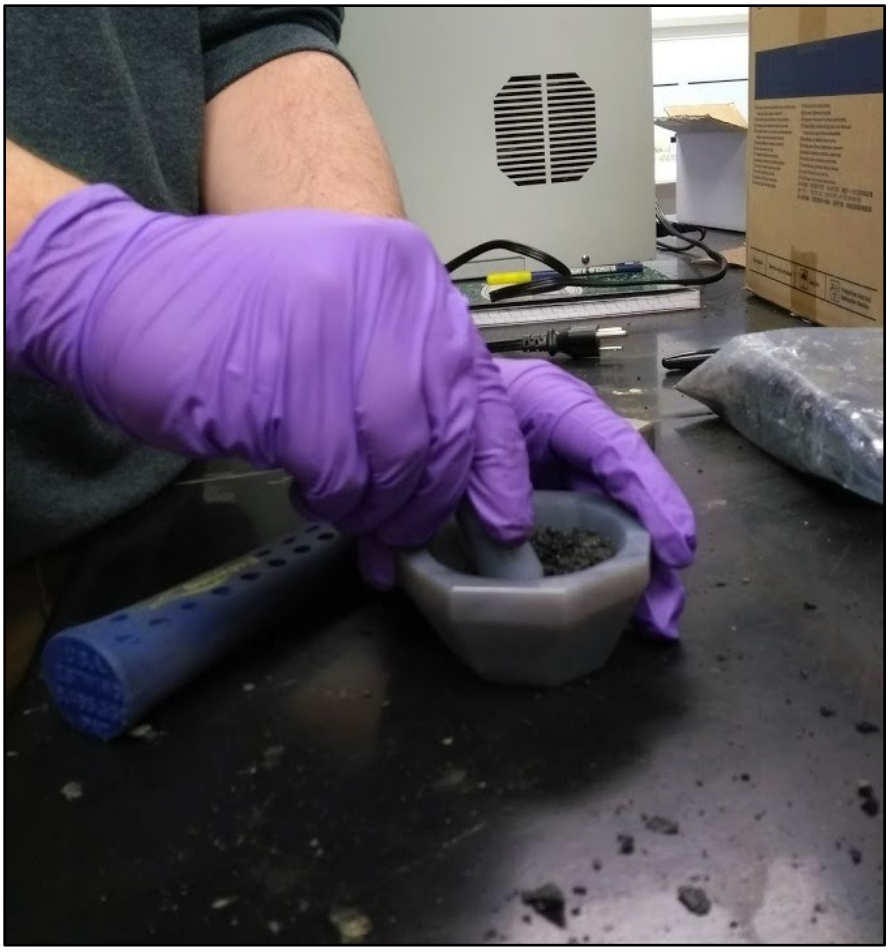

Figure A2-28: Grounding hammered sample with agate mortar and pestle.

3. Transfer the ground sample into a tungsten capsule along with the ball. Ensure that each cork ring is placed securely along the inside rim of each lid and that lids on each end are screwed on as tightly as possible. Otherwise, lids can loosen during shaking in the instrument and can lead to sample loss.
    - Never run a capsule in the ball mill with a ball and no sample as this will cause damage to the capsule.

Figure A2-29: Unassembled capsule, ball, lids, and cork rings.

4. Put the assembled capsule inside the SPEX Sample Prep 8000M ball mill holder and make adjustments to accommodate the size of the capsule. To secure it in place, first screw down the larger clamp, and then be sure to screw down the smaller clamp that is closer to the capsule holder.
    - Both clamps must be tightened as far as they can to ensure the capsule is not flung out of the holder, which could cause severe damage to the instrument.

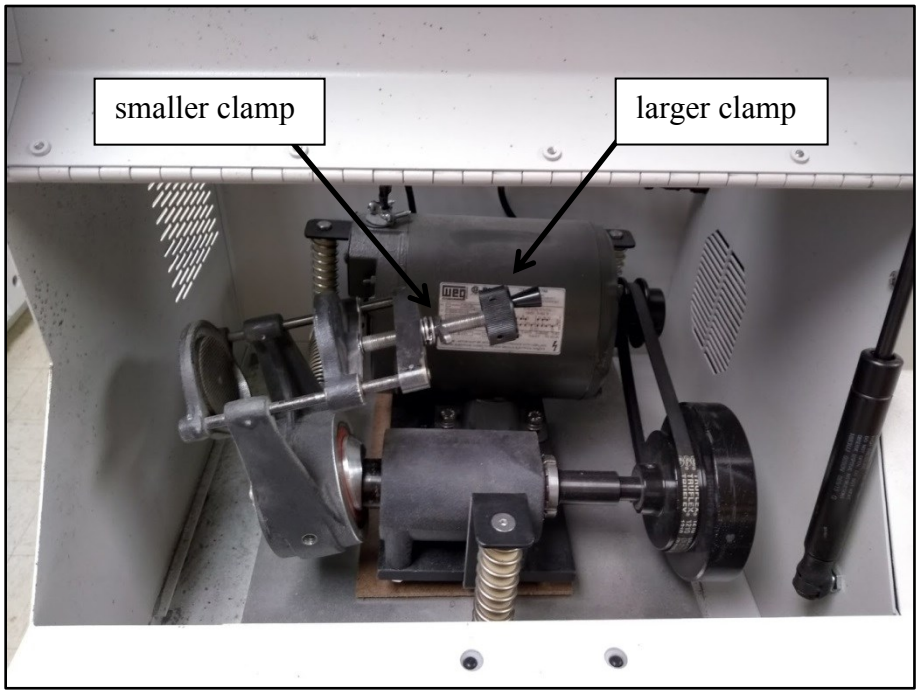

Figure A2-30: Inside view of the SPEX Sample Prep 8000M ball mill.

Figure A2-31: Placing the assembled tungsten capsule into its holder and tightening the clamps.

5. Shut and latch the lid of the instrument, turn it on, set the timer to count down from 5 minutes (or adjust time as needed), and press "start."
    - If the capsule should come loose during the run, immediately stop the run and shut off the instrument. Assess any damage and clean up any spilled sample inside the ball mill.

6. While the capsule is shaken back and forth in a figure eight motion, label the vial the sample will be funneled into. Write sample ID labels on both the glass side of the vial and on the plastic cap in case caps are accidentally lost or switched.

7. When the run is complete, remove the capsule from the holder by first untightening the smaller clamp and then the larger clamp. Shut and latch the lid and turn off the instrument if finished running samples.

8. Funnel the finely powdered sample into a labeled glass vial.

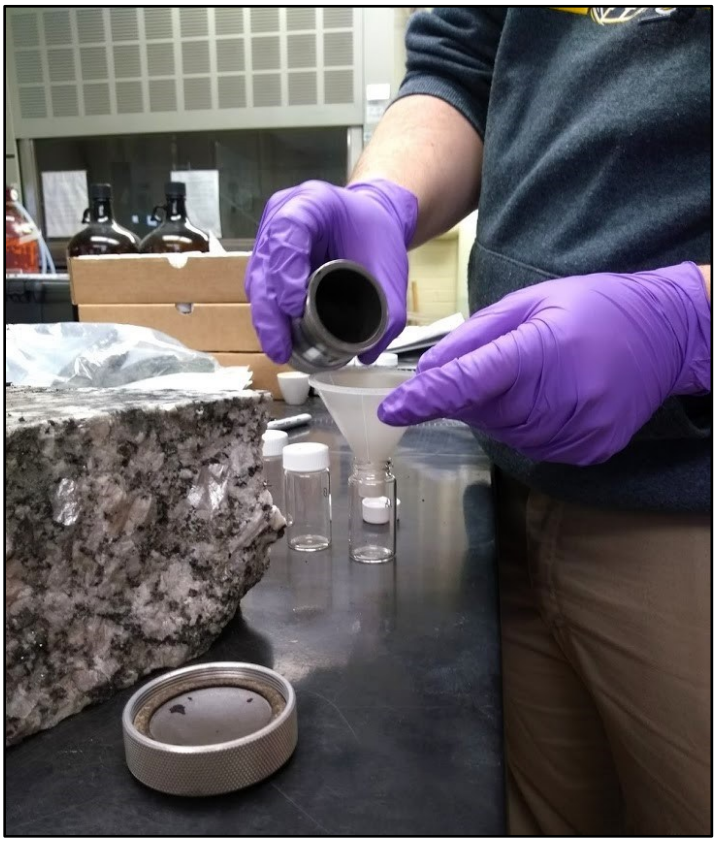

Figure A2-32: Funneling powdered sample into vial.

Clean-Up:

Wash the funnel with Milli-Q water and wipe with a Kimwipe to remove any powder residue. Disassemble the ball mill capsule for cleaning. Clean the cork rings with Milli-Q water only (methanol will cause them to deteriorate). Clean the ball, lids, and capsule with soap and water, rinse with Milli-Q water, and, lastly, rinse with methanol. Wipe the insides of the lids and inside of the capsule with a Kimwipe before placing everything on a towel to air dry.

Part 2: Purge and Trap Assembly Using a Chromium-Reducible Sulfur Technique

This process achieves a final filtration product of Ag_2S that is weighed to obtain the pyritic sulfur content of the sample (this assumes that all present sulfur was in the form of pyrite). Through mathematical manipulation, the pyritic iron content is calculated.

- Use nitrile gloves to avoid contamination of sample.
- Prior to running the samples, prepare the folded tin foil squares enclosing each filter. Label the outside with the sample ID. Using an analytical balance, record the weight for each of these foil/filter combinations.

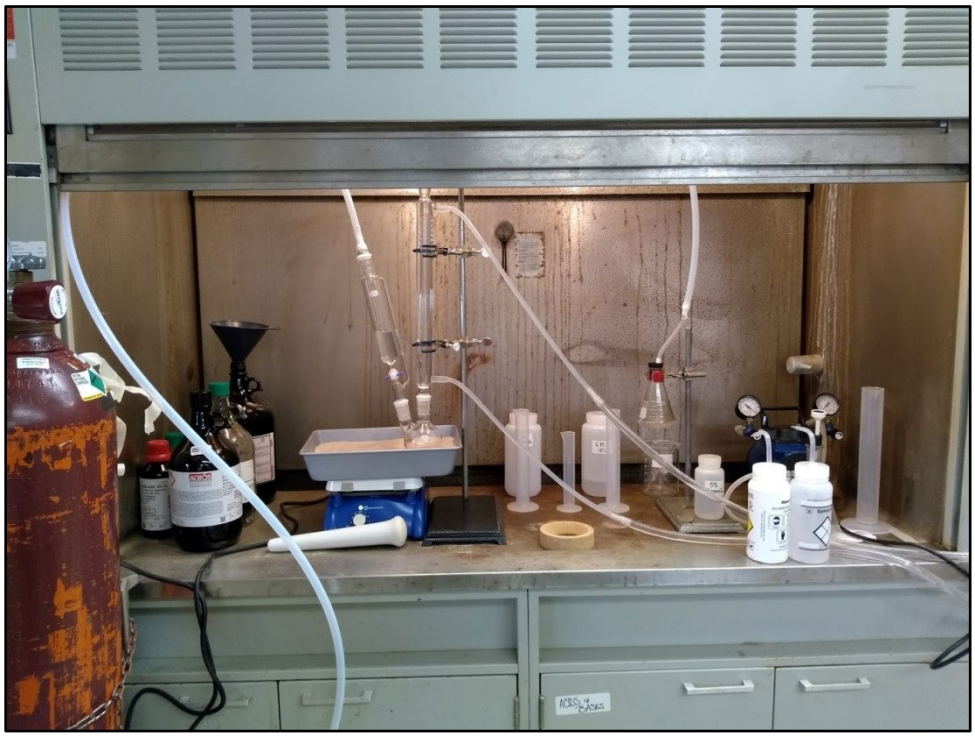

Figure A2-33: Degree of pyritization set-up to obtain pyritic sulfur and pyritic iron values.

1. Turn on the hot plate. Hook up the condenser to a running water source.
    - Temperature settings may vary between hot plates and will require experimentation to find what works best for the given equipment. A light boil is needed for the initial heating.
    - The tube running from the lower stem of the condenser should be connected to the water spout (may use tap water) while the tube connected to the upper stem runs to the drain.
    - The water running inside the condenser should be calm with few to no bubbles; lower the water pressure if necessary.

Figure A2-34: Hot plate turned on to begin heating the sand bath. The condenser is clamped into the ring stand with the upper tubing leading to the drain and the lower tubing attached to the running water supply.

2. Fold a piece of weighing paper diagonally in half and place it on the analytical balance. Tare the balance. Use a spatula to weigh approximately 0.05 g of powdered shale sample onto the weighing paper. Record the weight. Pour the sample into the round-bottom flask (rb-flask).
    - Clean the spatula with Milli-Q water and a Kimwipe.

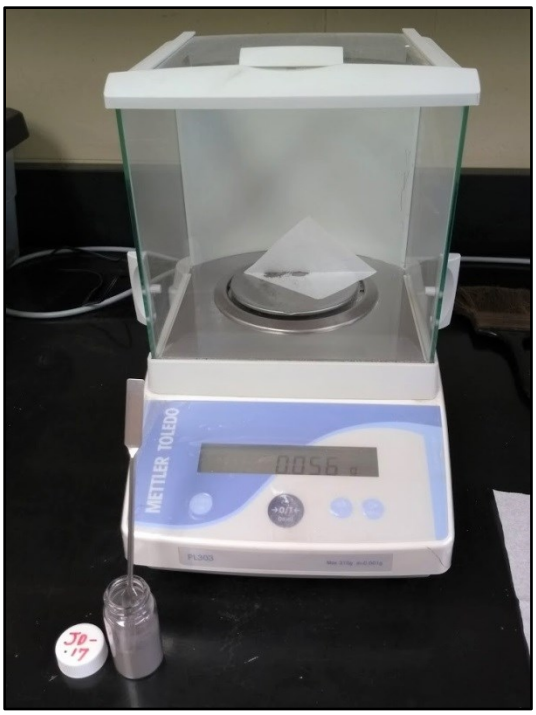

Figure A2-35: Weighing out powdered sample.

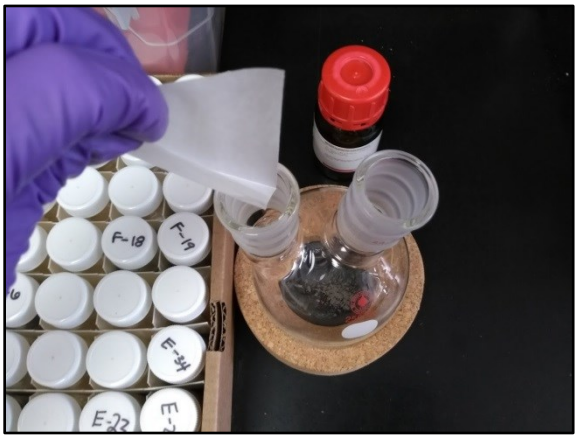

Figure A2-36: Pouring weighed sample into the rb-flask.

3. Re-use the same piece of weighing paper and place it back on the scale. Tare the weight. Weigh approximately 2.04-2.07 g of chromium powder. You do not need to record this weight. Pour the powder into the rb-flask.
    - Clean the spatula with Milli-Q water and a Kimwipe.

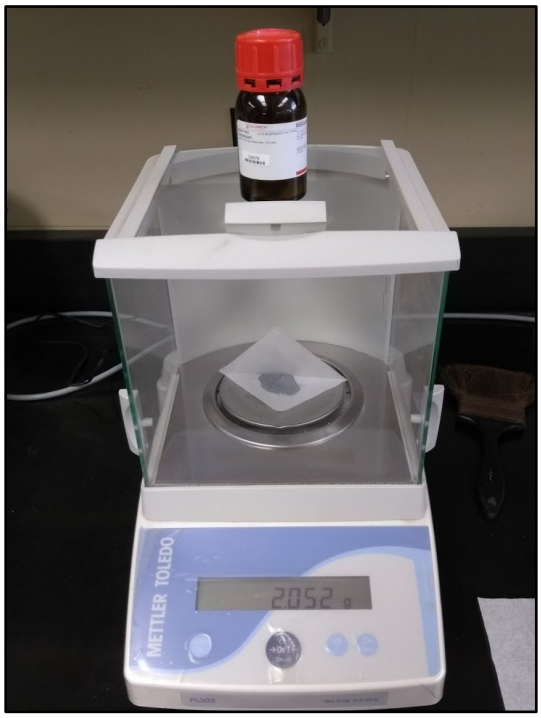

Figure A2-37: Weighing out chromium powder.

4. Measure the following volumes into separate graduated cylinders:
    - Zinc acetate = 40 mL
    - Ethanol = 10 mL (be exact)
    - Hydrochloric acid = 60 mL (be exact)

Figure A2-38: Measured volumes of zinc acetate, ethanol, and hydrochloric acid.

5. Put an Erlenmeyer flask (E-flask) into the clamp on the far right of the assembly. Pour the ZnAc into the E-flask.

Figure A2-39: Clamping the E-flask onto its ring stand.

6. Carefully, fit a glass pipette through a cork stopper so that only a small portion of the pipette is visible at the top of the stopper. Set this to the side. Place the removable tube/glass adapter combination into the top of the condenser. Fit the glass pipette/stopper combination into the end of the open tube. Next, fit the stopper into the open E-flask so that the pipette tip is beneath the surface of the ZnAc.

Figure A2-40: Pushing the glass pipette through the stopper.

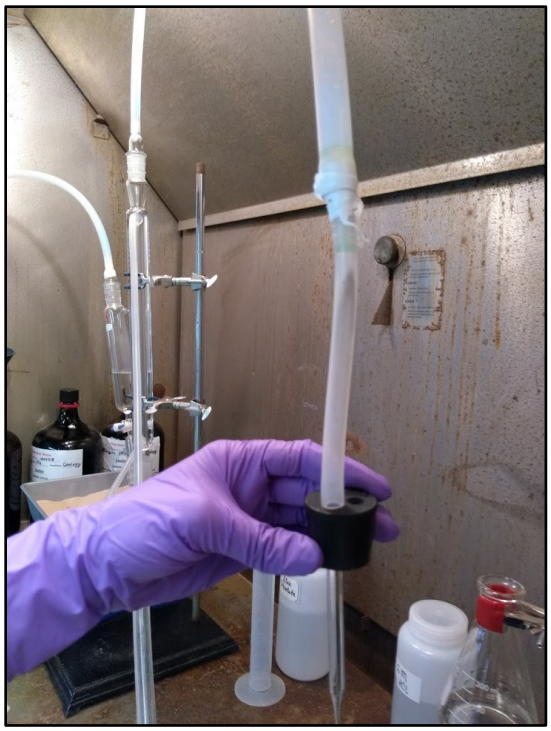

Figure A2-41: Attaching the glass pipette/stopper combination into the open end of the tube.

Figure A2-42: The E-flask with the stopper and glass pipette in place and attached to the tubing leading back to the condenser.

7. Pour the ethanol into the rb-flask and maneuver the flask so that it is connected to the bottom joint of the condenser. This will require loosening the clamps holding the condenser to accommodate the height of the rb-flask. The condenser should fit into the straight neck of the rb-flask. The rb-flask will be sitting in the sand bath.

Figure A2-43: Joining the rb-flask to the bottom of the condenser.

8. Fit the funnel into the slanted neck of the rb-flask. Ensure that the stopcock is in the closed position. Next, carefully pour the HCl into the funnel so that it trickles down the back wall.

Figure A2-44: Pouring the measured HCl into the closed funnel.

9. Attach the nitrogen tank tube to the top of the funnel.

Figure A2-45: Attaching the nitrogen tank tube into the top of the funnel.

10. Use the silver handle on the top of the nitrogen tank to fully open it; turn in the direction as indicated on the handle. Then, use the large maroon knob on the regulator to generate a

vigorous flow through the system. Flow should be great enough to produce strong bubbling in the E-flask. Set a timer for 5 minutes.

- This allows the system time to flush out any oxygen that may otherwise interfere with the reactants.

Figure A2-46: Nitrogen tank with silver handle on top to open and close the tank and the regulator with the large knob between the two gauges to increase or decrease the pull of flow.

11. During the 5 minutes, cut pieces of Teflon tape and apply them to all five connected joints in the assembly in order to prevent gas leakage.
    - Any leaks should be apparent by a hissing sound emanating from the specific joint. This may require adjusting the fit of the glassware pieces to ensure one joint is completely within the connecting joint to the fullest extent before applying the tape.
    - If running multiple samples throughout the day, tape scraps from a previous sample can be saved for the following one to provide extra coverage.

Figure A2-47: Tape around funnel/rb-flask joint and condenser/rb-flask joint.

Figure A2-48: Tape around nitrogen tube/funnel joint and removable tube/condenser joint.

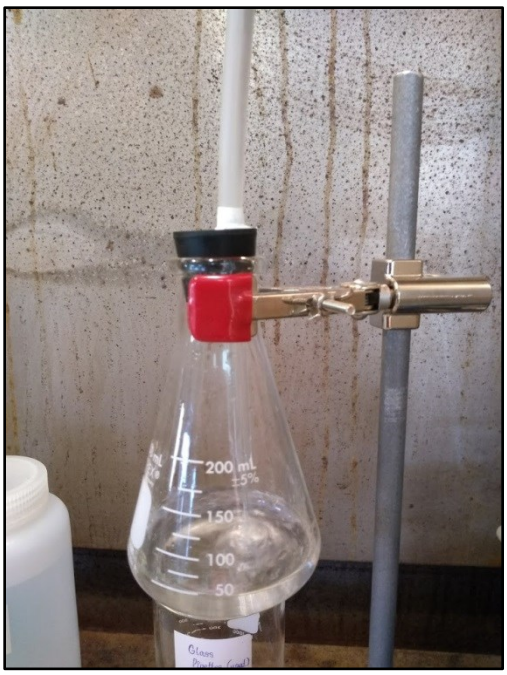

Figure A2-49: Tape around tubing and pipette connection.

12. Once the timer goes off and the joints have been taped, turn down the flow of N_2 gas so that a less vigorous, but steady stream is visible in the E-flask. Then, release the stopcock on the funnel to allow one drop of HCl at a time to be released into the rb-flask. Build up the sand around the sides of the rb-flask for insulation and to encourage faster boiling.
    - You will be pulling < 1 psi of N_2.
    - If this is not the first sample of the day, wait to turn on the hot plate until this point to avoid boiling the sample too soon.

Figure A2-50: Releasing the HCl in a steady drip from the funnel.

Figure A2-51: Building up sand around the rb-flask with an available ceramic pestle.

13. Once all of the HCl has been released, watch for the contents in the rb-flask to begin boiling.

- This boiling should not be intense. You do not want the contents to splatter against the walls of the flask. Boiling may occur as intense swirling on the surface of the green solution accompanied with some light bubbling.

14. Once boiling has commenced, set the timer for 1 hour. Give the set-up a gentle shake to stir up the contents in the rb-flask and prevent any sample from adhering to the walls of the flask. Shaking can be done by gently placing one hand on the funnel and the other around either the condenser or the ring stand holding the condenser. Give a light shake to produce a circular sloshing motion in the contents of the rb-flask.
    - During this 1 hour, periodically give the set-up a gentle shake to stir the contents of the rb-flask and re-build the sand mound surrounding the flask (approximately every 10-12 minutes).
    - Make adjustments to the nitrogen tank regulator as needed to maintain a constant, steady flow.
    - If the solution in the E-flask becomes cloudy, add more ZnAc. Keep track of this extra added volume on a scrap piece of paper.

15. When the timer goes off, turn off the hot plate and turn off the nitrogen flow. Close the nitrogen tank using the handle on top of the tank and turning it in the correct direction as labeled on the handle.

16. Lift the cork free from the E-flask and, using a Milli-Q squirt bottle, rinse off any solution on the pipette into the E-flask.

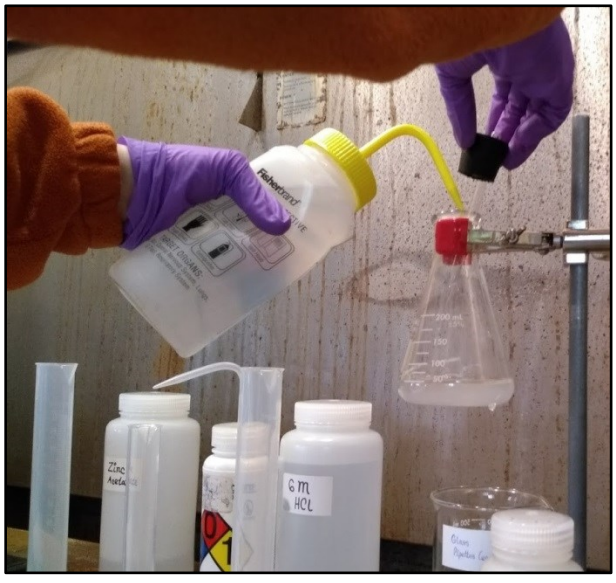

Figure A2-52: Rinsing the pipette with Milli-Q water.

17. Using a graduated cylinder, measure 20 mL of silver nitrate solution.

- More $AgNO_3$ is required if extra ZnAc was added to correct for cloudiness. Add the 20 mL in addition to the equivalent amount of extra ZnAc.
- Please note that the $AgNO_3$ solution is photosensitive and should be covered in aluminum foil to minimize exposure. When not in use, keep the solution stored in a cabinet and away from light.

Figure A2-53: Silver nitrate solution container wrapped in aluminum foil to reduce exposure to light.

18. Pour the $AgNO_3$ into the E-flask and briskly swirl the contents so that precipitate forms.
    - This precipitate is Ag_2S and is the final product that is captured on the filter paper.
    - Set this flask off to the side and begin disassembling the set-up for cleaning and/or preparation of the next sample.

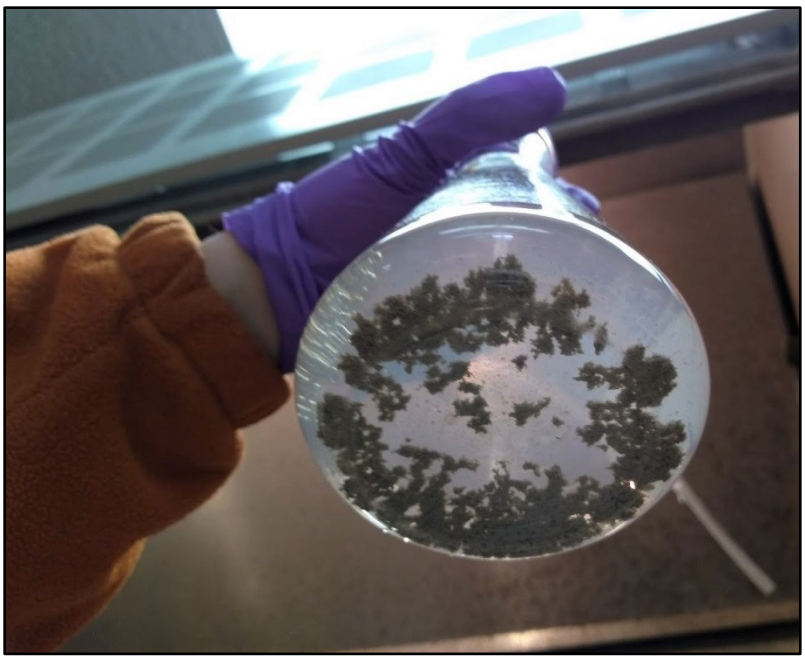

Figure A2-54: Precipitate forming and settling in the E-flask after swirling.

Clean-Up:

Peel off the Teflon tape pieces and either discard or keep the scraps for the next sample. Dispose of the pipette in the broken glass bucket (pipettes are not re-used in this procedure). Disconnect the tube/glass adapter combination that leads back to the condenser; rinse the adapter and insides of the tubing with ethanol and allow to air dry. Disconnect the funnel and rinse with ethanol; allow to air dry. Disconnect the rb-flask (use heat resistant gloves if it is still hot) and pour the contents into their own labeled waste container. Use Milli-Q water to quick-rinse the insides of the flask and pour this into the waste container as well. Then, wash the rb-flask with first Milli-Q water and then ethanol; allow to air dry.

The waste container for the rb-flask contents should be labeled as “chromium chloride and hydrochloric acid” as well as “corrosive.”

If continuing with another sample, proceed with the above steps again until the sample is on the 1 hour countdown before returning to the previous sample awaiting filtration. When ready, proceed to step 19.

19. Plug in vacuum and attach the vacuum hose to a large filtration flask. Use a Milli-Q squirt bottle to wet the surface where the filter will be placed.

20. Carefully, unfold the edges of the pre-weighed foil/filter combination. Using forceps, remove the filter and place it on the filtration stage. Be sure to center the filter so that no gaps in coverage exist. Then, turn on the vacuum.

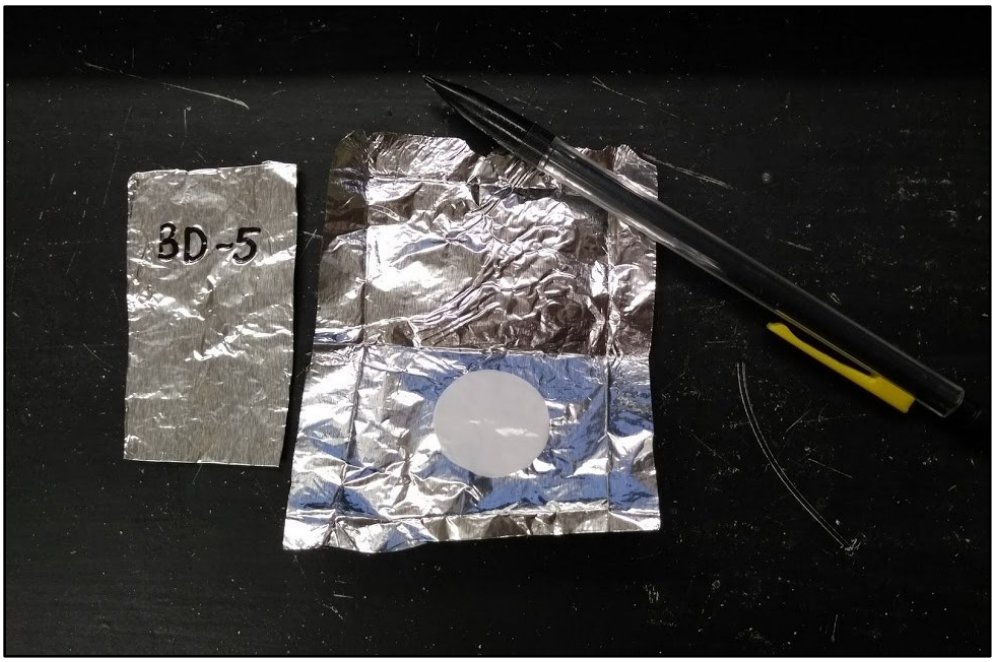

Figure A2-55: Labeled foil/filter combination.

Figure A2-56: Placing the filter on the filtration stage.

21. Attach the fitted plastic funnel over the filter stage and screw down into place. Test the seal of the filter by squirting Milli-Q water into the funnel.
    - If there is a hissing sound, the vacuum should be shut off and the funnel removed so that adjustments can be made to the positioning of the filter.

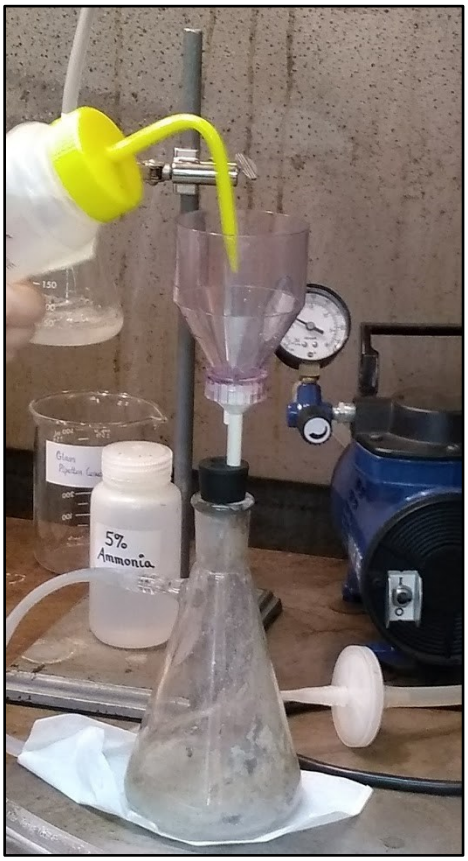

Figure A2-57: Using Milli-Q water to check for successful filter coverage.

22. When the seal has been tested and approved of, swirl the contents of the E-flask and pour out a small portion into the funnel. Repeat this several times.

Figure A2-58: Pouring out E-flask contents into filtration system.

23. Once all contents of the E-flask have been poured and filtered, use an ammonia squirt bottle to rinse the insides of the E-flask for any remaining final product and pour this into the filter.

24. Pour more ammonia into the filtration system to dissolve as much solid material on the filter as possible. Repeat this ammonia rinse until satisfied.

25. Use the Milli-Q squirt bottle to rinse the insides of the funnel clean of any remnants/residue. Repeat this several times until satisfied.

26. Once all solutions have filtered through, remove the funnel, turn off the vacuum, and gently detach the vacuum hose from the filtration flask.

27. Use forceps to carefully remove the filter and place it back into its foil wrapper. Fold the filter in half to retain its content and then carefully fold the foil and close off all edges.

Figure A2-59: Filter with final product of Ag_2S.

28. Place the finished sample(s) into a furnace heated at 70°C in order to remove any moisture prior to weighing. Leave the sample(s) overnight to dry (approximately 16-24 hours) and then weigh the foil/filter combination(s) to obtain the weight of the foil/filter combination + sample. A final weight is calculated by taking the difference between this weight and the initial weight.

Figure A2-60: Furnace used for drying samples.

Clean-Up:

Wash the plastic filtration funnel with Milli-Q water and wipe it dry with a Kimwipe to remove any lingering residue; allow to air dry. Wash the E-flask with a brush and Milli-Q water; allow to air dry. Empty the contents of the large filtration flask into their own designated waste container. This flask does not need to be cleaned for re-use in this procedure.

The waste container for the large filtration flask contents should be labeled as "zinc acetate and silver nitrate" as well as "toxic waste."

Chromium reduction reagents for the above chromium-reducible sulfur technique:

1. 6 M HCl in 1 L:
    - Add 500 mL of 12 M HCl to 500 mL of Milli-Q water.

2. zinc acetate solution in 1 L:
    - Weigh out 30 g of zinc acetate powder.
    - Fill a 1 L container approximately ¾ full of Milli-Q water and add the powder.
    - Dissolve the powder using a stir plate and stir bar.
    - Once dissolved, add remaining Milli-Q water for a complete 1 L container.

3. 0.1 M silver nitrate solution in 500 mL:
    - Weigh out 8.493 g of $AgNO_3$ powder
    - Fill a 500 mL container approximately ¾ full of Milli-Q water and add the powder.
    - Dissolve the powder using a stir plate and stir bar.
    - Once dissolved, add remaining Milli-Q water for a complete 500 mL container.

4. 5% ammonia solution:
    - Add 200 mL of Milli-Q water to a 250 mL container.
    - Add 12.5 mL of concentrated ammonia to the container.
    - Shake container to mix the solution.
    - Add remaining Milli-Q water for a complete 250 mL container.

Part 3: Preparation for ICP-OES

The following process is designed to obtain the HCl-extractable iron (acid soluble iron) portion of each black shale sample. With this value and the pyritic iron values found through the above experimental procedure, the DOP equation can be used to assign a value for each sample.

- Use nitrile gloves to avoid contamination of sample.

1. Weigh approximately 0.1 g of powdered shale sample using a semi-microbalance Record the weight and transfer the sample to a labeled 15 mL test tube. To prepare standards, skip to step 8.

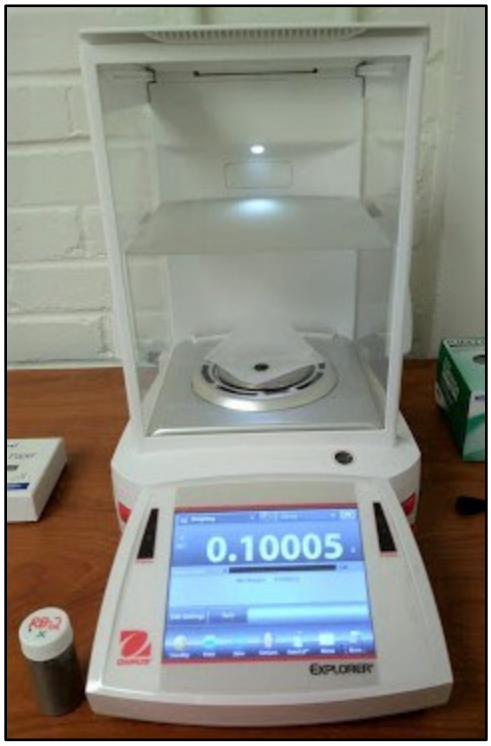

Figure A2-61: Weighing sample on semi-microbalance.

Figure A2-62: Weighed sample in a labeled 15 mL test tube.

2. Turn on the hot plate to heat the sand bath. Pre-measure 5 mL of 12.1 HCl into a graduated cylinder and 10 mL of Milli-Q water into a separate graduated cylinder.

Figure A2-63: Pre-measuring 5 mL of HCl.

3. When the sand bath has been heated to allow for boiling, remove the cap on the test tube containing the sample and pour in the measured HCl. Stick the test tube into the sand bath so that it can stand upright. Set a timer for 1 minute.

Figure A2-64: Boiling sample for 1 minute.

4. When the timer goes off, remove the test tube and immediately add the measured Milli-Q water. Cap the test tube.

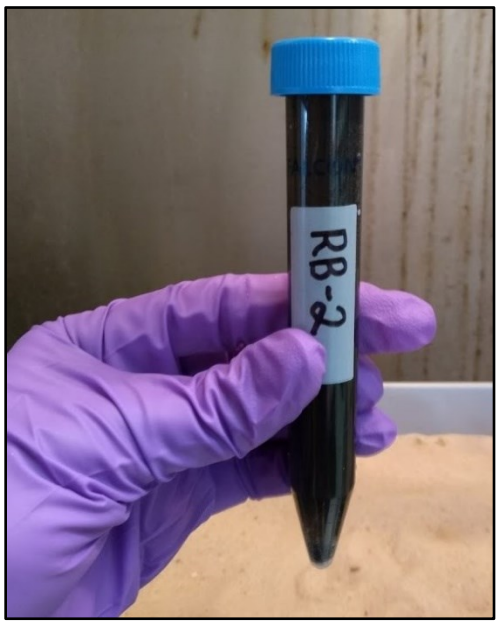

Figure A2-65: Quenched sample with 10 mL of Milli-Q water.

5. To filter the sample, first pour the solution into a clean beaker. Use a syringe of appropriate volume to extract the solution. Attach a filter to the syringe and eject the solution into a new, labeled 15 mL test tube. Discard the filter. Syringes can be re-used if using a cleaning solution of 2% HNO_3 between samples.

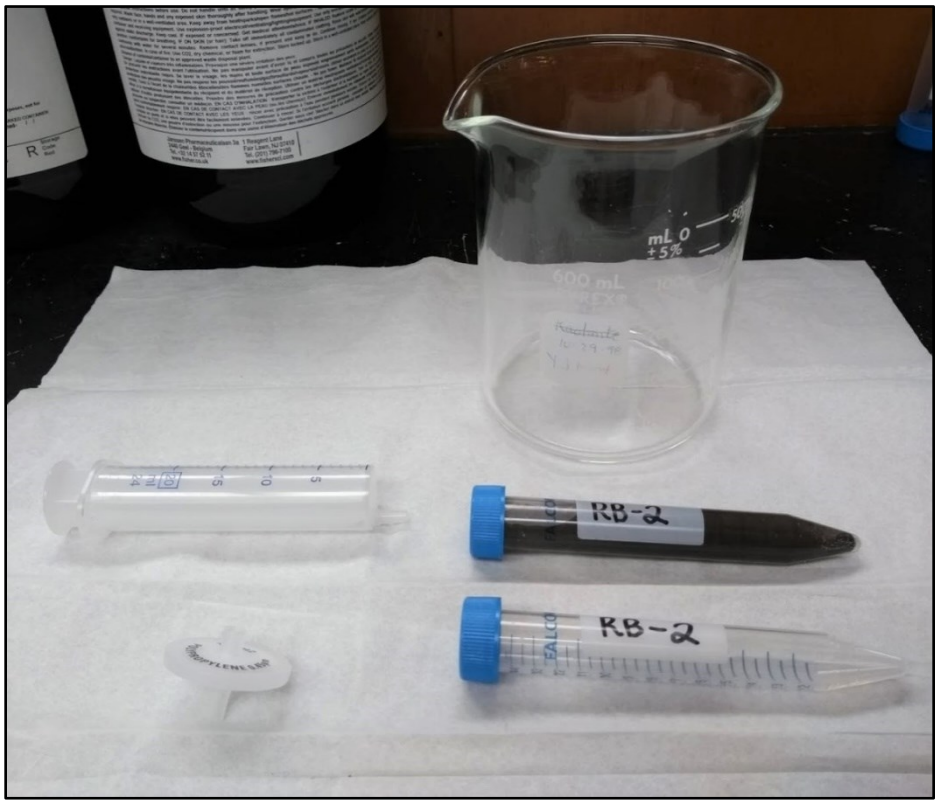

Figure A2-66: Materials needed for filtering samples include a beaker, a syringe, a filter, and a new test tube.

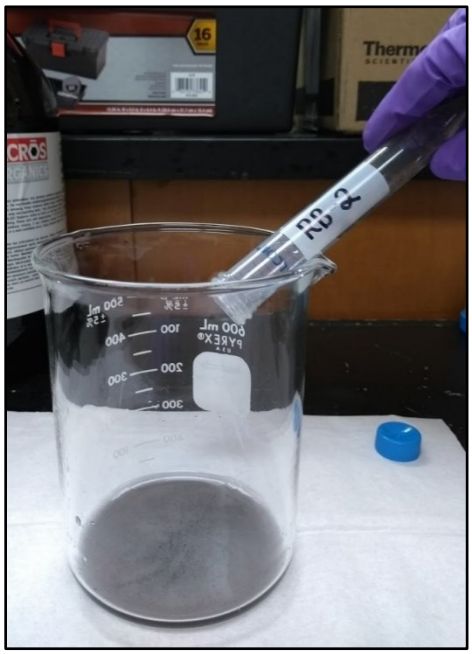

Figure A2-67: Pouring solution into beaker.

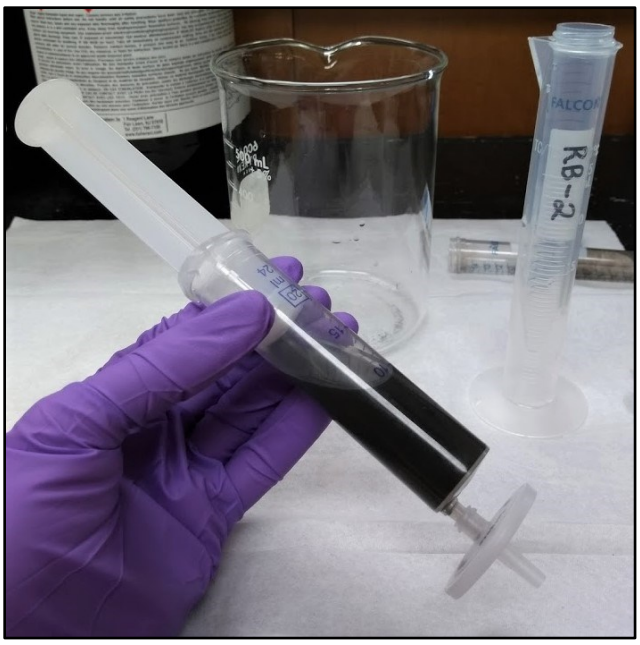

Figure A2-68: Solution in syringe with filter attached.

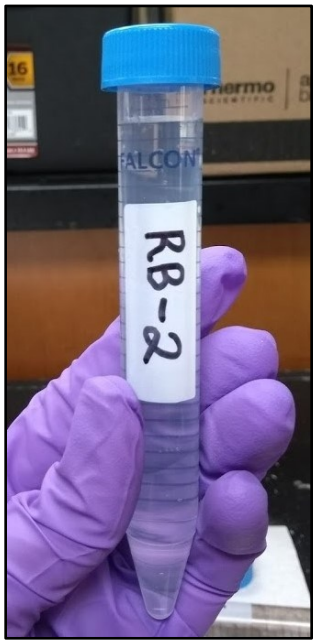

Figure A2-69: Filtered solution in a new test tube.

6. To dilute the sample so that its concentration can be detected on the ICP-OES, extract 1 mL of the filtered sample and add it to a 50 mL test tube. Fill the test tube with Milli-Q water to the 50 mL mark.
7. For the ICP-OES, samples must be prepped in 15 mL test tubes. Extract 15 mL of the diluted solution and transfer to a new, labeled 15 mL test tube.

8. To prepare standards for the ICP-OES, weigh approximately 0.1 g of powdered shale sample using a semi-microbalance. Record the weight and transfer the sample to a Teflon bomb.

9. Under a fume hood, use a pipette to add 1 mL of HF and 3 mL of HNO_3 to the sample. Cap the samples and place them on a hot plate covered with aluminum foil; keep at low heat (approximately 140°C) for 24 hours.
    - Make sure the caps are on semi-tight.
    - ➢ Extreme caution must be taken when working with HF; wear eye protection, gloves, close-toed shoes, and a lab coat.

10. After 24 hours, remove the samples from the hot plate, but keep them inside the fume hood. Place them on large Kimwipes in case of spills. Take off the caps and arrange them on the Kimwipes in the same order the uncapped samples will be placed back on the hot plate.

11. Place the uncapped samples on the hot plate and increase the temperature to approximately 172°C.

12. Allow the samples to dry down to a disk or pea ball shape. Some do not take this form and require even greater care with observation. Once a sample has dried down, remove it from the hot plate and add 1 mL of HCl and 3 mL of HNO_3. Cap the sample.

13. Once all samples have been removed and treated, place the samples back on the hot plate and adjust the temperature to 140°C for 24 hours.

14. After 24 hours, uncap the samples, dry them down, and add 1 mL of H_2O_2 and 3 mL of HNO_3. Place capped samples back on the hot plate at 140°C for 24 hours.

15. After 24 hours, uncap the samples, dry them down, and add 3 mL of HNO_3. Place capped samples back on the hot plate at 140°C for 24 hours.

16. After 24 hours, uncap the samples, dry them down, and add 0.5 mL of HNO_3. Transfer the sample to a labeled 15 mL test tube.

17. Proceed with steps 5-7 to complete sample preparation for standards.

18. Run the samples on the ICP-OES.

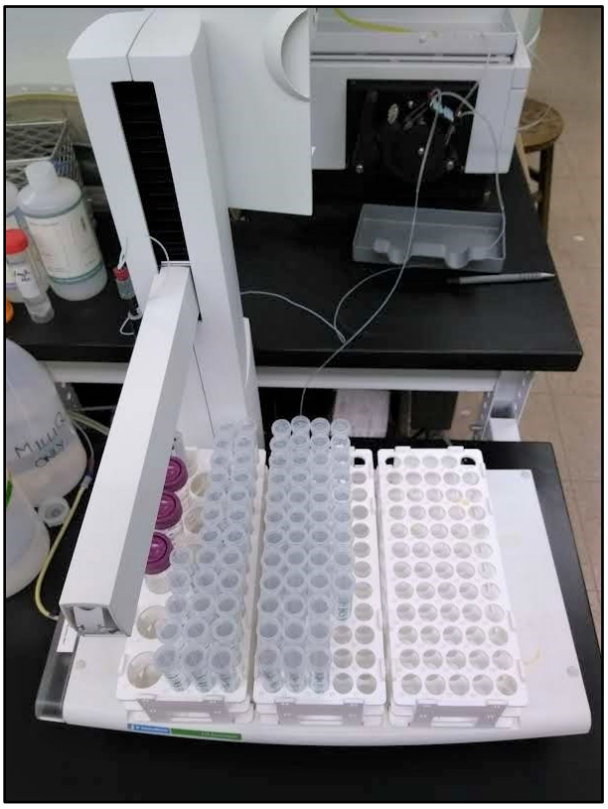

Figure A2-70: Samples ready to be measured on the ICP-OES.